
CARBON FIBER REINFORCEMENT FOR CONCRETE ENGINEERING

THESIS

HANDED IN ON THE
UNIVERSITY OF NATURAL RESOURCES AND
APPLIED LIFE SCIENCES, VIENNA
INSTITUTE FOR CONSTRUCTIONAL ENGINEERING

for attainment the academical degree

„GRADUATE ENGINEER“

ASSESSOR

O. Univ.-Prof. Dipl.Ing. DDr. Konrad Bergmeister

Institute for constructional engineering
UNIVERSITY OF NATURAL RESOURCES AND
APPLIED LIFE SCIENCES, VIENNA



Wolfgang WENZL

Vienna, December 2006

To attend thankfully

my parents Josef and Ingeborg

as soon as my brother Oliver

PREFACE

I would like to take the opportunity to thank all those who assisted me in succeeding this work. My special thank applies to O.Univ.Prof. DI. DDr. Konrad Bergmeister for provision of the subject, supervision of the diploma thesis as well as the possibility to work on this problem at the University of Natural Resources and Applied Life Sciences.

A very special thank applies to my mentor, Miss Univ.Ass.DI Dr. Andrea Rathmanner who always supported me with all her commitment and who stood at my side during organisation and execution of the experiments.

Furthermore I would like to gratefully thank the company Isosport – Eisenstadt for the provision of CFK – lamellas, the company Lafarge – Perlmooser for cement and various additives as well as the company Doka for the provided formworks.

Special thanks, too, to my fellow students Rudl, Mary, Christian and all the others for the wonderful, merry and nonetheless informative hours over my academic years.

Most of all, my thanks go to my parents and my brother who believed in me and stuck by throughout all the heights and depths of my life.

Table of contents

Carbon fiber reinforcement for concrete engineering

Preface	III
Abstract	VII
1. Introduction	
<i>1.1. Starting situation</i>	<i>1-1</i>
<i>1.2. Problem</i>	<i>1-1</i>
2. General part	
<i>2.1. Concrete</i>	<i>2-1</i>
2.1.1. Historical development	2-1
2.1.2. Definition of concrete	2-2
2.1.3. Cements	2-2
2.1.4. Aggregates	2-6
2.1.5. Water	2-8
2.1.6. Water/cement ratio	2-9
2.1.7. Additives	2-10
2.1.8. Concrete classes	2-12
<i>2.2. Structural steel</i>	<i>2-14</i>
<i>2.3. Reinforced concrete</i>	<i>2-18</i>
<i>2.4. Alternative reinforcement methods</i>	<i>2-19</i>
2.4.1. Prestressed concrete	2-19
2.4.2. Fiber concrete	2-22
2.4.3. External reinforcement	2-24
3. Carbon fibers	
<i>3.1. General</i>	<i>3-1</i>
<i>3.2. Manufacturing of CFRP-lamellae</i>	<i>3-1</i>
3.2.1. Manufacturing of carbon fibers	3-1
3.2.2. The pultrusion process	3-3
3.2.3. The laying procedure	3-6
3.2.4. Extrusion	3-7
<i>3.3. Properties of the composite</i>	<i>3-7</i>
3.3.1. Creeping and relaxation	3-7
3.3.2. Fatigue behaviour	3-7

3.3.3. Durability	3-7
3.3.4. Electric and thermal properties, lightning stroke hazard	3-8
3.4. <i>Types and applications</i>	3-9
3.4.1. Prefabricated CFRP-lamellae	3-9
3.4.2. CFRP-cable	3-10
3.4.3. CFRP strengthened concrete	3-12
3.4.4. CFRP textiles	3-12
3.4.5. CFRP-foils	3-12
3.4.6. Carbon fiber composites	3-13
3.5. <i>Fire protection</i>	3-14
3.6. <i>Safety concept</i>	3-16
3.7. <i>Quality assurance</i>	3-17
4. Material description and fabrication	
4.1. <i>Material description</i>	4-1
4.1.1. Fabrication of meshes based on carbon fiber lamellae	4-1
4.1.2. Concrete mixture	4-4
4.1.3. Aggregates	4-4
4.1.4. Moisture test of aggregate	4-6
4.2. <i>Comparison with a SCC</i>	4-8
4.3. <i>Preparation</i>	4-11
4.3.1. Preparation of formwork	4-11
4.3.2. Concrete – preparation and casting	4-12
4.3.3. Base concrete	4-15
4.3.4. Storage of the slabs	4-16
5. Experimental part	
5.1. <i>Experimental set-up</i>	5-1
5.1.1. Three-point bending test	5-1
5.1.2. Schematic illustrations	5-4
5.1.3. Set-up of measuring unit	5-6
5.2. <i>Experiments</i>	5-7
5.2.1. Mounting of specimens	5-7
5.2.2. Tensile bending test	5-8
5.3. <i>Results</i>	5-9
5.3.1. Crack evolution and distribution	5-9
5.3.2. Ultimate failure criteria	5-11
5.3.3. Demolition of the slabs	5-13
5.3.4. Results	5-15
5.4. <i>Analysis of the results</i>	5-23

6. Pull out tests

6.1. <i>Simplified pull-out test</i>	6-1
6.1.1. Preparation	6-1
6.1.2. Test setup	6-2
6.1.3. Evaluation	6-3
6.2. <i>Standardized pull-out test</i>	6-4
6.2.1. Roughness of the lamellae	6-4
6.2.2. Pull-out test in general	6-7
6.2.3. Testing variants	6-9
6.2.4. Bursting effect resulting from bonding ...	6-12
6.2.5. Experimental set-up of the pull-out tests	6-13
6.2.6. Manufacturing	6-14
6.2.7. Data acquisition system	6-17
6.2.8. Test results	6-18
6.2.9. Analysis of the results	6-20
6.3. <i>Simplified evaluation</i>	6-21

7. Summary

Literature

Bibliographie

Appendix

Picture register	A-1
Table register	A-3
Figure register	A-6
Produktion of Carbon Fiber Plastics	A-9
Mechanism of SCC	A-13
LOG-IN Data for the evaluation program	A-16
Test protocol	A-20
Force – strain – curve	A-21
Influence facts of loading rate to the concrete	A-24
Release for publication	A-26

KURZFASSUNG

Bewehrung aus Kohlenstofffasern im Betonbau

Diese Diplomarbeit beschreibt Forschung im Bereich der Anwendbarkeit von Kohlenstofffasern als Ersatz von herkömmlicher Stahlbewehrung bei Betonplatten. Dank der Korrosionsbeständigkeit haben Kohlenstofffaser Lamine bereits ein großes Anwendungsspektrum im konstruktiven Ingenieurbau.

Bei der untersuchten Anwendung für die Kohlenstofflamelle handelt es sich um einen neuen Bewehrungsgittertyp, der aus verwobenen Lamellenstreifen hergestellt wird. Die Bewehrung wird mittels 3-Punkt Biegezugversuche getestet, die Rißweiten, Rißabstände und die Ergebnisse mit denen von herkömmlicher Stahlbewehrung verglichen.

Zusätzlich zeigen Auszugsversuche das unterschiedliche Verbundverhalten von verschiedenen Laminatoberflächen. Die Flexibilität dieses neuartigen Bewehrungssystems ermöglicht die Bewehrung von Beton in nahezu allen Formen.

ABSTRACT

Carbon fiber reinforcement for concrete engineering

This diploma thesis summarizes investigations on the feasibility to reinforce concrete slabs with carbon fiber laminate and to substitute common steel reinforcement. Due to their corrosion resistance carbon fibers show an extensive scope of application in structural engineering.

The investigated application for the carbon lamella is a new type of reinforcement grid, which consists of woven carbon lamella bars. The reinforcement is tested with 3-point flexural tests.

The crack widths and the crack distances are measured and compared those of steel reinforced slabs. Additionally, pull-out tests describe the bonding behaviour of different surfaces of the lamellas.

The flexibility of this reinforcement enables to strengthen concrete in nearly every shape.

1. Introduction

1.1. Starting situation

Structures are planned and designed for a life time of generally 80 – 100 years. Due to time dependent effects or unexpected circumstances like a change of use, fire, earthquake etc. during operation an adaptation according to the state of the art may be necessary.

Nowadays different solutions are available for this problem, e. g. strengthening of floors and binding girders or downstand beams, but the technical and financial expenditure usually is considerable.

In Europe there are mainly used extrusion pulled carbon fiber lamellae for the strengthening of structures and rehabilitation of structural members, whereas the applied methods depend on the kind of structural member, static system and properties of the material. After cleaning and preliminary treatment of the surfaces the lamellae are glued by means of epoxy resin on the structural members consisting of reinforced concrete, timber or steel. New methods have been developed where the lamellae are glued directly in slots. The bearing capacity depends on the actual boundary conditions and may be enhanced by the following measures:

- Strengthening of the tensile zone
- Strengthening of the compression zone
- Shear - strengthening (bearings, columns...)
- Strengthening of columns (to avoid buckling)

The weak link of these systems is commonly the adhesive, a fact that is more pronounced at higher temperatures. This may be an additional risk in case of fire, if the strengthened members are not protected.

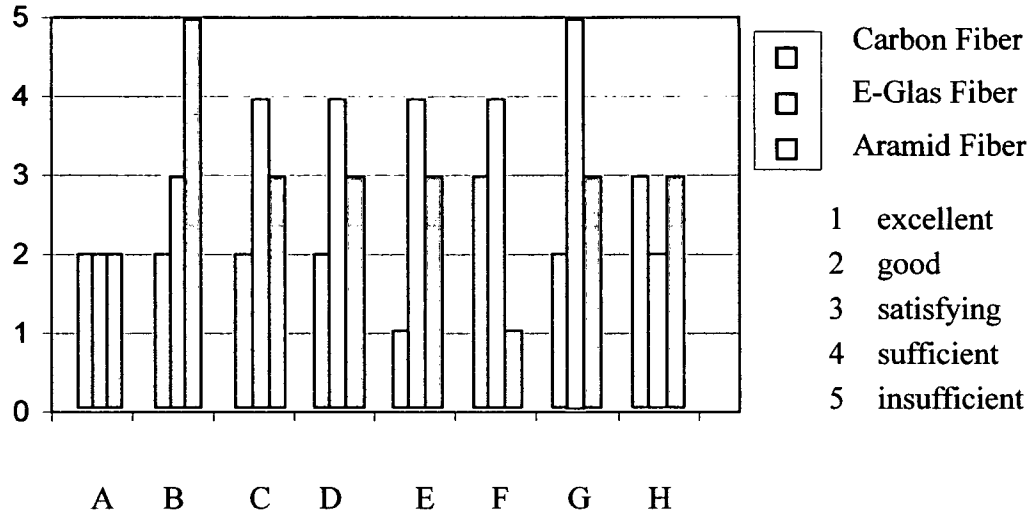
An alternative method is the strengthening by use of woven carbon fibers, where the advantage consists in the total coverage independent of the shape of the structural member.

1.2. Problem

In this thesis the possibility of a new reinforcement for concrete is examined. Instead of the traditional steel reinforcement with flat or ripped bars or grids we used grids of plaited carbon fiber reinforced polymer (CFRP) lamellae and investigated their effect on load capacity in a bending test. The choice fell on CFRP-lamellae due to

their good mechanical performance compared to E-glass and Aramid fibers (see Figure 1.2-1).

The CFRP exhibits many advantages compared to steel like lower specific weight, higher tensile capacity and Young Modulus and excellent fatigue and corrosion resistance properties. The main disadvantage is the high price, which depends on type of product (high modulus, high strength or normal fibers).



A - tensile strength B - ultimate strength C - Young's Modulus
 D - time depending behaviour E - fatigue
 F - density G - alkali resistance H - price

Figure 1.2-1 Qualitative comparison of different types of fibers

For the tests high strength lamellae with the laminate identification C 200/14 (length: 2000 mm, width: 80 mm, thickness: 1,4 mm) were used, modified to a length of 1800 mm and a width of 10 mm and plaited to grids. The lamellae exhibited different roughness on both sides.

The total test program consisted of 6 concrete slabs with a thickness of 10 cm: 2 slabs with double-layer and 2 slabs with single-layer carbon fiber grids, for reference test 1 slab with CQS 8 resp. CQS 6 steel grids.

Since experimental investigations are concerned only few references are available. Within this thesis the following themes are treated:

- Processing of the CFRP-lamellae
- Manufacture of the grids
- Fabrication and storage of the concrete specimens
- Bending test
- Evaluation of the results
- Reference concrete with grading curve
- Roughness measurements on the lamella
- Standardized and non-standardized pullout tests
- Verification of test results

The continuation of the test series can be found in the PhD-thesis of Guggenberger who varied the distance between the lamellae, the lamella width and the concrete specimen thickness. The influence of the surface roughness of the lamellae has also been investigated. A self compacting concrete (SCC) was used and tested in a 4-point-bending test.

2. General part

2.1. Concrete

2.1.1. Historical development

Concrete was already known in the antique. Caligula built up a mole consisting of concrete close to Naples in 37 – 41 a. D., whereas limestone, pozzolan soil and volcanic rocks acted as binding material. The Romans produced also masonry with concrete resp. cast masonry. A stone matrix between masonry shells or a wooden form was bound through a castable fine mortar or already mixed before. As binding materials there were used lime hydrate, grinded bricks and volcanic ash. The effect was a hydraulic hardening of the mortar, i. e. not through reaction with air, but with water and hence also under water. The hydraulic hardening means high resistance and insolubility in water and enables every kind of water constructions. During the Middle Ages concrete was used, but fell increasingly into oblivion.

The French engineer Belidor introduced the word “concrete” in 1753. In England cement was produced already since the middle of the 18th century (Roman Cement). In 1824 Joseph Aspdins from Leeds in England applied for a patent for the “Portland cement”. The decisive change did J. C. Johnson, namely the burning of the limestone – clay mix beyond the sinter limit. In this way the production of Portland cement began. In 1857 Alois Kraft produced for the first time Portland cement in Perlmoos close to Kufstein in Austria.

In 1855 the French F. Coignet applied for three patents, which represent the basic properties of concrete technology:

- Economical use of water
- Mixing machines for an economical production of large amounts of concrete
- Reusable forms
- Compacting by stamping

He added also steel bars to the concrete and constructed in this way, long before Joseph Monier, the first structural elements (walls, floors, tubes, etc.) consisting of reinforced concrete. The English W. B. Wilkingson addressed in 1854 the important aspect of the fire resistance of concrete. In Germany there was developed the concrete pump in 1929, which enabled the transport of plastic concrete. Furthermore the concrete vibrator was invented. Another invention of the 20s represents the use of compressed air (shotcrete). Finally, in the 60s and 70s the amount of transport

concrete increased rapidly. Nowadays the portion of transport concrete is about 35 – 60% of the total production. [1]

2.1.2. Definition of concrete

According to the Austrian standard ÖNORM B 4200 normal concrete consists of cement, water, aggregates and additives and exhibits a gross density between 2000 and 2800 kg/m³. This standard is valid for concrete which is produced at the construction site as well as for pre-fabricated concrete elements and for transport concrete according to ÖN B 3307.

2.1.3. Cements

Cements have to comply with the Austrian standard ÖN B 3310. Cement must be protected against moisture (also from air), stored separately according to type and quality and may content only easy crushable bulbs before use. For suitability tests the same type and quality of cement must be used as afterwards in the construction.

If the supplier is changed then suitability tests have to be performed in order to identify changes of the properties of fresh and hardened concrete. In Austria there are mainly used the following 5 cement types: Portland cement (PZ) 275, 375 and 475, iron Portland cement (EPZ) 275 and blast furnace cement (HOZ) 275.

The main difference of these cements is the grind fineness, which affects crucially the hardening process. The specific surface is increased through a finer grinding. This leads to a faster hydration and hence to an increased early resistance. [1]

Cement is available in sacks or loose as silo cement, whereas the imprint on the sacks indicates the manufacturer, type and strength class of the cement, standard, seal of the accrediting testing laboratory and waste disposal code.



Figure 2.1.3-1 The most important test and quality seals of cement

For a better distinction the cement sacks and the imprints have different colours (s. Table 0-1).

Cement	sack		Silo cement delivery note
	Colour	Imprint	
PZ 275	Ecru	black	white
EPZ 275	Ecru	red	pink
HOZ 275	Ecru	magenta	magenta
PZ 375	Ecru	green	green
PZ 475	red	black	red

Table 2.1.3-1 The main cement colour codes

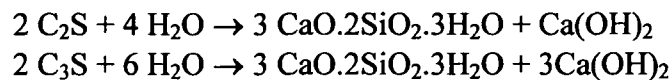
The cement types PZ 275 and PZ 375 should not be stored more than one month, otherwise the strength may be reduced [4]:

After 3 months: 10 – 20 %
 After 6 months: 20 – 30 %

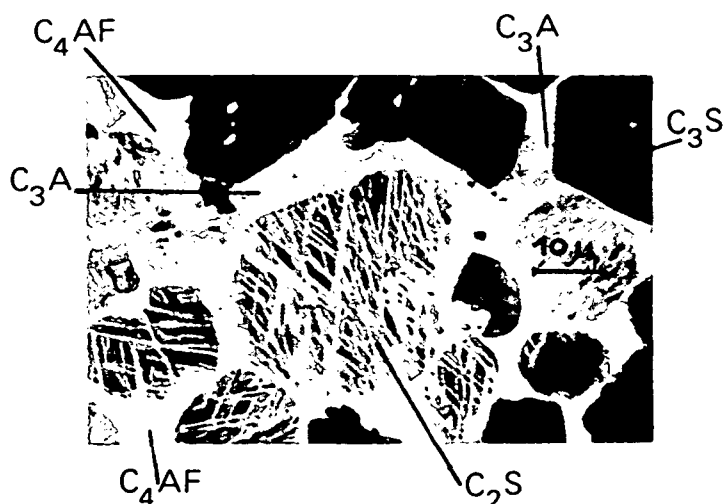
Cement consists of lime and clay or marl with a suitable constitution. Minerals rich in lime and clay (SiO_2 , Al_2O_3 , Fe_2O_3) are mixed with a ratio of clay : CaO = 1 : 1.7, finely milled and sintered in the rotary furnace at 1400 – 1450 °C. The achieved cement clinker is ground to fine powder which consists of compounds of calcium oxide with silicon, aluminium and ferric oxide. Portland cement consists of:

50 %	3 $\text{CaO} \cdot \text{SiO}_2$	Tricalciumsilicate (C_3S)
20 %	2 $\text{CaO} \cdot \text{SiO}_2$	Dicalciumsilicate (C_2S)
10 %	3 $\text{CaO} \cdot \text{Al}_2\text{O}_3$	Tricalciumaluminate (C_3A)
10 %	4 $\text{CaO} \cdot \text{Al}_2\text{O}_3 \cdot \text{Fe}_2\text{O}_3$	Tetracalciumaluminateferrit (C_4AF)
less than 1 %	$\text{CaO} \cdot \text{SiO}_2$	Monocalciumsilicate

The rest is formed by Mg-, alkali- and sulphur compounds. The aluminium ion is able to act as anion (substitution of Si) as well as cation. C_3S and C_2S react in the following manner:



The first reaction product are needle-like crystals which felt during the hardening process and hence contribute mainly to the strength. [5]

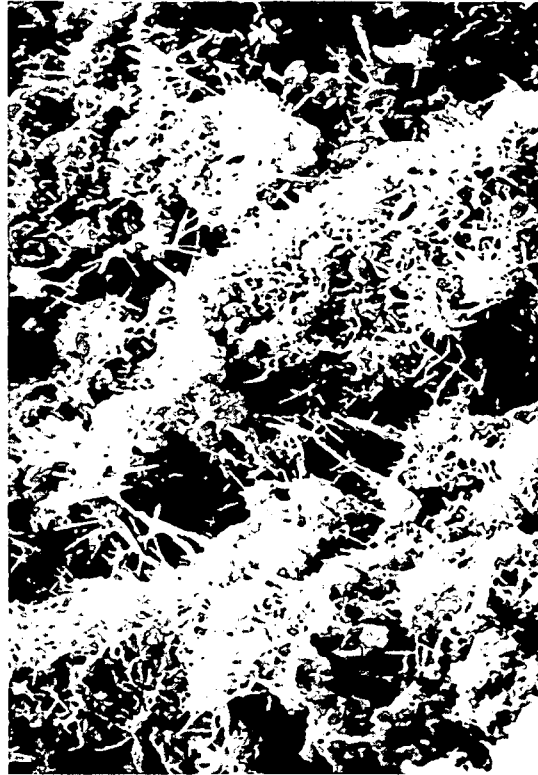


Picture 2.1.3-2 Microphoto of a ground surface concrete

The free calcium hydrate reacts strongly alkaline and protects the steel reinforcement against corrosion. It appears in the form of coarse crystals or finely distributed in amorphous state and due to its water solubility in porous structures it can easily be leached out (e. g. efflorescence). By diffusion of carbon dioxide it is transformed into limestone (carbonation) and as consequence the steel will corrode.

Gypsum is added during the milling of the cement in order to retard the very rapid hydration by binding the C₃A-component. Too much gypsum resp. sulphuric water during operation may cause a pressure of gypsum or creation of ettringite, which in compound with water forms needle-shaped crystals with a higher demand of volume and hence the cement stone is destroyed.

After the hydration process an amount of water of about 25% of the cement mass is bound chemically to the cement components. This is only possible if the total amount of water accounts for 35 – 40%. A part of it adheres in some way in the gel region and cannot participate in the hydration process. The liquid mix of cement and water (paste) hardens to cement stone.



Picture 2.1.3-3 Cement stone, $w/c = 0.5$, after 7 days, 5000 times enlarged

Especially at the beginning the hydration products are not formed contemporaneously, but successively. If the hardening is accelerated, the initial strength in fact is higher, but the final strength often decreases because due to the abbreviation of the second hydration level less long-fibered calcium hydrosilicates are formed.

Shortly after mixing water with cement the paste becomes stiff temporarily, a phase which may be liquefied by vibrations (thixotropy). As a consequence concrete should be cast and compacted during the first hour. Since the hydration of cement is an exothermic reaction, heat is released. The higher the final strength, the higher is the amount of released heat. Cements with a high initial strength exhibit a larger heat release during the first days, whereas cements with a low heat release show a slower strength development. The average heat release during total hydration per 1 g cement amounts for 500 J, whereas the various clinker phases contribute with different amounts. Since the hydration is a chemical process it is accelerated at high temperatures, decelerated at low temperatures and stopped at the freezing point.

Large structures are critical (e. g. dams) because the released heat cannot flow off easily and an increase in temperature of about 30 – 40 degrees may be possible. If the temperature gradient between

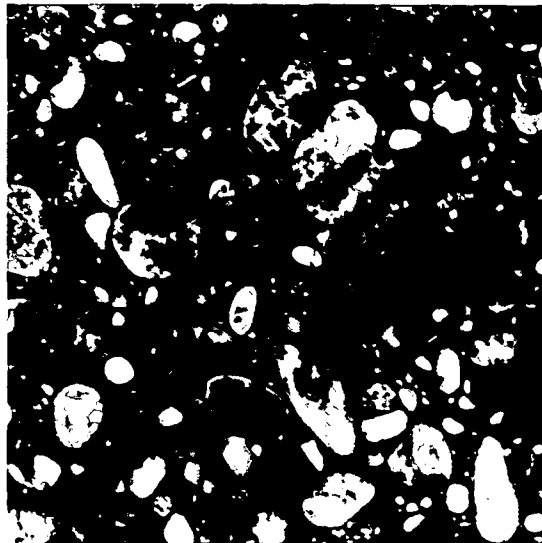
the surface and the core of the structural element exceeds a limit of about 10 – 15 degrees, cracks will be formed.

The final strength of the cement stone is determined fundamentally by the pore space, whereby the hydration speed depends on the fineness and chemical composition of the cement and on temperature and moisture conditions during the hardening. The capillary pore space increases with increasing amount of water in the cement paste and hence the strength of the hardened concrete is reduced. Additional consequences are increased shrinkage, water suction and permeability and a poor resistance against chemical and frost impacts.

The moisture content in the first hardening stage is of crucial importance because the hydration can be activated only by an adequate amount of water. Early dry up leads to strong shrinkage and stops the hardening, an effect that may be noticed through formation of sand on the edges. [4]

2.1.4. Aggregates

As aggregates usually a mix of grains is used which is bound by the cement stone similar to a natural conglomerate. If the grain size is less than 4 mm it is referred to as mortar, beyond 4 mm as concrete. [4]



Picture 2.1.4-1 Structural constitution of concrete

The aggregates must not contain any material that may affect the hardening and durability (e. g. adobe) and for this purpose they are cleaned with water. Additionally, the aggregates are separated with filters in different grain sizes.

According to the fracture surface the aggregates are classified in round grains (more than the half surface is naturally rounded) and square-edged grains (more than the half surface is square-edged). [1]

A mix of aggregates is characterized through the grading curve which is obtained by a series of sieves with different mesh size. After each sieve the residue is measured and noticed as a fraction of the total weight. The largest grain must be less than $\frac{1}{4}$ of the smallest dimension of the element and must not exceed 1.25-times the smallest distance between reinforcement for single layers and 0.8 times for multi layers. [6]

Due to the different shapes of the grains they cannot be divided exactly, so within a size class a certain amount of smaller and larger grains may appear (s. Table 0-1).

Grain size	Smaller grain	Larger grain
≤ 4 mm	15 %	10 %
> 4 mm	10 %	10 %

Table 2.1.4-1 Limits for the content of smaller and larger grains

Modern concrete mixing equipments compose the desired grading curve with single fractions. Due to the increased ratio between surface and volume the demand of water is higher for a fine grain than for a coarse one. [6] The standard ÖN B 3304 regulates the favourable and acceptable grain composition for mixtures with the largest grain of 4 mm, 8 mm, 16 mm, 22 mm and 32 mm.

For the best composition of the grains the amount of voids is minimized. If one or more fractions are missing, the grading curve becomes discontinuous. It is also possible to use only one fraction of aggregates (“single grain concrete”).

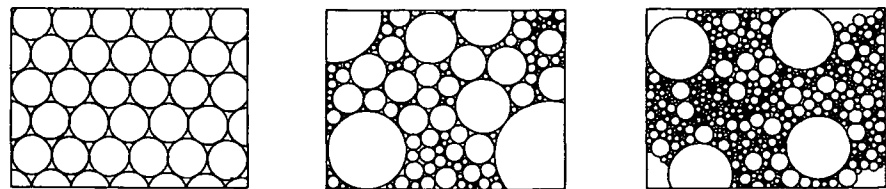


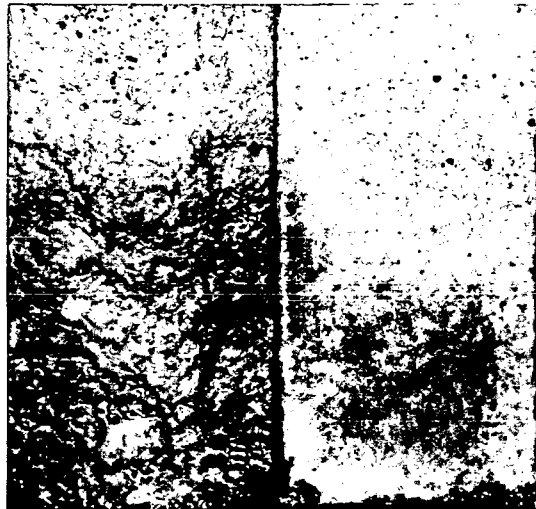
Figure 2.1.4-1 Various grain mixtures (schematic) [4]

Depending on strength and frost resistance the aggregates are divided into classes I, II and III. For class I the allowable amount of brittle grains is 5 %. In the case that it is higher the freeze resistance has to be proved according to ÖN B 3304 chapter 4.10. Concrete with class I aggregates is frost resistant and highly resistive against chemicals. Exceptions are subaqueous concrete,

pump concrete, internal fairfaced concrete and concrete with maximum grain of 4 mm.

Aggregates with more than 5 % brittle grains belong to class II if it is proved according to ÖN B 3304 chapter 4.9 that the strength is not influenced negatively. They are not frost resistant and usable for all concretes where class I is not required explicitly.

Aggregates with brittle grains between 5 and 20 % and without proof of frost resistance and strength are counted among class III. The meal grains consist of the fine fraction below 0.25 mm grain size, hence the cement is included. An optimum quantity of meal grains is necessary for a good workability, to avoid decompositions, for waterproof concrete and to improve the surface of fairfaced concrete. Grading curves with little fine sand are not recommendable.



Picture 2.1.4-2 Content of meal grains: at the left too little, at the right ok

2.1.5. Water

Any potable water is suited principally for production of non-reinforced concrete, RC and prestressed concrete. Water may not be suitable, which content substances that

- decelerate or avoid hardening (e. g. sugar, vegetable mould acids),
- create air pores in an uncontrolled way and hence decrease the strength of the concrete (e. g. seaweed, oils and lipids, suspensions, various inorganic salts),
- lead to corrosion of embedded steel.

Such substances may contain water that is contaminated by domestic and industrial wastes. If the water is taken from rivers, it has to be ensured that no wastes are conducted into the river. Brooks from fens may contain substances which disrupt the hardening (vegetable mould acids). [1] The amount of suspensions (e. g. clay, silt) must not exceed 2 g/l. Steel corrosion may be induced by chlorides and H₂S. If doubts exist about water quality a certified laboratory should be consulted.

The chloride content of natural potable water in Austria is less than 100 mg/l, which according to the international state of the art is harmless for RC and prestressed concrete. Water with a chloride content much more than 300 mg/l should not be used for prestressed concrete. Gypsum or other sulphates destroy the cement stone.

2.1.6. Water/cement ratio

Decisive for the quality of concrete is the ratio of mass between water and cement in the fresh concrete. Cement is able to bind chemically only 25% of its mass, but for the total hydration additional 10 – 15% are necessary. Concrete with a w/c value > 0,4 exhibits excess water that creates additional capillary pores in the cement stone and decreases the strength. High w/c-ratios have the following disadvantages:

- Low strength
- Water permeability
- Weather sensibility
- Higher evaporation
- Higher shrinkage
- cracking

Hence the most important rule in concrete technology:

The lower the w/c value the higher the strength and durability!

For this purpose so-called additives have been developed (details see chapter 2.1.7). However, not too less water must be used in order to enable total compacting, i. e. the air pores must be kept at a minimum. [1] The influence of the w/c-ratio on strength can be seen in Table 2.1.6-1. If the w/c-factor is increased e. g. from 0.4 to 0.75, the strength decreases about 60%.

w/c ratio	0.4	0.5	0.6	0.7	0.8
Compressive strength (in %)	100	83	64	48	37

Table 2.1.6-1 Concrete strength vs. w/c-ratio

From the w/c-ratio result also the so-called consistence classes of fresh concrete which represent a measure for the workability. [6] The consistency should be chosen according to the disposable equipment so that the concrete can be cast without decomposition and compacted without coarse pores. In Austria the consistency is tested by two standard procedures – the spreading measure and the compacting measure (ÖN B3303). [1]

class	consistency	Spreading measure in cm	Compacting measure	Compacting through	Application useful for
K1	stiff	---	1.45 – 1.26	Strong vibrators	Only large elements, forbidden for close reinf.
K2	Stiff plastic	≤ 37	1.25 – 1.16	vibrators	Elements with moderate dimension and wide meshed reinf.
K3	plastic	38 - 43	1.15 - 1.09	vibrators	RC, prestressed concrete, pump and fairfaced concrete
K4	soft	44 - 50	1.08 – 1.04	Vibrating carefully, picking	Close reinf., rangy elements
K5	very soft	51 - 60	---	Vibrating carefully, picking	Very close reinf., rangy elements, subaqueous concrete

Table 2.1.6-2 Concrete consistencies [6]

2.1.7. Additives

Certain demands on concrete (e. g. resistance against frost and thaw salt, very early or very late hardening) cannot be fulfilled through a change of cement content, composition of aggregates or water content. In this case the use of additives is necessary.

Additives may be liquid or powdery substances that are added in very small quantities (usually in ‰ of the amount of cement) and influence by physical and / or chemical effects the properties of fresh and hardened concrete. The effectiveness of additives depends also on the “right” composition of concrete. In the following table various types of additives and the according regulations are listed.

Effect	label	regulation
Fluidise	BV	ÖN B 3333
Fluxing agent	FM	Richtlinie f.
Air pore generator	LP	Fliessbeton
Antifreeze	FS	RVS 8.01.71
Air pores and fluidise	LPV	ÖN B 3332
Sealant	DM	Richtlinie des ÖBV
Hardening decelerator	VZ	-
Hardening accelerator	BE	-
Grout assistance	EH	-

Table 2.1.7-1 Common types of additives

A series of additional additives is available. In the case that additives are used, three basic demands have to be fulfilled:

- Efficiency
- Harmless
- Free of chlorides

Efficiency means that the additive yields the change of the desired concrete properties. An additive is harmless if other properties are not influenced negatively so that the concrete may become unacceptable for the intended use.

The chloride content must be specified by the manufacturer on the packing. In order to avoid steel corrosion the limit is 0.002 ‰ chloride referred to the cement mass for the maximum allowable dose of the additive.

The efficiency of an additive depends strongly on the components of the concrete, mixing and casting temperature, consistency, other additives etc. Specifications of the manufacturer about dose may be interpreted only as a standard value. [1]

2.1.8. Concrete classes

In this section the differences between the previous Austrian standard ÖN B 4200 part 10, the new Austrian standard ÖN 4700, the Eurocode 2 and the DIN 1045 are listed.

	C12/15	C16/20	C20/25	C25/30	C30/37	C35/45	C40/50	C45/55	C50/60
F_{ck}	12	16	20	25	30	35	40	45	50
f_{ck,cube}	15	20	25	30	37	45	50	55	60
F_{ctm}	1,6	1,9	2,2	2,6	2,9	3,2	3,5	3,8	4,1
E_{cm}	26.000	27.500	29.000	30.500	32.000	33.500	35.000	36.000	37.000
f_{ctk;0,05}	1,1	1,3	1,5	1,8	2,0	2,2	2,5	2,7	2,9
f_{ctk;0,95}	2,0	2,5	2,9	3,3	3,8	4,2	4,6	4,9	5,3

Table 2.1.8-1 Concrete strength classes and specifications according to EC2 (in N/mm²) [10, 12]

	B 15		B 25		B 35	B 45		B 55	
B_{w200}	15		25		35	45		55	
E_b	26.000		30.000		34.000	37.000		39.000	

Table 2.1.8-2 Concrete strength classes and specifications according to DIN 1045 (in N/mm²) [10]

		B 20	B 25	B 30			B 40	B 50	B 60
f_{ck}		15	18,8	22,5			30	37,5	45
f_{cwk}		20	25	30			40	50	60
f_{ctm}		1,9	2,2	2,6			3	3,5	4,1
E_c		27.500	29.000	30.500			32.500	35.000	37.000
f_{cd}		10	12,5	15			20	25	30
f_{ctk}		1,3	1,5	1,8			2,1	2,5	2,9
τ_d		0,22	0,24	0,26			0,28	0,31	0,33

Table 2.1.8-3 Concrete strength classes and specifications according to ÖN 4700 (in N/mm²) [19]

		B 225		B 300			B 400	B 500	B 600
$\beta_w=W_{28}$		22,5		30			40	50	60
E_b		26.000		30.000			35.000	39.000	43.000

Table 2.1.8-4 Concrete strength classes and specifications according to ÖN 4200 part 10 (in N/mm²) [2,3]

Explanations of specifications and indices

According to EC 2

f_{ck}	characteristic compressive strength of cylinder after 28 days
$f_{ck,cube}$	characteristic compressive strength of cube (150 mm) after 28 days
f_{ctm}	Average tensile strength with $f_{ctm} = 0.3 \cdot f_{ck}^{2/3}$
E_{cm}	average secant Young's modulus
$f_{ctk;0.05}$	5% fractile
$f_{ctk;0.95}$	95% fractile

According to DIN 1045

β_{w200}	compressive cube strength (a = 200 mm) after 28 days
E_b	Young's modulus

According to ÖN B4700

f_{ck}	characteristic long time strength in the structure (= 75% of f_{cwk})
f_{cwk}	characteristic cube compressive strength (5%-fractile is decisive)
f_{ctm}	Average tensile strength
E_c	average Young's modulus
f_{cd}	design compressive strength
f_{ctk}	characteristic tensile strength (5% - fractile)
τ_d	shear stress

according to ÖN 4200 part 10

$\beta_w = W_{28}$	average cube compressive strength (a = 200mm) after 28 days
E_b	Young's modulus

If the strength is measured on cubes with a = 150 mm (a = 300 mm), the value has to be multiplied by the factor 0.93 (1.10).

2.2. Structural steel

The chemical element iron (Fe) is a metal with a density of 7860 kg/m³ and a melting point of 1536°C. Pure iron is soft and exhibits a low yield (100 N/mm²) and ultimate strength (200 N/mm²) but a high strain at fracture (50%). Natural iron appears only in chemical compounds, most frequently as iron oxide. Ores exhibit a content of iron between 20% and 70% and can be found in different types like e. g. magnetite, hematite, limonite and siderite (Erzberg in Styria).

Steel is defined as iron that is forgeable without treatment afterwards. This is achieved through the addition of metallic and non-metallic alloying additions, whereas the maximum content of carbon is limited by 2% of the mass. Carbon increases the strength but decreases the toughness and weldability. A well weldable steel contents less than 0.2% of carbon. [9]

Alloys with more than 2% carbon are referred to as cast iron. As it can be seen in the next figure by thermal analysis the various stable phases of the Fe – C alloy depended on the temperature can be detected.

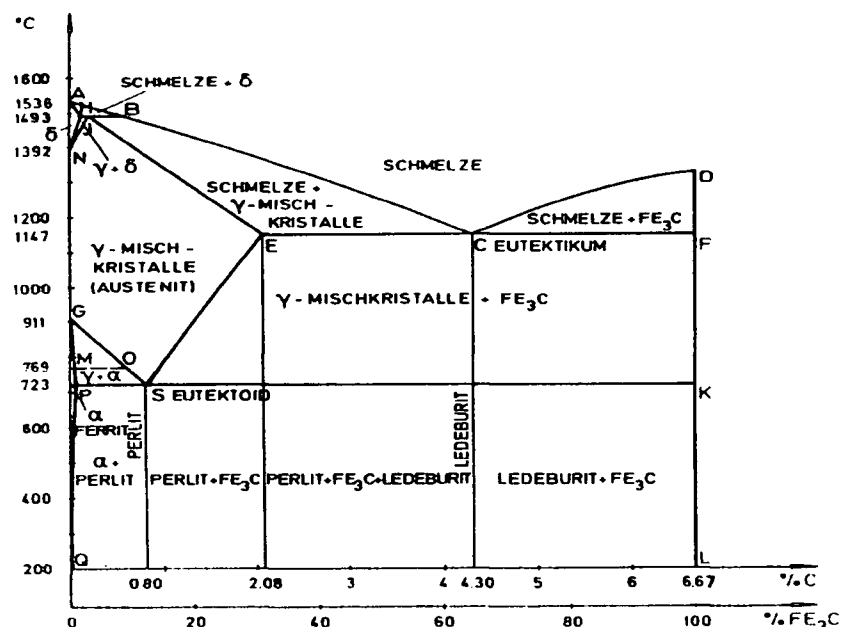


Figure 2.2-1 Ferrum-carbon-diagramm

By variation of amount and type of alloying additions and specific application of various processes the properties of steel can be adapted to the intended use. If the amount of metallic alloying additions is kept below a determined limit it is referred to as non-

alloy steel. Dependent on the demands one distinguishes between standard, quality and stainless steels. Structural steels are non-alloy steels that are provided for further processing. Demands are put regarding

- Strength
- Chemical composition
- Technological properties
- Production process
- Delivery condition
- Surface condition

These demands must be considered in correlation due to the fact that the change of one property generally leads to a change of all other properties. [7]

The strength (yielding and fatigue resistance) is determined in uniaxial tests. The most commonly applied steel test is the uniaxial tension test whereas a bar is clamped on both ends and stressed in tension. The applied force is transformed into stress and the extension into strain. As a result you get a stress-strain diagram of a uniaxial tension test (s. Figure)

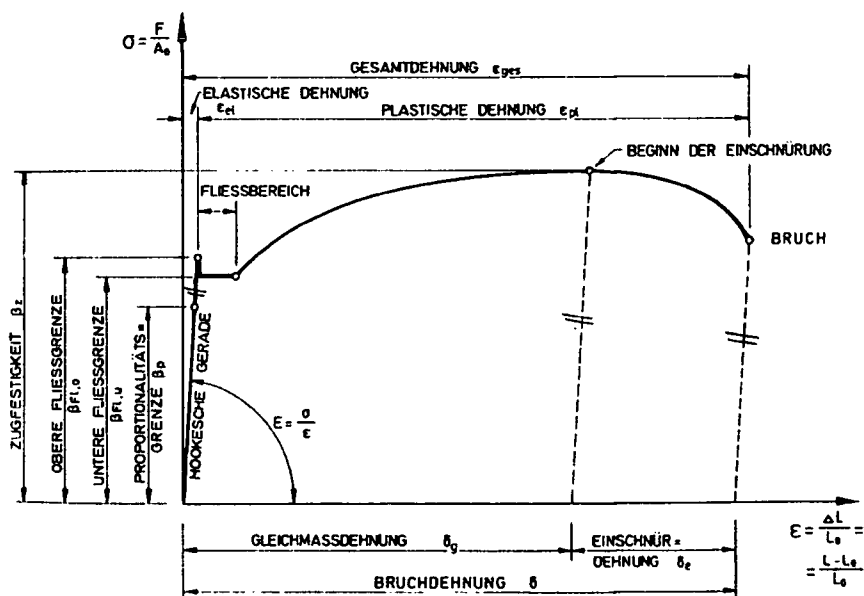


Figure 2.2-2 Stress-strain-diagram [7]

In RC construction there are used usually flat or ripped bars and grids with a high elongation at fracture. The nominal diameter of ripped bars corresponds to the diameter of flat bars of the same weight. According to the Austrian standard ÖN B 4200 part 7 the

steel sorts are divided into groups with corresponding yield and ultimate strength. [2] Structural steels are identified as following:

- Code for steel St
- Code for minimum tensile strength in N/mm², e. g. 560
- Code for quality B, C, D

The Young's Modulus is quantified with 206000 resp. 210000 N/mm². [7]

According to the manufacturing it is distinguished between:

- steel with as-rolled hardness with and without heat treatment whose strength depends on the chemical composition and
- cold rolled or cold formed steel whose strength is achieved by twisting, moulding or stretching.

Steel for RC should exhibit:

- High strength and deformation capability
- Good adhesion properties
- Suitability for bending
- Fatigue resistance ($2 \cdot 10^6$ cycles)
- Weldability

In the future steel for RC will be standardised in the EVN 10 080 which at the moment exists as a draft. Steel products for RC are sorted according to:

- Strength
- Ductility class (H = high ductile, N = normal ductile)
- Dimension (diameter 6 – 40 mm)
- Surface properties (flat bars with moderate bond strength and ripped bars with high bond strength) and
- Weldability

Ripped steel exhibits much higher bond strength as flat steel and hence an effective limitation of crack widths is possible. The mechanical properties are characterised by strength, stress-strain diagram, ductility, Young's modulus and fatigue resistance.

Steels with as-rolled hardness show a pronounced yielding plateau with following strength increase, a characteristic which is almost missing for cold formed steels. Due to the poorly pronounced yielding the yielding point for cold formed steel is defined as the stress corresponding to a plastic deformation of 0.2%.

In Austria and Germany and in the future Eurocode 2 the value for the Young's modulus is 210000 N/mm². [10]

Product	bars	bars	bars	bars	bars	mats	mats
Code	BSt 220	BSt 420	BSt 500	BSt 550	BSt 600	M 500	M 550
Group	I	III	IV	BSt 550	V	M IV	M 550
Form	flat	ripped	ripped	ripped	ripped	flat, profiled or ripped	
Yield strength	220	420	500	550	600	500	550
Ultimate strength	360	460	560	620	670	560	560
Young's modulus	206000	206000	206000	206000	206000	206000	206000
Stress limit	240	420	500	550	600	-	-
Strain [%]	0.4	0.4	0.4	0.4	0.4	-	-

Table 2.2-1 Steel classes according to ÖN 4200 part 7 (units in N/mm²) [6]

Properties		Strength classes				
		4.6	5.6	8.8	8.8	10.9
				d < 16 mm	d > 16 mm	
Ultimate strength	Nominal value	400	500	800	800	1000
	Minimum value	400	500	800	830	1040
Lower yield strength	Nominal value	240	300	-	-	-
	Minimum value	240	300	-	-	-
0.2% yield strength	Nominal value	-	-	640	640	900
	Minimum value	-	-	640	660	940

Table 2.2-2 Steel classes according to DIN ISO 898 (units in N/mm²) [6]

	BSt 220	BSt 420	BSt 500	BSt 550	BSt 600
f_{yk}	220	420	500	550	600
Ultimate strength	360	460	560	620	670
f_{yd}	191	365	435	478	522

Table 2.2-3 Steel classes according to ÖN 4700 (units in N/mm²) [19]

f_{yk} characteristic yield strength
 f_{yd} design yield strength

2.3. Reinforced concrete

Reinforced concrete as a composite material is economic only if concrete and steel are used according to their suitable load bearing capacity, i. e. concrete for compressive and steel for tensile stresses. [10]

The fundamental requirement for the functionality of reinforced concrete is the similar temperature coefficient of steel and concrete. Otherwise any change in temperature would cause different strains and hence stresses in the adhesive region and the bonding between steel and concrete would be destroyed. [11]

The tensile strength of concrete is only about 10% of the compressive strength. In the most cases this small tensile strength is exceeded due to shrinkage and temperature effects. So it is necessary for structural elements that the steel reinforcement takes up tensile forces. In compression elements or in reinforced pressure zones the steel is loaded also in compression.

The bonding between the two materials must not exhibit any slip. This may be guaranteed through a good embedment in the concrete and a suitable surface of the steel. Bars with a ripped surface have a high resistance against pullout of the concrete. [2]

Due to the alkalinity of the cement stone the steel is protected against corrosion, if the concrete cover amounts at least 2 – 3 cm.

Crucial influences on the bond strength are:

- Form of the interlocking
- Concrete strength
- Compaction of the concrete
- Concrete coverage
- Shear stress resp. shear reinforcement
- Steel diameter (small influence)

The resistance against pullout of a steel bar is a consequence of:

- Adhesion between steel and concrete
- Friction due to shrinkage and deflection forces
- Shear resistance of concrete due to mechanical interlocking

The sum of all kinds of resistances is called bond strength. [2] It is assumed in the design of the cross section that there exists no slip between steel and concrete (rigid bond).

Bending moments create tensile stresses in the cross section of a reinforced concrete element. If the tensile stresses lie below the tensile strength of the concrete (state I = uncracked), the theory of strength may be applied. After exceeding the tensile strength cracks will be formed which don't transfer tensile forces (state II =

cracked). The cracked cross section is decisive for the ultimate strength and hence for the design.

In a reinforced concrete structure under service loads the appearance of fine cracks between 0.1 – 0.3 mm width is characteristic, whereas larger crack widths may cause damage. The limitation of crack widths below this limit is achieved by structural measures like:

- Sufficient concrete coverage
- More thin bars are better than less thick bars (ratio surface/volume)
- Small distance between bars

The durability of reinforced concrete elements is reduced drastically by damaged steel reinforcement. To ensure the quality of a building the proof of ultimate strength has to be accomplished by the proof of serviceability and durability, hence different limit states must be proven:

- Ultimate limit state (loss of strength, equilibrium or stability)
- Service limit state (large deformations, vibrations or cracks)

In the standards (e. g. EC 2) the proofs are completed through structural rules. Actually, this combination represents a quality ensure. [12]

2.4. Alternative reinforcement methods

2.4.1. Prestressed concrete

The fact that concrete is very well suitable for compressive stresses but exhibits a poor performance if loaded in tension lead to the idea to reduce or even eliminate tensile stresses in the concrete. This can be achieved through induction of compressive stresses in the tensile zones, so that the superposition of the stresses remains below a limit which may be critical for the durability of the concrete. [13]

The method of prestressing concrete with high strength steels creates a stress state opposite to dead and traffic loads and hence external forces until a certain level don't induce tensile stresses. If the pretension is high enough the concrete remains uncracked and cross sections can be designed for state I.

Time dependent shrinkage and creep of the concrete lead to a shortening of the prestressed structure and of the prestressed steel, too. Therefore the pretension decreases and the compressive zones change into tensile zones. Steels with a low strength are not suited for prestressed concrete because the possible pretension may be compensated by the mentioned losses after 3 – 4 years. Unallowable high stresses and formation of large cracks would be the consequences. This could be observed in the first prestressed concrete structures where the pretension stress was only about 6 kN/cm².

High strength steels allow pretension stresses until 120 kN/cm² and behave actually as springs with large strain at high pretension force, so the relative small shrinkage and creep shortening leads to a small reduction of prestressing force.

It depends on the position of the prestressed steel relatively to the centre of the concrete cross section, whether the pretension creates only compressive or also tensile forces. If the steel is arranged in the core area of the cross section, only compressive stresses arise. In the case that it is below the core area there are induced tensile stresses on the upper side of the beam. [2]

For this purpose different models dependent on demands and loads have been developed:

- Straight pretension elements
- Curved pretension elements

Various methods exist for prestressing concrete:

- Prestressing without cable (used only in exceptional cases, e. g. for short-time measures)
- Pretensioned concrete (the prestressing force is induced in the element through the adhesion between steel and concrete, e. g. pre-fabricated elements)
- Prestressing with subsequent adhesion (after the hardening of the concrete, a specific mortar is pressed between the cables and the surrounding tube)
- Prestressing without subsequent adhesion (the steel is surrounded by a corrosion protective medium and installed with the tube before the casting of the concrete; it is prestressed after the hardening of the concrete)
- External prestressing (s. chap. 2.4.3)

A keyword for the design of prestressed elements is the class or the grade of pretension. Basically three classes are distinguished:

-
- Class I: no tensile stresses exist, cross section remains in state I, probability of cracking is very low
 - Class II: tensile stresses are allowed, cross section remains in state I, probability of cracking is low
 - Class III: tensile stresses are not limited under short time loading, under permanent loading a full or limited pretension is necessary, the cross section changes to state II, probability of cracking is very high.

Dependent on position and arrangement of prestressed elements and their effect on the concrete (cutting force) the following differences arise:

- Centred straight cable course
- Eccentric cable course
- Parabolic cable course
- Several cables
- Buckled course of cable in pretensioned concrete with external prestressing

For prestressed elements a minimum quality of C 25/30 according to Eurocode 2 must be met. Every prestressed member has to be approved, whereas a system may consist of several elements like anchoring body, coupling, jacket tube and prestressing steel. The testing of the prestressing steel regarding guarantee, information and standard values takes place in two different kinds:

- Suitability test before beginning of production
- Quality monitoring during production

In the case that deviations between standard and approval arise only the specifications of the approval are valid!

Nowadays also prestressing elements consisting of carbon fiber reinforced polymer are available, e. g. LEADLINE™ Carbon Fiber Reinforced Plastic Rod from Mitsubishi Chemical Corporation.

Finally, the most important advantages and disadvantages of prestressed concrete compared to RC are summarised:

Advantage:

- Reduction of dead load
- Smaller beam heights for equal span
- Larger spans due to reduced dead load
- Full prestressing enables state I of the concrete and hence water impermeability and special corrosion resistance
- High performance materials can be used more economically
- Bending deflections are reduced

-
- Possibility of further construction methods (cantilevering, timed shifting, ...)

Disadvantages

- Increased costs due to anchoring, jacket tube and wharf shackle
- Danger of stress corrosion cracking of prestressed steel
- Design of structure is more expensive because the time dependent properties of concrete have to be considered
- Prestressed concrete may be economic only for large spans [13]

2.4.2. Fiber concrete

For the production of fiber concrete natural or synthetic fibers of organic or inorganic origin are admixed to the fresh concrete. These are embedded in the hardened cement paste and act as a reinforcement, i. e. they reduce the tension. This reinforcement must not be compared with the standard steel reinforcement, because arrangement and distribution of the fibers don't correlate.

A limitation of crack widths or a division in many fine and hence harmless cracks may be achieved through fibers with a high tensile strength. Orientation and distribution of the fibers during the admixing depend on the process condition like e. g. mixing procedure, so they may be distributed

- homogeneously according to position and orientation
- mainly in one plane with different orientation (e. g. shotcrete)
- homogeneously over the cross-section and oriented uniaxially (e. g. extruded concrete products)

Numerous types of fibers with different properties are available. Dependent on the basic material and processing, fibers can be divided into four groups:

- synthetic organic fibers (aramide-, PE-fiber,...)
- synthetic inorganic fibers (steel-, glass-, carbon-fiber,...)
- natural organic fibers (hemp, jute,...)
- natural inorganic fibers on mineral basis

Candidates of the first two groups are of major importance for the production of fiber composite materials.

Due to the fact that the hardened cement paste matrix under tensile loading exhibits a much lower elongation at rupture than the fiber material, the matrix fails before the fiber reaches the ultimate

strength. Prior to cracking the fibers transfer only a very low amount of tensile forces, whereas the contribution depends on the ratio between ultimate strain of the fibers and concrete. The tensile strength of the fiber can only be utilised if the embedment in the matrix is long and strong enough. Otherwise the bond breaks before the full activation of the fiber itself.

The critical fiber content is defined as the fiber content in vol.-%, which is adequate to fulfil the demands, the minimum length is described by the critical length. The critical fiber content increases if the fibers are oriented inhomogeneously in plane or space instead of in the direction of loading, because only a part of the fibers becomes effective.

Ritter D. [Stahlfaserbeton – Festigkeitsuntersuchungen und Computermodellierungen, Institut für Konstruktiven Ingenieurbau, BOKU Wien, 1999] simulated the distribution and orientation of the fibers. The same problem arises if the length of the fibers lies below the critical length.

Two variants could be determined in the tests:

- case 1: A subcritical fiber length leads to a pullout of the fiber before the tensile strength is reached
- case 2: The fibers are anchored so deep that the tensile strength is decisive and the optimum utilisation is possible

Fiber concrete exhibits the following enhanced properties compared to non-reinforced concrete:

- delayed and controlled cracking
- tough fracture
- increased impact and shock resistance
- decreased crack sensitivity at fast temperature changes

In combination with an additional steel reinforcement, fiber concrete may be used advantageous:

- for dynamic loaded structures (due to seismic actions, explosions, shocks, billows)
- for industrial floors, airport anchorage, bridge coatings,...)
- for thin-walled elements like shells, tanks, folded structures, tubes
- as steel fiber shotcrete in mining and tunnel construction and for rehabilitation of RC and prestressed concrete structures
- as repair mortar for silos, dams, bridges, curtains or elements with high fire resistance

For these briefly listed possibilities shredded fibers, laminae and rods consisting of carbon fibers are utilised [14].

2.4.3. External reinforcement

Basically it has to be distinguished between new buildings and the rehabilitation of structures (especially bridges) with external prestressing. Currently, in Germany and Austria the external prestressing is utilised only for new bridges with caisson cross sections, where the prestressing elements lie outside the concrete in the caisson. Therefore the caisson acts as protection and due to the free access a continuous inspection is possible.

Besides the conventional construction (prestressing elements with adhesion) and the prestressing of exclusively external elements there exists also the so-called mixed construction, whereas a part of the prestressing elements is in adhesion with the concrete and the rest is arranged externally. Dependent on conditions, in the case of rehabilitation of bridges the external prestressing elements are arranged inside or outside the caisson.

The prestressing of bridges with external elements exhibits several advantages compared to conventional prestressed bridges:

- Detection of corrosion damage by visual inspection
- Interchangeability and restrechability of prestressing elements
- Easier concreting of footbridges
- Reduction of weight due to thinner footbridges
- Utilisation of higher prestressing force
- Lower friction losses of external prestressing elements compared to elements with adhesion
- More robust construction through an increased amount of steel
- Only small stress variations act on the prestressed steel, which favours the durability
- Better surface quality of bridge floors due to the absence of air vent tubes

Disadvantages:

- The utilisation of the full static height of cross section is not possible
- Manufacturing of anchorage and deviation elements requires special care and is relatively expensive
- High degree of reinforcement of anchorage elements

-
- Due to the missing adhesion an additional load bearing reserve of the prestressed elements may be activated only conditionally
 - Currently the elements for external pretension are still more expensive than prestressing with adhesion

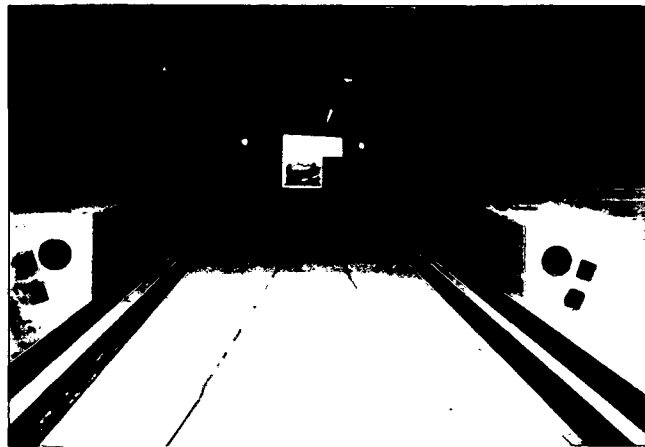
Beside the construction of new bridges with external pretension, in the last years the rehabilitation and strengthening of existing bridges with external prestressing elements gained a major importance. If a reduced load bearing capacity of an existing building is determined, the level of decompression may be increased by an additional external pretension force. As a consequence the durability will be improved and long-term corrosion damage (e. g. cracks in the region of coupling joints) may be avoided.

The external pretension forces are anchored either by existing dead-end and supporting transverse girder or by subsequently casted anchor body which exhibit a high shear strength. It is proven, that this construction technique is controllable and that the durability of structures is enhanced significantly [15].

External reinforcement is not limited to bridge construction, but in the last years also other methods have been developed and utilised in a meaningful way. An example are CFRP-lamellae for the strengthening of timber bridges, RC beams, masonry, silos, floors etc. The development of mesh-type foils made of carbon or glass fibers enabled the strengthening of columns by wrapping. Glass fiber mats found utilisation as geo-textiles.

The lamellae resp. the mesh are glued on the surface or into slots of the structural element by means of epoxy resin. Conditions for a proper functionality are the cleaning of the surface, elimination of surface roughness, observation of climatic conditions and an accurate distribution of the bonding agent and press of the lamellae against the surface. The fire protection represents an additional problem because the resin exhibits a drastic loss of strength at elevated temperatures (see chap. 3.5).

In the following pictures a few possibilities of external reinforcement in bridge construction are shown.



Picture 2.4.3-1 Internal view of the Hünenburg bridge, external prestressing elements VBF-CMM D for timed shifting [30]

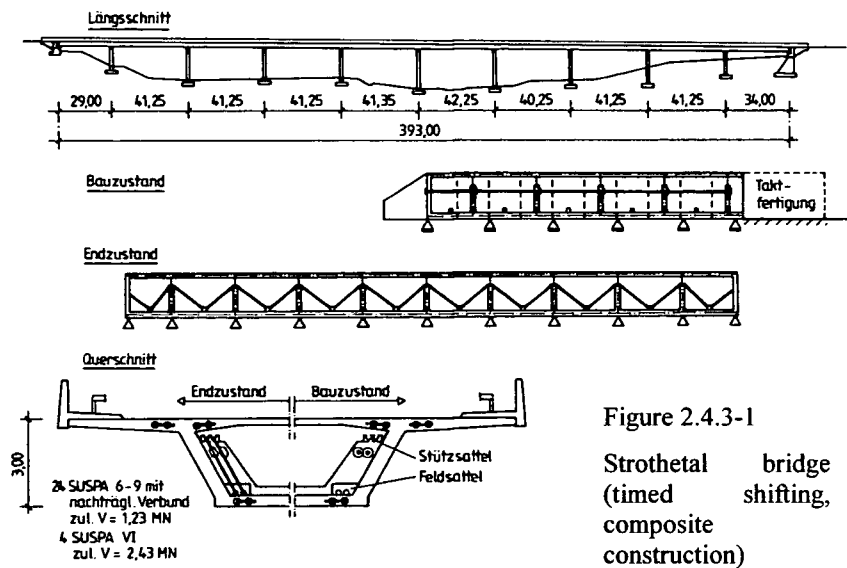


Figure 2.4.3-1

Strothetal bridge (timed shifting, composite construction)



Picture 2.4.3-2 Internal view of Rümmecke bridge (exclusively external prestressing elements)

3. Carbon fibers

3.1. General

Carbon, glass and Aramid laminates count to the category of fiber composite materials that consist of resin with embedded reinforcement fibers. In composite structural elements the fibers are loaded mainly in tension, whereas the resin provides form stability and load transmission between the fibers. Carbon fibers are used as short fibers (length: a few mm), long fibers (rods or laminae) or as textiles.

In aerospace and aeronautical engineering, where high strength and low weight is of crucial importance, fiber composite materials are utilised already since 40 years. After this first successful applications there raised interest also in the automotive industry about the new materials and special products have been developed. During the last decade finally, structural engineers began to use fiber reinforced composites for strengthening measures and in very aggressive environments, where other materials don't exhibit a sufficient resistance [16].

3.2. Manufacturing of CFRP-lamellae

3.2.1. Manufacturing of carbon fibers

Carbon fibers are known already since 1879, as Thomas Alva EDISON produced them from bamboo fibers for his first filament lamp. Nowadays they are manufactured from Polyacrylnitril (PAN) or pitch fibers by thermal degradation (carbonisation). The PAN-fiber usually is the same product which is used for woven cloths, whereas the pitch fiber is a waste product from the petrochemical industry and hence the costs are relatively low.

The original PAN-fiber (precursor) is stretched 2 – 3 times after the extrusion process, washed and stretched again by a factor 15 at 200 – 300°C. In this process several thousand parallel fibers are involved and a strong orientation of the molecule chains in longitudinal direction is yielded. The Young's modulus increases from initially 4000 N/mm² to 15000 N/mm².

The subsequent carbonisation takes place at temperatures of about 1600°C whereas during the pyrolysis all non-carbon elements are eliminated. The resulting yield of carbon fibers amounts about 50%

of the PAN-fiber. Tensile strength and Young's modulus increase continuously during the first step of the carbonisation until 900°C. At the end the Young's modulus reaches about 230000 N/mm² and the strength more than 4000 N/mm².

For a further increase of the Young's modulus of the carbon fiber it is stretched mechanically at 3000°C in argon atmosphere which yields a pronounced band or layer structure with van der Waals binding in transverse and covalent binding in longitudinal fiber direction. Hence carbon fibers are sensitive against mechanical actions in transverse direction. The diameter of the fibers lies between 5 and 8 µm and the amount of carbon is 92 – 99,99%.

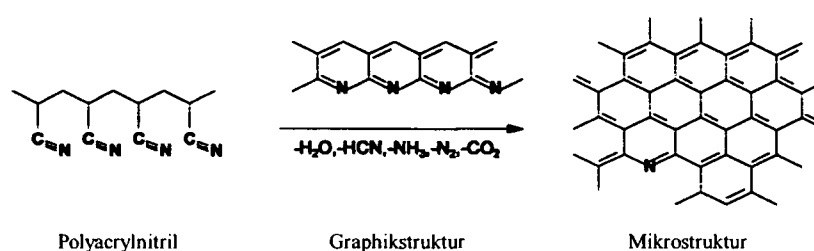


Figure 3.2.1-1 Chemism of manufacturing and microstructure of carbon fibers

Three types of fibers are distinguished:

- N (normal)
- HT (high tenacity)
- HM (high modulus) fibers

The highest achievable strength is currently about 7000 N/mm² and the highest modulus about 900000 N/mm² [17].

For the production of hybrid fibers there are used carbon fibers with different Young's moduli and strength. The fibers with a low Young's modulus but high strain at rupture are prestressed so that the Young's modulus becomes linear in the laminate. This technique enables the manufacturing of cheap carbon fibers with low Young's modulus [18].

S&P Laminate (Hybrid)

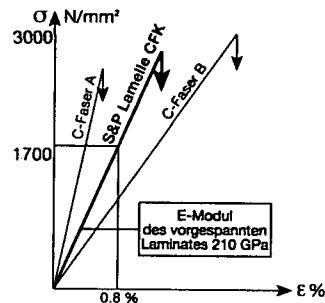


Figure 3.2.1-2 Young's modulus of prestressed hybrid laminate

3.2.2. The pultrusion process

Carbon fibers usually are produced and delivered in the form of roving. Nowadays 1-k until 320-k roving wrapped on coils are available, whereas a 3-k roving for example consists of 3000 single fibers.

CFRP-lamellae are manufactured in the pultrusion process by pulling many dozens of rovings through an impregnation bath, forming to lamellae and subsequent hardening. This method enables the production of quasi-endless unidirectional reinforced profiles with good mechanical properties in longitudinal direction, whereas the transversal mechanical performance depends on the matrix system. The single procedures of a pultrusion equipment are:

- Bringing together the rovings
- Impregnation with liquid matrix material
- Forming and hardening in a heated form
- Post-hardening in hot air stream
- Pull off with rubber crawler
- Roll up and/or cutting equipment

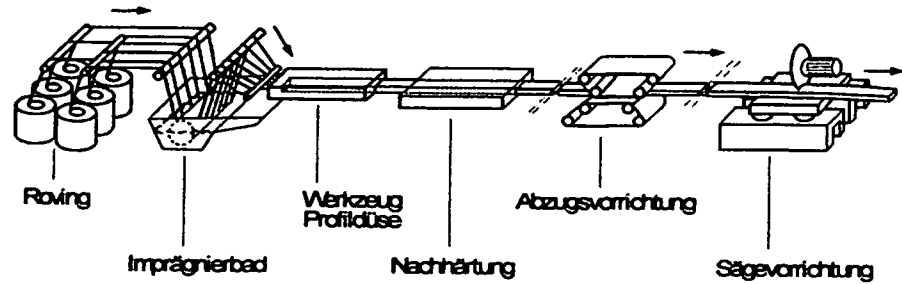


Figure 3.2.2-1 Single procedures of a pultrusion equipment

The density of the most common fibers is between 1.80 and 1.84 g/cm³ and of the epoxy resin matrix exhibits a density between 1.10 and 1.20 g/cm³. The apparent density may be calculated with the mixing rule and amounts about 1.60 g/cm³.

The tensile strength of an unidirectional layer parallel to the fibers may be calculated with sufficient accuracy by means of the mixing rule:

$$\sigma_{longitud,u} = \sigma_{fiber,u} \cdot \phi + \sigma_{matrix,u} \cdot (1 - \phi)$$

Equation 3-1

whereas ϕ means the fiber content per volume.

The elastic properties of an unidirectional layer can be described by four independent basic elasticity parameters which are derived from the Young's modulus of the fiber and the matrix and the fiber content. The so-called technical modulus of elasticity of an unidirectional layer parallel to the fiber is also calculated with the mixing rule:

$$E_{longitud} = E_{fiber} \cdot \phi + E_{matrix} \cdot (1 - \phi)$$

Equation 3-2

The transversal and longitudinal Poisson's ratio can be determined in a similar simple way, Young's modulus transverse to the fibers and the transversal and longitudinal shear modulus may be solved by continuum mechanics.

In the following tables there are listed the main parameters of a lamella with a fiber content of 60% and 70% respectively.

Fiber type	Longitud. tensile strength [Mpa]	Transverse tensile strength [Mpa]	Interlaminar shear strength [Mpa]	Longitud. strain at rupture [%]
High tenacy	2600 -3000	40 - 50	50 - 70	1.8
High modulus	2200 - 2600	30 - 40	40 - 60	0.8

Table 3.2.2-1 Strength values of CFRP-lamellae with 70% fiber content [17]

Fiber type	Longitud. Young's modulus [Mpa]	Transverse Young's modulus [Mpa]	Shear modulus [Mpa]	Poisson's ratio longit./transv.
High tenacy	150000	8000 - 10000	5000 - 6000	0.28
High modulus	300000	7000 - 9000	4000 - 5000	-

Table 3.2.2-2 Technical elasticity parameters of CFRP-lamellae with 70% fiber content [17]

Fiber type	Longit. temp. coeff. [$10^{-6}/^{\circ}\text{C}$]	Transv. temp. coeff. [$10^{-6}/^{\circ}\text{C}$]	Longit. heat conductivity [W/mK]	Transv. heat conductivity [W/mK]
High tenacy	0.3	36	6	0.6
High modulus	-0.7	36	26	1.1

Table 3.2.2-3 Thermal properties of CFRP-lamellae with 60% fiber content [17]

Fiber type	resistance Longitud. [$\Omega\cdot\text{m}$]	resistance transverse [$\Omega\cdot\text{m}$]
High tenacy	$50 \cdot 10^{-6}$	$7.500 \cdot 10^{-6}$
High modulus	$30 \cdot 10^{-6}$	$5.000 \cdot 10^{-6}$

Table 3.2.2-4 Electric resistance of CFRP-lamellae with 60% fiber content [17]

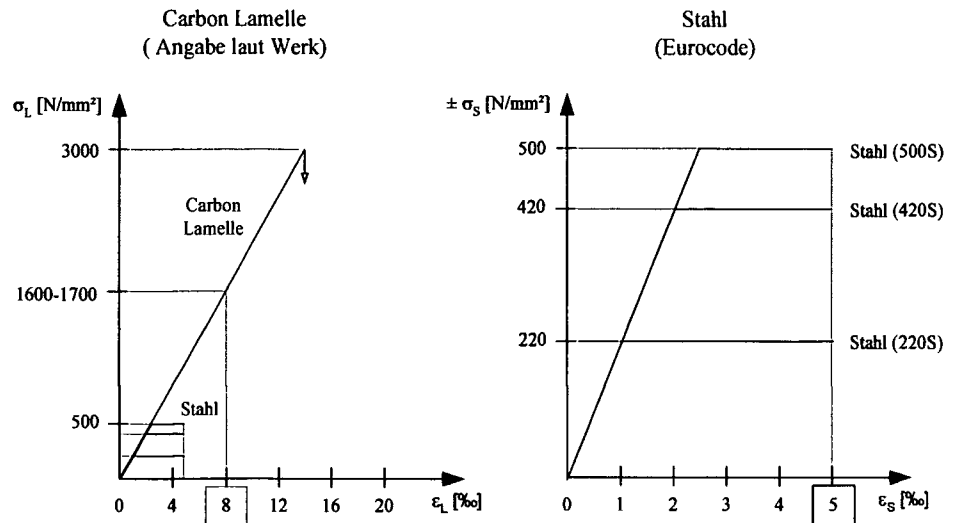


Figure 3.2.2-2 Comparison of Young's moduli of CFRP-lamellae and steel
(Steel = Stahl)

3.2.3. The laying procedure

The laying procedures are characterised by impregnating the textile with resin or by superimposing several resin-textile layers. In this way two-dimensional structures are covered, whereas duroplastics and thermoplastics act as resin. The first cure through a chemical reaction and the latter liquefy at high temperatures and solidify at low temperatures. Unsaturated polyester (UP), epoxy (EP) and vinylester count to the category of duroplastics, whereas polyamide (PA), polycarbonat (PC) and polyoxydemethanol (POM) are thermoplastics. In the following table the principal differences between duroplastics and thermoplastics are listed.

	advantages	disadvantages
duroplastics	High chemical resistance	No possibility of subsequent forming
	Small creeping	
	High temperature resistance	
thermoplastics	Low cycle time at production	Pronounced creeping
	Subsequent forming	

Table 3.2.3-1 Properties of duroplastics and thermoplastics

As adhesives there are utilised solvent-free two-component structural adhesives on the base of epoxy resin with polyamine hardener and eventually quartz powder. The hardening takes place through polyaddition where in fact no by-products originate and almost no shrinkage can be observed.

From the building physics point of view at least 30% of the surface of the structural element should be water vapour permeable. This may be achieved by the use of water vapour permeable adhesives on the base of PU- or acrylate.

3.2.4. Extrusion

This process is suitable for the production of small prefab units. The resin is mixed with short fibers and injected in a form, whereas due to the short cycle time mainly thermoplastics are used.

3.3. Properties of the composite

3.3.1. Creeping and relaxation

Longitudinal creeping and relaxation of unidirectional CFRP-lamellae can be neglected because the stiffness of the lamella is dominated by the carbon fibers. In transversal direction the lamellae are sensitive like plastics due to the dominant behaviour of the epoxy matrix.

3.3.2. Fatigue behaviour

CFRP-lamellae exhibit an excellent fatigue behaviour in longitudinal direction. Unlike steel they are insensitive to friction fatigue which is important for the bridging of cracks under cyclic actions. In the most cases the fatigue behaviour of the base material (timber, concrete, aluminium, steel) or of the adhesive may be critical.

3.3.3. Durability

According to the current experience you may suppose that CFRP products are long term stable under the chemical environment which is typical for structural engineering. The epoxy matrix may become critical before the carbon fibers.

3.3.4. Electric and thermal properties, lightning stroke hazard

Like the mechanical properties also the electric and thermal properties of CFRP-lamellae are extremely orthotropic. Also the fiber itself exhibits an anisotropic behaviour: in longitudinal direction heat and electricity are conducted, whereas in transverse direction it behaves like an isolator.

Due to the fact that CFRP-lamellae don't act as electric isolators in longitudinal direction, but on the other side they are not good conductor, in case of a lightning stroke the lamellae could be damaged. The temperature of the fibers may exceed 400°C and burn the epoxy matrix, so the forces between the fibers cannot be transmitted any more.

In the most cases the lightning stroke hazard does not exist because the lamellae are protected inside of buildings or bridges (caisson). Should they be applied on masts or curtains, protection measures have to be performed. [17]

In the following list the advantages and disadvantages of strengthening measures with carbon fibers are listed.

- High, controllable tensile strength and stiffness (dependent on fiber type)
- High Young's modulus
- Creeping in longitudinal direction negligible
- Excellent fatigue behaviour
- Chemical resistance against acids, alkalis and solvents
- Temperature resistant
- Corrosion resistant
- Low density
- Resistant against short and long term actions
- Antimagnetic
- Flexible application (textiles can be formed arbitrarily)
- No location of joints at large spans

Disadvantages:

- Electric and thermal conductivity in longitudinal direction
- Isolator in transverse direction
- Allowable strain until 2% (leads to large deflection of beams and slabs)
- High price
- Low strain at fracture (brittleness)
- Necessary fire protection
- Protection against UV-light

3.4. Types and applications

3.4.1. Prefabricated CFRP-lamellae

Lamellae are delivered on rolls with a thickness of 1 – 2 mm, 50 – 300 mm width and 250 m length. Due to their small strain lamellae are suitable to increase the stiffness of a structural member, whereas textiles are utilized typically to increase the ductility. In the case of structural rehabilitation, the aim is usually to limit crack widths and depths by exploiting small strains or by prestressing. The allowable strain should not exceed 0.6 – 0.8 %, because large cracks would favor the decoupling of the lamella. [20, 21]

In the following figure the decoupling due to excessive shear loading is shown schematically.

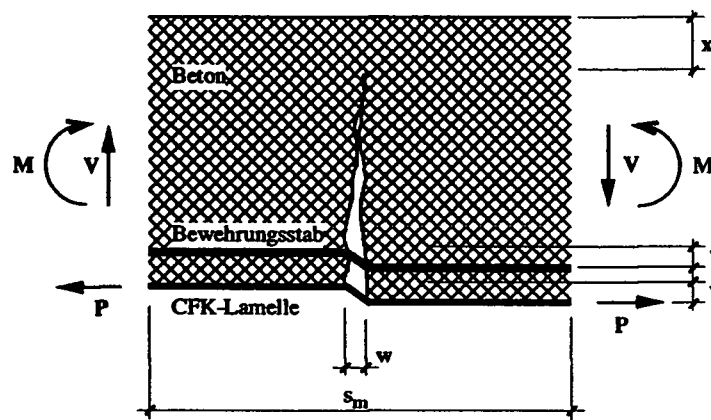


Figure 3.4.1-1 Shift in a bending crack due to large shear stress [22]

M	bending moment
V	shear load
v	shift
w	crack width
w_{crit}	critical crack width (if exceeded, no load transfer is possible)
x	neutral axis
s_m	average crack distance
Beton	concrete
Bewehrungsstab	reinforcement

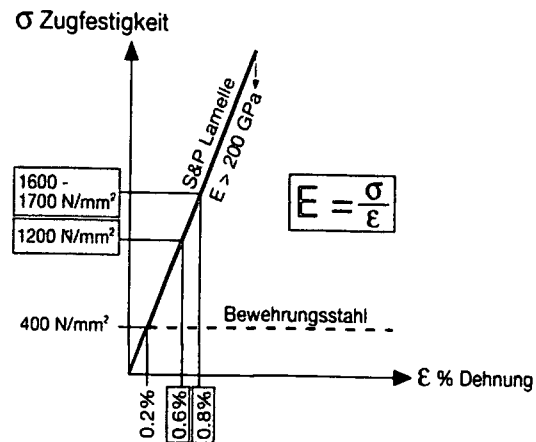


Figure 3.4.1-2 Tensile strength of the CFRP-lamella for design [18]

3.4.2. CFRP-cable

CFRP prestressing cables are usable principally like prestressed steel for pretension with or without adhesion of structural concrete. The main difference consists in the different operating lines and hence in the different behaviour for tensile loading. Steel exhibits nearly a linear elastic – ideal plastic material behaviour, whereas carbon fibers show a linear elastic behaviour until rupture. The consequence is a reduced ductility of an element which is prestressed with CFRP cables. A higher ductility may be achieved by the use of additional conventional reinforcement.

Connecting CFRP wires with a diameter of 5 mm to parallel bundles may have future potential. The fiber volume content of the cable varies between 68 – 72% and a cable with 241 strands reaches a load capacity of 12000 kN. A CFRP cable with the same load capacity as a steel cable weighs only 1/8. Especially for large spans, the low weight leads to a larger equivalent Young's modulus as it can be seen from the following table. [16]

horizontale range [m]	Relative equivalent E-modulus [Gpa]	
	Steel	CFK-cabel
5	210	165
500	196	165
1000	163	163
1500	128	162
2000	98	159

Table 3.4.2-1 Relative equivalent Young's modulus

Already in 1991 on the factory area of BASF in Ludwigshafen there were used 4 additional prestressed bundles each consisting of 19 CFRP-strands for a large prestressed concrete bridge. Since 1994 at the EMPA in Zürich reliable prestressing systems have been developed so that a general application may be suggested. [25, 26, 27]

According to the following figure the maximum stress of the CFRP-cable is about 2500 N/mm² at a strain of 1.6% and the Young's modulus 150000 N/mm². The steel strands exhibit a higher modulus of elasticity and strain (200000 N/mm² resp. 5%).

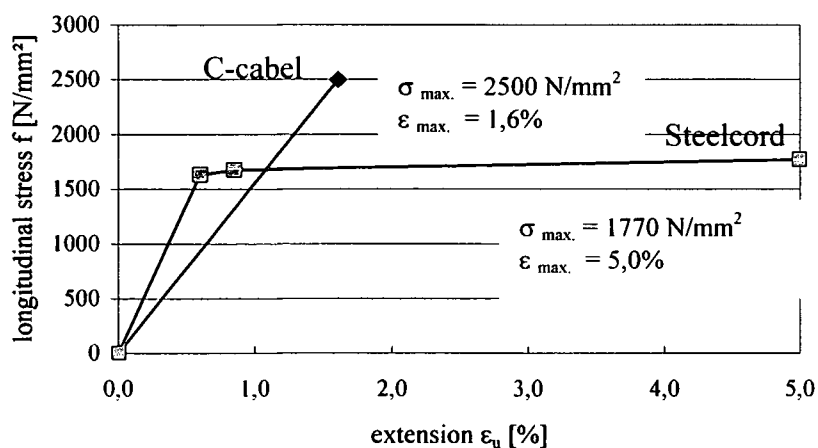


Figure 3.4.2-1 Operating line of prestressed steel and CFRP cable

3.4.3. CFRP strengthened concrete

Fiber concrete will be used for a broad application range in the future. Steel, glass, hemp and carbon fibers have the advantage of high strength and stiffness and high resistance against corrosion also in carbonized regions.

3.4.4. CFRP textiles

The fibers are braided in both directions, so a bi-directional fiber mesh with a fiber content of about 10 – 20% originates. Due to the waved arrangement of the fibers resulting from the weaving process at first they are drawn straight-lined under tensile forces and hence larger strains arise. There are used glass fibers in both directions or carbon fibers in one and glass fibers in the other direction. Dependent on surrounding conditions alkali-proof (AR) glass or non-treated E-glass is used, because uncoated glass is corrosion sensitive in alkaline medium.

3.4.5. CFRP-foils

CFRP-foils are 0.15 - 0.45 mm thin single- or multi-layered foils consisting of unidirectional arranged and totally stretched carbon fibers with 2 – 3% glass fibers in transverse direction for fixing purposes. The content of carbon fibers usually lies between 20 and 50%. Arrangement of the fibers in the loading direction leads to highest stiffness and strength.

For a load transfer to the steel reinforcement in a RC element rupture of the tensile zone is necessary. The strain of the foil is hereby decisive for the limitation of crack widths and depths. However, a too large strain of the foil may induce a shift of the shear crack and hence a decoupling of the foil.

The strengthening effect of CFRP-foils depends primarily on the properties of the fibers. The influence of the resin matrix on the load capacity may be neglected. Hence the theoretical fiber cross-section and not the values of the composite is decisive for the design of C-foils. If the theoretical fiber thickness is unknown, it can be calculated as the ratio between weight and density of the carbon fiber:

$$S = \frac{m_{\text{C-Faser}}}{\rho_{\text{C-Faser}}}$$

Equation 3-3

In the case that the fibers are laminated by hand on building site it is recommendable to diminish the fiber properties by a factor 1.2, because various influences like damage of the fibers during rolling or non optimal arrangement of the fibers may lead to a reduced load capacity. [23]

For lamellae always the total cross-section is decisive because the fiber content is known more accurately.

3.4.6. Carbon fiber composites

Young's modulus and tensile strength of carbon fiber composites may be presumed to be log-normal distributed with a coefficient of variation of about 5%. [19]

Besides the carbon fibers, the aramide fiber (known under the brand mark Kevlar) is widely used for composite materials with low weight and high toughness. Critical is the loss of strength under ionizing radiation e. g. solar light. [16]

In the following tables resp. diagram the carbon and glass fiber composite materials are summarized and the operating line is shown.

	fibrous-direction	fibrous-order	E-modulus [N/mm ²]	f _t [N/mm ²]	ε _u [%]	fibrous-content	f _{ct} [N/mm ²]
foil (lying): C-fibrous	uni - opposite	stretch	240.000	4.800	2,0	20-50%	>1,0
			400.000	3.200	0,8		
			600.000	2.400	0,4		
tissue G-fibrous	bi - opposite	≈≈≈ wavy	70.000	>1.700	2,5	10-30% as direction	>0,5
Lamellae C-fibrous	uni - opposite	stretch	150.000	>2.500	1,7	ca.70%	>1,5
			200.000	>2.500	1,3	ca.70%	>1,5
cabel C-fibrous	uni - opposite		200.000	>2.500	1,3	ca.70%	

Table 3.4.6-1 Overview of carbon and glass fiber composite materials

<i>BSI 550</i>	comparison: Isotrop	210.000	$(f_t / f_y) > 1,08$ $f_{t,k} > 594$	$\epsilon_{uk} >$ 5%	$\alpha_{t,CFK} \approx 0 \text{ K}^{-1}$ $\alpha_{t,Stahl} = ,2E^{-5} \text{ K}^{-1}$
----------------	---------------------	---------	---	-------------------------	---

Table 3.4.6-2 For comparison: structural steel

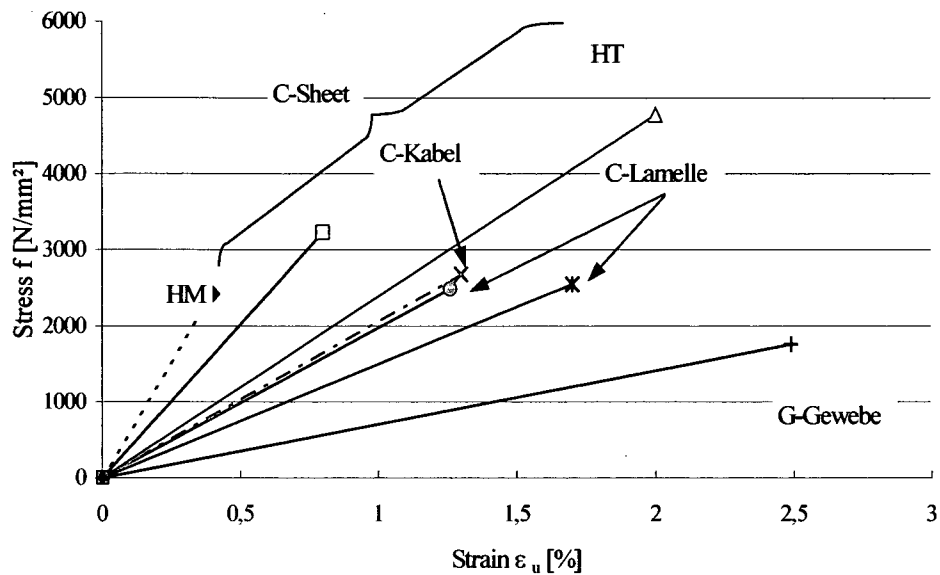
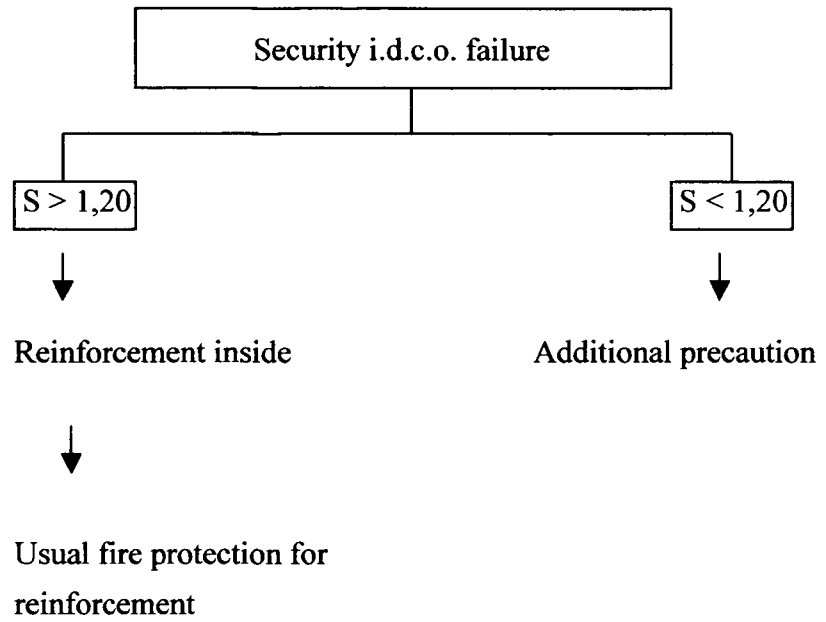


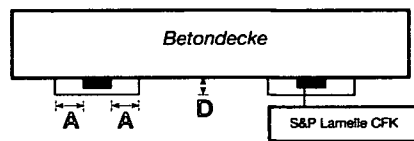
Figure 3.4.6-1 Operating line of composite materials

3.5. Fire protection

If strengthening measures with steel or CFRP-lamellae are performed it has to be considered that the adhesives are resistant only until 60 – 80°C. In the case of fire the epoxy matrix would burn and the lamellae decouple from the surface. Hence the lamellae must be protected by fire protecting measures. An example is given in the next figure.



Beispiel: Brandschutzplatten



The Security in the case of failure S of the lamella S gives information, what kind of prevention must be used.

Feuerwiderstand	A = 100 mm (D)	A = 200 mm (D)
F 30	2 x 20 mm	2 x 20 mm
F 60	2 x 40 mm	2 x 30 mm
F 90	> 110 mm	2 x 40 mm
F 120	> 110 mm	> 110 mm

Figure 3.5-1 Fire protection measures [18]

3.6. Safety concept

For a subsequently strengthened structure the following dangers and uncertainties have to be considered:

- Uncontrolled planning, construction and operation
- Dashing vehicles, falling bodies
- Climatic stresses
- Impairment dependent on time and loading history
- Omissions and misactions
- Mistakes during planning, construction and operation

Hence the strengthening may fail during operation, but the resulting damage must be assessable so that the risk can be minimized. For this reason a subsequently strengthened structure should exhibit a global safety factor > 1.0 after failure of the strengthening element and under specified operation. [24]

The missing plastic deformation capacity of CFRP-lamellae must be considered for design because else the load capacity may be overestimated. If shear in the tensile zone is decisive an increased global safety factor should be used, e. g. $\gamma = 2.1$ (rupture without warning) according to the DIN standard.

Bending failure of a conventional RC structure generally takes place after large deformations and wide opened cracks. By embedding single fiber ropes with lower strain at rupture the failure of lamella may be pre-warned acoustically and visually. Deformations and cracks must be kept limited and hence state II should not be exceeded.

Physical adhesion forces originate from molecular interaction between adhesive and the materials which have to be connected. This forces depend on type of molecules and distance between themselves and are negatively influenced by dirt, dust and fat. Therefore an accurate treatment of the surfaces is of crucial importance.

The concrete surface must resist the shear and tensile stresses induced by the CFRP. Due to the fact that the cohesion forces in the adhesive and the adhesion forces between CFRP-lamella and adhesive resp. adhesive and concrete are 2 – 3 times higher than the surface tensile strength of the concrete, it must be proofed by tests that the surface tensile strength of the concrete does not remain under 1.5 N/mm^2 . The concrete should exhibit a minimum age of 6 weeks. If the surface tensile strength of the concrete is less than 1.5

N/mm², strengthening of a structure with glued reinforcement is **not recommendable**. [23]

3.7. Quality assurance

To assure the calculated resistance and the accurate application of composite materials, all process and application steps must be supervised continuously. The quality of the workmanship is controlled through internal and external supervision, whereas the first consists of testing the:

- surface tensile strength of the concrete resp. leveling mortar
- adhesion of the primer on CFRP-lamellae
- hardening of the adhesive
- even surface of glued lamellae
- record and check of surrounding conditions during gluing work

In the case of complicated strengthening measures additional CFRP-lamellae are glued and tested in the pull – off test where the adhesive pull strength is measured and the type of failure can be observed. **After hardening of the adhesive the pull – off test must yield concrete failure.**

The internal supervision is controlled by the external supervision. Additionally, the unevenness of the CFRP-lamellae and the existence of voids in the adhesive (by tapping) must be checked in order to avoid a premature decoupling. It must be assured that the application is performed by qualified and supervised staff.

4. Material description and fabrication

This chapter describes the fabrication of reinforcement meshes based on carbon fiber lamellae as well as their use and application. Furthermore the construction of the formwork, the concrete mixture used, the concreting itself, and storage of the finished slabs is documented and illustrated by means of pictures, tables and graphs.

4.1. Material description

4.1.1. Fabrication of meshes based on carbon fiber lamellae

The material used for the fabrication of the meshes was provided by the company Isosport, located in Eisenstadt. The dimensions of the carbon fiber lamellae are: 2.00 m long, 8 cm wide and 1.40 mm thick.

Two types of lamellae were available:

Lamella type 1: C150/2000
Lamella type 2: C200/2000

These two types are mainly used in the sports industry for products such as rackets, ski linings etc. Lamella type 2 – C200/2000 was used for the preparation of the mesh. The fiber content of the lamella amounts 70 % and the fibers are aligned in parallel resulting in a Young's modulus of more than 200,000 N/mm². In order to obtain the desired slab dimensions of l/w/h = 180/40/10 cm the lamellae had to be further prepared and cut to size.

The final lamellae had a length of 180 cm, a thickness of 1.40 mm and a width of 10 mm.

The lamellae used as cross elements to improve the stiffness of the mesh have been cut to a length of 40 cm. The longitudinal and cross lamellae have then been woven in such a way to ensure optimal stiffness of the mesh. Three series of specimens have been fabricated, each consisting of 2 slabs.

For the first series 2 meshes have been deployed for each slab, whereas for the second series only 1 mesh per slab was used.

Regarding the third series one slab using a CQS 6 steel mesh and another slab using a CQS 8 steel mesh have been prepared and were subjected to a bending test to obtain reference values.

It was shown that plaiting the carbon lamellae instead of gluing them was sufficient enough to obtain a reasonable stiffness of the mesh. The following listing shows the advantages resulting from this fabrication technique:

- Easy fabrication – little physical effort
- Plaiting is not very time consuming
- High stiffness of mesh according to grid spacing
- Easy handling due to little weight
- Easy installation of mesh into formwork
- Less reinforcement needed compared to steel fabrics

The carbon fiber meshes have been mounted without any further preparatory treatment, however the method of production results in a smooth and a rough side of the material.

On one hand this difference in roughness has not been accounted for in the bending tests but on the other hand also pull out test have been conducted to analyze the influence of different surface roughness (see also Chapter 6: “Pull out tests”).



The picture on the left side shows the base material used for fabrication of the meshes. The lamellae delivered were 200 cm long, 8 cm wide and 0.14 cm thick. Also the shorter cross elements are shown (marked in red).

Picture 4.1.1-1 Base material for production of CFRP-sheets

The sketch below outlines the different mesh arrangements used for the specimen series 1 and 2, in the way they have been embedded

in concrete. Further important parameters are summarized in the table beneath.

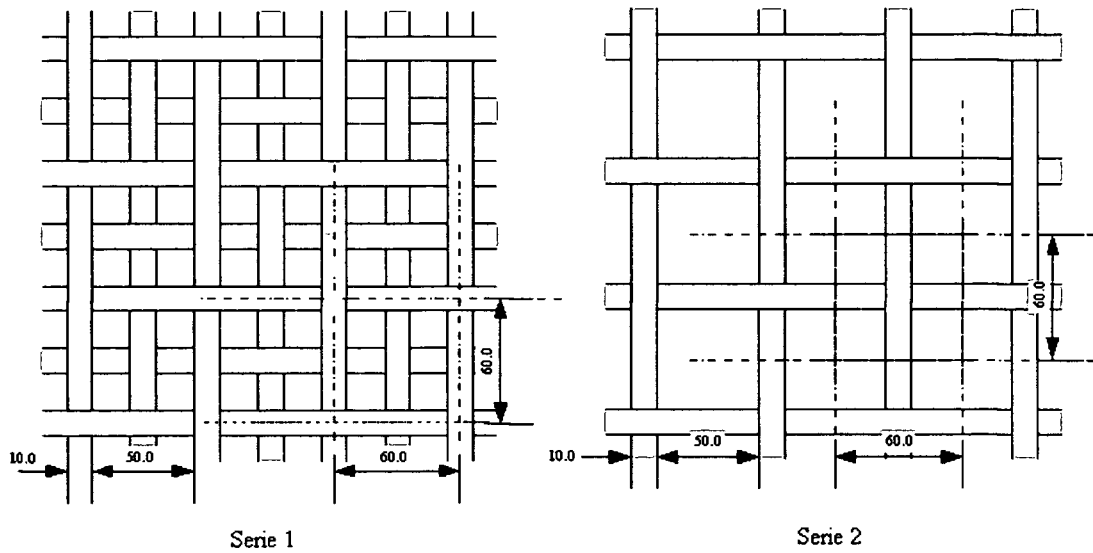


Figure: 4.1.1-1 Sheets of series 1 and 2

series		1	2	3	4
deskription	—	CFK	CFK	steelmatt	steelmatt
longitudinal grid	[cm]	1	1	CQS 8	CQS 6
transversal grid	[cm]	1	1	CQS 8	CQS 6
grid size	[cm*cm]	ca.6*6	ca.6*6	15*15	15*15
number of matt	—	2	1	1	1
rough top side	—	rough	rough	ripped	ripped
and lower side	—	smooth	smooth	ripped	ripped
measure of matt	[kg]	0,55	0,55	3,881	2,254
armor account at longitudinal departure	[Vol.-%]	0,385	0,21	0,377	0,283
salb number	—	1 bis 2	3 bis 4	5	6

Table 4.1.1-1 Dimensions of CFRP-sheets and reference slabs

4.1.2. Concrete mixture

Aim of the concrete mixture is to ensure a minimum strength of B300 or B30, according to EC2 this notation corresponds to a concrete strength of C25/30. The materials used for the mixture are listed in the table below.

Concrete composition		
cement species	PZ 475	5,00 g/cm ³
addition	0/4	2,70 g/cm ³
W/Z-account	0,6	1,80 g/cm ³
flow medium	Profluid AX	0,20 kg

Table 4.1.2-1 Composition of concrete

The table on top of it does not only list the materials used but also gives information on the amounts of each component, which however will be subject to change – more details will be given in Chapter 4.1.3.

4.1.3. Aggregates

Sand with a maximum grain size of 4 mm was used as aggregate. The sand was stored outside and was covered with plastic to protect it from weathering.

During sieving the humid weight of the aggregate amounted 2037 g. The weight when dried was 2021 g, thus the inherent humidity amounts to 0.80 %. Furthermore the aggregates do not contain any organic contaminations.

Thus the sample has an original weight of 2021 g – weight when dried.

Results of the sieving process are depicted in the next graph and summarized in the following table.

grain size in [mm]	0,063	0,125	0,25	0,5	1	2	4	8	11
initial weight 2021 in g	1989	1935	1645	1247	984	681	113	2	0
backwardness in %	98,4	95,7	81,4	61,7	48,7	33,7	5,6	0,1	0
passage in %	1,6	4,3	18,6	38,3	51,3	66,3	94,4	99,9	100

Table 4.1.3-1 Values of dry grading curve

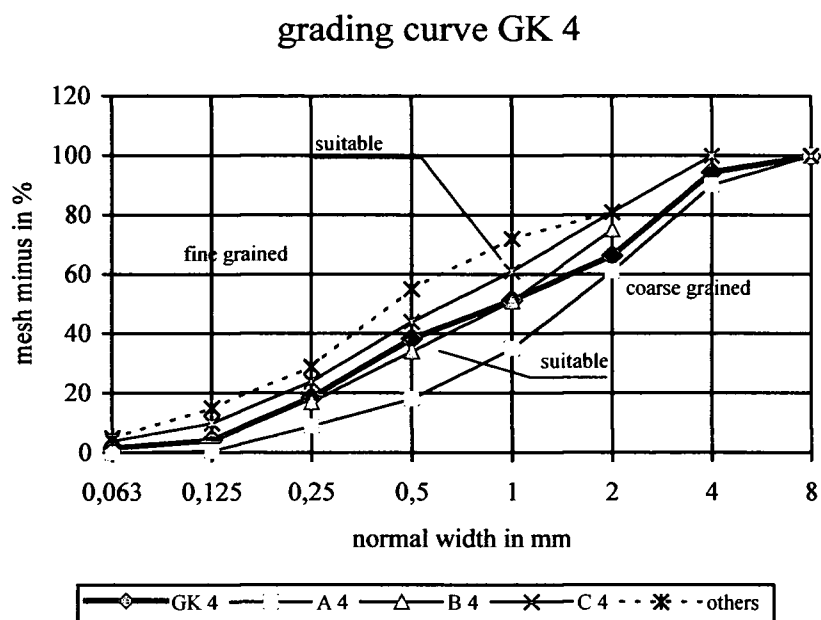


Figure 4.1.3-1 Single grading curve for maximum grain size 4

The next figure shows the grain size distribution with a maximum grain size of 4 mm. The sections A, B, and C, as well as the extended section are missing. The sections A and C are also called the limiting grading curves, i.e. section A mainly contains coarse grains and only few fine grains to provide a dense packing, whereas in section C fine and very fine grains are dominant resulting in a disadvantage for processing (more cement paste will be needed). The optimum grain size distribution is represented by section B, or should be at least above this section. [1]

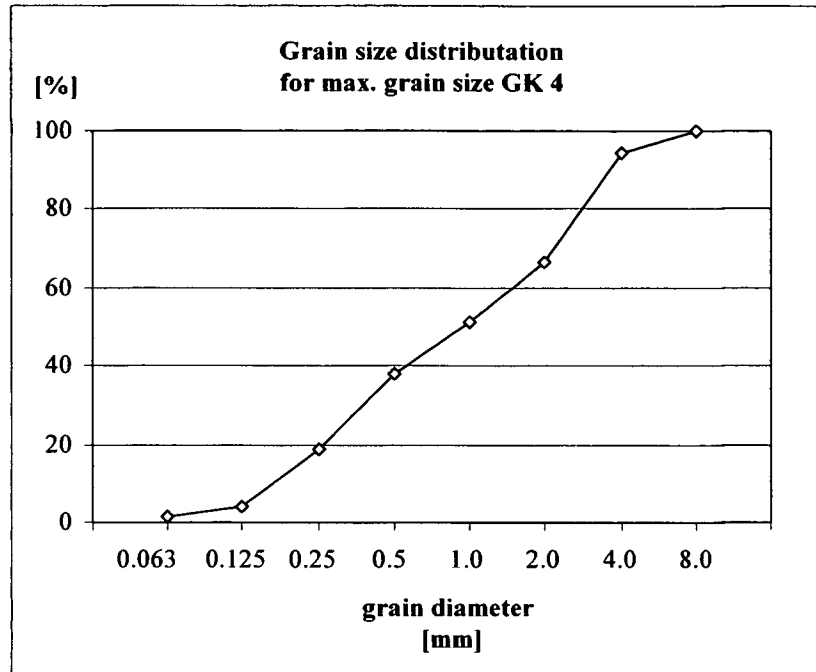


Figure 4.1.3-2 Grain size distribution for maximum grain size 4

4.1.4. Moisture test of aggregate

The desired concrete has a minimum strength of class B 30 / B 300, a water-cement ratio of 0.6, and a consistence of K3 (high-slump concrete).

In order to achieve these properties, it is essential to measure the moisture content of the aggregate and if necessary alter the mixture ratio for the concrete. The total amount of water needed depends not only on the desired degree of consistence, but also on how the concrete will be compacted and on the type of aggregate and its grain composition.

The following outlines the steps conducted to determine the water content of the aggregate:

Two samples were taken from the sand kept in the open – but covered - , one from the surface and one from the inner of the sand heap. Each sample had a weight of 5.00 kg and was then placed into a tin bowl with a weight of 6.60 kg adding up to a total weight of 11.60 kg. The wet sample was then covered by pouring spirit and ignited. To ensure optimum drying the sample was thoroughly mixed with a steel lance during the burn off. After a short cooling time the sample was weighted again and a reduced weight of 4.8 kg was measured. A reduction in weight by 0.20 kg corresponds to an

initial moisture content of 4 % for the aggregate. The same values were found for both samples.

Thus a different amount of water will be needed to obtain a water-cement ratio of 0.60. The following tables show the original and altered concrete recipe for a slab with dimensions $l/w/t = 180/40/10$ cm, hence a volume of $V = 0.072 \text{ m}^3$, and a weight of 180 kg when assuming a density for reinforced concrete of $G = 2,500 \text{ kg/m}^3$. The amount of solvent needed was calculated based on the cement content.

original concrete composition, W/Z - account with 0,60			
	[kg]	[Gew.-%]	[Vol.-%]
cement amount	25,72	14,29	9,62
addition amount	138,65	77,03	73,74
water amount	15,43	8,57	16,37
flow medium	0,2	0,111	0,27
total:	180kg	100%	100%

Table 4.1.4-1 Concrete composition in weight and volume percent

Given a weight difference of 0.20 kg, which corresponds to a moisture content of 4 % for the aggregate, a correction value for the amount of water and aggregate was determined and new values were calculated. The updated amounts are listed in the next table.

Based on these corrected values a concrete with the desired properties can now be prepared and used.

trim concrete composition, W/Z - account with 0,60			
	[kg]	[Gew.-%]	[Vol.-%]
cement amount	25,72	14,29	9,62
addition amount	144,2	80,11	78,16
water amount	9,88	5,49	11,95
flow medium	0,2	0,111	0,27
total:	180kg	100%	100%

Table 4.1.4-2 Corrected concrete composition in weight and volume percent

4.2. Comparison with a SCC

The abbreviation SCC stands for “Self Compacting Concrete”. This type of concrete has already been broadly applied in Japan between 1980 and 1990. The major advantage of this product, as already its name states, is the ability to self compact merely by its own weight without the need of any additional vibration tools. The consistence of this concrete is far above K 5 i.e. has a slump of more than 60 cm.

During the last decades the use of self compacting concrete for manufacturing of precast concrete elements but also for ready-mixed as well as site-mixed concrete has increased in Europe.

The new generation of highly efficient solvents allow to prepare concrete at very small water-cement ratios ($W/C < 0.40$) with only little dosage and additionally do not delay the build up of strength. These new liquefiers are based on a modified Phenoxy resin and may be combined with other products such as air-entraining agents, micro silica, blast furnace slag, and fly ash.

With addition of the new liquefiers it was possible to substantially decrease water consumption, thereby introducing the positive side-effect of reduced capillary porosity.

This results in a higher quality concrete with increased durability due to reduced ingress of harmful substances – and if necessary also providing increased tightness. Similarly have the properties of the hardened concrete such as strength, deflection behaviour, and shrinking been improved.

Due to its self compacting ability, this type of concrete is ideally suited for the fabrication of slender structural members with a high degree of reinforcement. There is no danger of demixing while feeding the concrete into the formwork. Perfect results for exposed concrete surfaces can be realized easily. [28]

The major disadvantage of SCC can be found in its increased production costs, however when compared to conventional concrete a decrease in expenditure for vibration tools and thus man hours is achieved.

A dissertation dealing with the combination of SCC and carbon fiber reinforcement meshes is already available. In the following an excerpt of this work will be given. Table 4.2-1 shows the concrete recipe used and figure 4.2-1 and 4.2-2 represent grading curves of the aggregates employed.

used material		[Gew.-%]	[Vol.-%]
water	----	8,43	20,14
cement	EHZ 275	19,15	15,26
grain size	0/4	50,47	44,49
gain size	4/16	21,63	19,15
flow medium	----	0,32	0,76

Table 4.2-1 Composition of SCC [29]

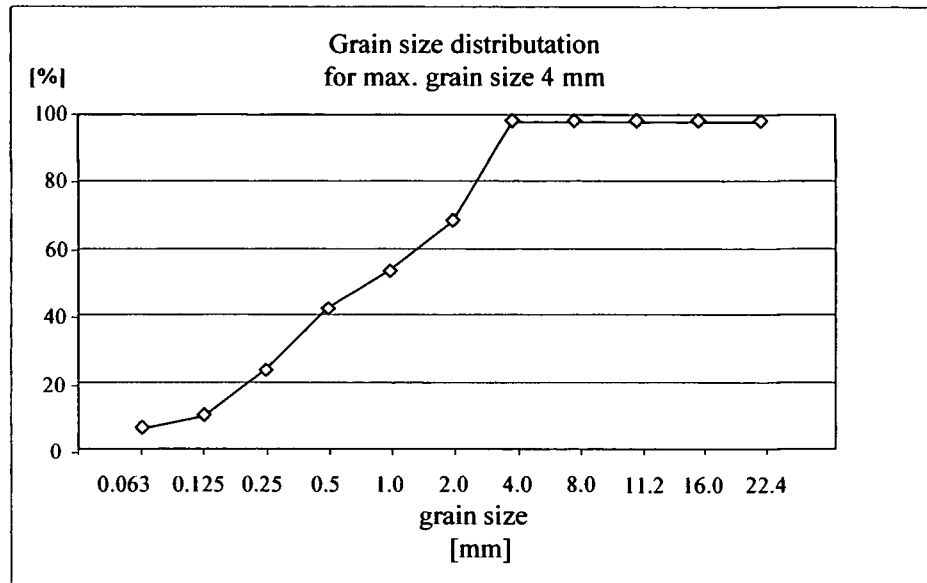


Figure 4.2-1 Grain size distribution for SCC with maximum grain 4

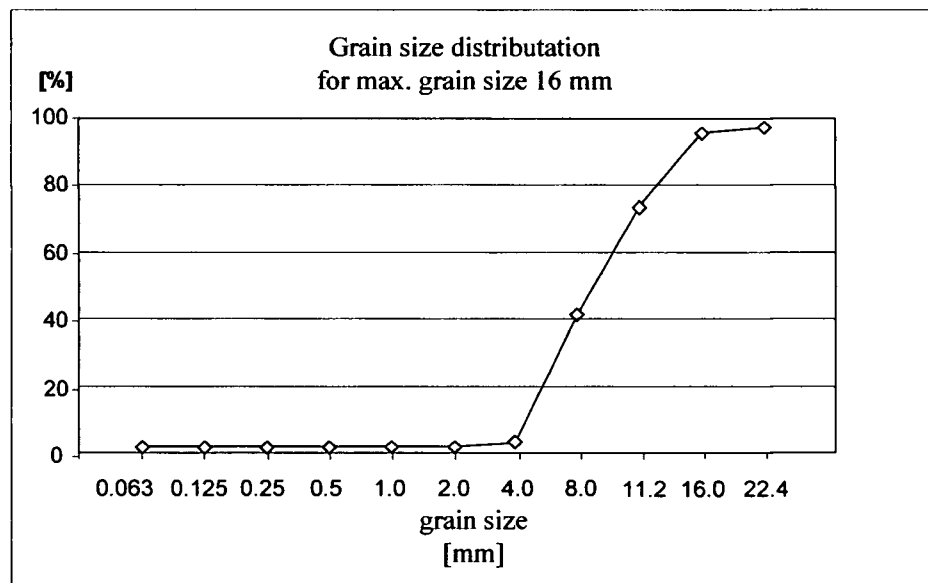


Figure 4.2-2 Grain size distribution for SCC with maximum grain 16

In order to obtain a statement of quality for the SCC – three prisms with dimensions of 100*100*400 mm and three cubes with dimensions of 150*150*150 mm were produced using base concrete. All specimens were stored for 28 days at a constant temperature of 20° C, and then subjected to a bending tensile test as well as a compression test. [29]

series Nr.	cement type	consistency	W/Z - account	grain [mm]	tensile bending- tightness [N/mm ²]	pressure- tightness [N/mm ²]	measure [kg/m ³]
—	—	—	—				
1-3	normal	K 3	0,61	4	4,30	38,10	2291
4-6	SCC	K 5	0,55	16	3,70	42,70	2240
7-9	SCC	K 5	0,55	16	5,00	47,80	2213
10-12	SCC	K 5	0,55	16	6,10	51,50	2248

Table 4.2-2 result of analyses about zero concrete [29]

4.3. Preparation

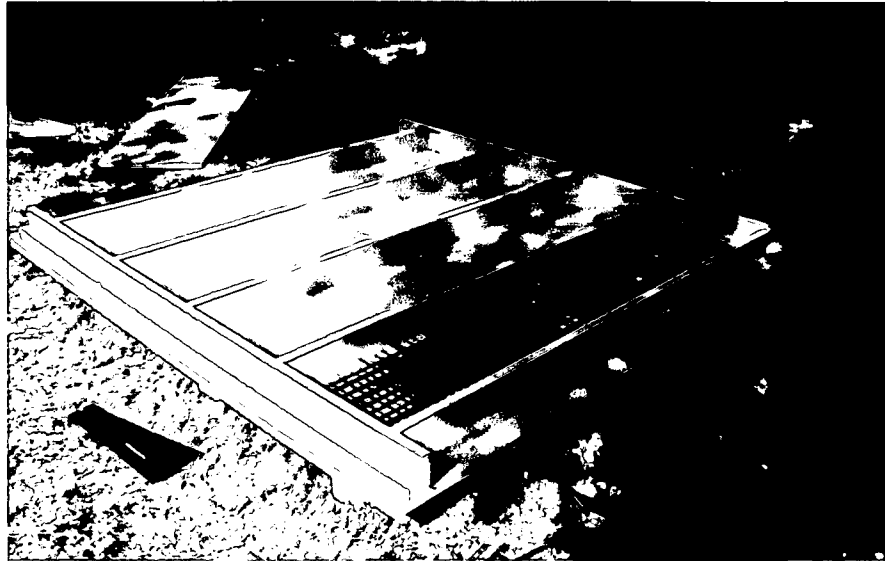
4.3.1. Preparation of formwork

The preparation of the form work was carried out at the campus of the University of Applied Sciences. The shuttering panels have been provided at no charge by courtesy of the company DOKA. The conceptual model of the formwork allowed to place 4 slabs with dimensions of l/w/t = 180/40/10 next to each other.

After completion of the formwork all joints and gaps were sealed with transparent Silicone, since the aggregate has a particle size range of 0/4 mm and is thus relatively fine. Before concreting the bottom and lateral walls were coated with forming oil. This helps to avoid sticking of the concrete and will ease the dismantling of the formwork.

Picture 4.3.1-1 shows the finished formwork and Picture 4.3.1-2 shows the sealing of the joints with Silicone.

Furthermore the formwork was supported by simple timber bearings to allow for easy transportation by a stacker truck to different work places. Additionally it was possible to easily adjust the horizontal alignment of the construction for concreting.



Picture 4.3.1-1 Finished formwork with sheet reinforcement



There are two reasons for sealing the joints:

- Avoid ingress of fine grains and laitance beneath the side elements and thus avoidance of elevation during hydration
- Reuse of the formwork – since it will be needed for further series

Picture 4.3.1-2 Sealing of joints

The above figure also illustrates the use of spacers between the side walls which have been removed later during concreting. The battens mounted on top of the formwork should avoid distortion of the side walls while concreting.

4.3.2. Concrete – preparation and casting

The type of aggregates and solvent used as well as the corrected values of the concrete mixture have already been presented in Chapter 4.1.4.

The concrete was prepared strictly according to the recipe using a gravity mixer. Before pouring the concrete into the formwork several samples have been taken in order to conduct a slump test.

To determine the consistence of the concrete a so called slump table is needed, which is standardized as follows:

- 21 mm plastic bonded surface refined plywood panel with a 2 mm sheet metal cover with a centered cross groove
- table dimensions: 70*70 cm
- 20 mm thick angle cleats to stiffen the corners of the supporting frame
- a back square to limit lift height at 40 ± 1 mm, and a footboard
- hinge and lifting handle
- a truncated pouring gate made of sheet metal
- 4*4 cm timber tamper

At first the surface of the slump table and the inside of the pouring gate have to be wetted. Next the pouring gate is positioned at the table center and fixed by stepping on the salient holding bars. The concrete has to be poured into the hopper as 2 layers of equal height and each of them will be compacted by 10 tamper strokes. Eventually the top will be drawn off and the table cleaned thoroughly.

Thirty seconds after filling the hopper it will be lifted vertically. Next the slump table will be lifted and dropped repeatedly by moving the lifting handle 15 times at an interval of 2 seconds until the limit stop at 4 cm height without jerk or shock. This should ensure that the mixture spreads out uniformly on the table building a slump body. In case the slump body is not uniform no measurements shall be taken and the test needs to be repeated.

The diameter of the slump body is obtained by taking the average of 2 measurements in the directions parallel to the lateral edges of the table. The slump test has to be carried out two times in order to get representative results. [1]

In our case two samples have been taken and the results of the slump test are summarized in the table below.

designation of spreading measure			means of two probe
	spreading m.	means	
probe 1	39 auf 38 cm	38,5 cm	39,50 cm
probe 2	40 auf 41 cm	40,5 cm	common K 3

Table 4.3.2-1 Results of the slump test

The average slump value amounts 39.50 cm which is equivalent to a consistence grade of K 3, and thus will guarantee perfect casting of the slabs.

After cleaning the formwork the inside was thoroughly coated with forming oil. At first the concrete cover of 2.5 cm was cast and drawn off. Next the carbon fiber reinforcement mesh was placed on and slightly pressed against the fresh concrete surface. This procedure was repeated in layers applying steady compaction work until the upper edge of the formwork where the top surface received a smooth and clean finish.

Additionally two ribbed concrete steel crooks with a diameter of 8 mm have been installed in the slab for transportation reasons.

The next couple of pictures illustrate two working steps: casting of the concrete cover and positioning of the reinforcement mesh and also the type and position of the ribbed steel crooks.

Further it was observed that the securing to prevent floating of the carbon fiber mesh due to its light weight was not necessary.



Picture 4.3.2-1 Casting of the concrete cover



Picture 4.3.2-2 Positioning of the reinforcement sheet

4.3.3. Base concrete

Simultaneously base concrete test cubes and prisms were prepared and subjected to compression and tensile-bending tests after 28 days at the laboratory of the company Lafarge – Perlmoser.

The compression test was carried out according to the Austrian standard ÖNorm B 3303 with a loading speed of $0.60 \text{ N/mm}^2\text{s}$, the bending test was conducted at a loading speed of $0.06 \text{ N/mm}^2\text{s}$ on a three-point bearing.

Since the concrete test cubes had a side length of only 15 cm, but the standard ÖN B 3303 references the test results - compression strength - for cubes with a 20 cm side length, it was necessary to convert the results. Table 4.3.3-1 lists the results of both the compression and bending test for both specimen types each represented by 3 samples.

Pressure- and tensile bending tightness of base concrete				
	part	measurement	pressure tightness	mean
cube	3	15*15*15cm	38,80 N/mm ²	38,10 N/mm²
			38,70 N/mm ²	
			36,80 N/mm ²	
	part	measurement	tensile bending tightness	
prism	3	15*15*60cm	4,30 N/mm ²	4,30 N/mm²
			4,30 N/mm ²	
			4,20 N/mm ²	

Table 4.3.3-1 Mechanical properties of base concrete

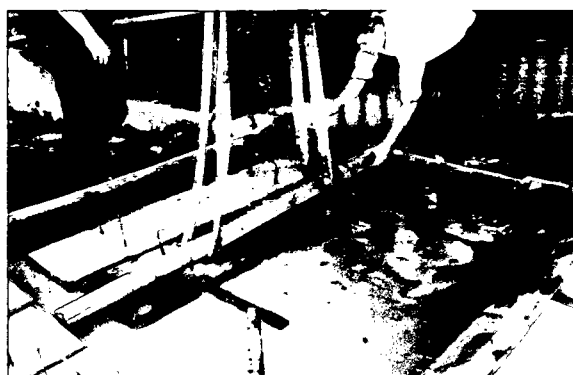
The results of the test showed that the concrete quality fully meets the desired requirement of a B 30 / 300.

4.3.4. Storage of the slabs

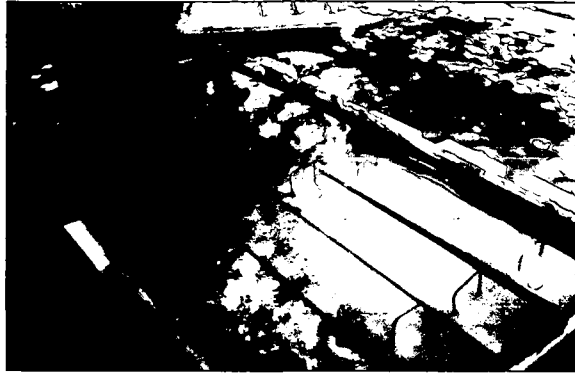
The preparation of the slabs was conducted during summer. Since no climatic chamber was available it was decided to store the slabs in especially designed water basins.

After 3 days of curing the formwork was dismantled and the slabs were lifted at the ribbed steel crooks into the water basins with the help of a stacker truck.

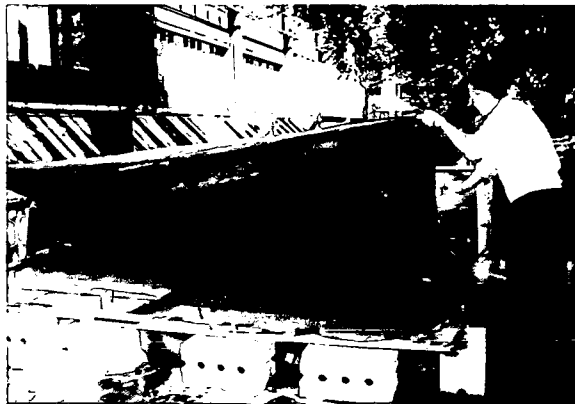
The slabs were then kept inside the basins for another 25 days to minimize cracks due to shrinking and creeping processes during curing. In order to protect the slabs from direct insolation the basins were covered with a plastic canvas.



Picture 4.3.4-1
Transport of slabs
to the water basin



Picture 4.3.4-2 Storage of slabs under water



Picture 4.3.4-3 Covering of basins

Once the concrete has fully cured, the slabs were taken out of the basins and taken to the testing lab. The slabs were cleaned and all steel crooks were removed in front of the testing lab. Eventually the slabs were lifted with an overhead crane and mounted on the testing machine.

5. Experimental part

This chapter describes the experimental set-up, mounting of the slabs, results of the tensile bending test, graphical analysis, and measurement system by means of illustrations such as photographs, sketches and diagrams.

5.1. Experimental set-up

5.1.1. Three-point bending test

The slabs were subjected to a three-point bending test by using an electronically controlled testing machine. The load was applied – force/displacement controlled - at a speed of 3.00 mm/min except for experiment number 5 and 6. The latter experiments were conducted at a loading speed of 1.80 mm/min, since in this case the reference slabs with conventional steel reinforcement were tested. The average duration of a test was 40 minutes per specimen.

Deflection of the specimens was measured in two ways:

- via a direct displacement transducer of the testing machine since it is force displacement controlled
- via an external inductive displacement transducer placed on the slab center – the measured displacement is thus free of any distortion of the testing machine during the experiment

The data obtained from the tests is then represented by stress-strain or stress-deflection diagrams and evaluated. The principal parameters that determine the shape of these curves and consequently the deflection behaviour of the concrete are the loading speed, load duration and concrete strength. Furthermore one has to distinguish between a constant loading speed and constant deflection speed, which considerably influence the shape of the curves. [10]

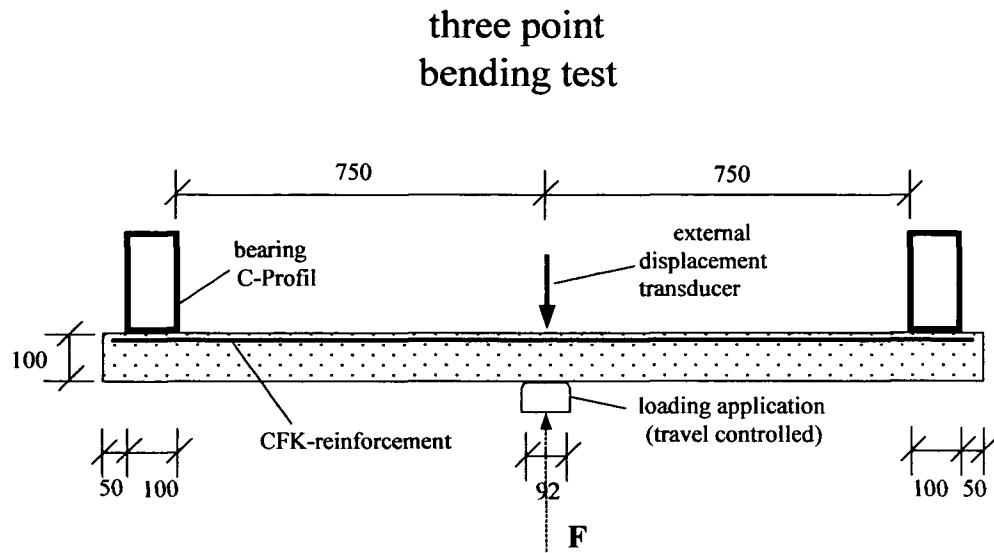


Figure 5.1.1-1 Test setup

The data analysis was carried out with a software package distributed by the company Meßphysik, Laborgeräte Ges.m.b.H. The evaluation of the tensile bending tests for synthetic products was done according to international standards (DIN EN 63, DIN 53 452, DIN 13 927).

This type of test determines strength and deflection stability of plastics when subjected to bending by a three-point load. The sample has to be mounted at the bearings without inducing stress the load is then applied at the center of the sample causing shear, compression and tensile stresses to develop, however shear and compression stresses need to be kept at a low level.

Based on the experiment the following properties can be determined:

- history of bending stress until failure
- strain history at edge fiber until failure
- deflection history until failure

The lever arm of the carbon fiber reinforcement amounts 7.50 cm when taking into account a slab thickness of 10 cm and a concrete cover of 2.5 cm.

The bending stress equals the extreme fiber stress at each moment of the experiment. It is defined as the ratio between bending moment and moment of inertia of the specimen.

$$\sigma_f = \frac{M}{W}$$

Equation 5-1

σ_f bending stress [N/mm²]

M bending moment [Nmm]

W section modulus [mm³]

The bending moment and moment of inertia are calculated as follows:

$$M = \frac{F * l_v}{2}$$

Equation 5-2

F bending force [N]

l_v bearing pitch [mm]

$$W = \frac{b * h^2}{6}$$

Equation 5-3

b slab width [mm]

h high cross section [mm]

Combining the above equation gives the following expression for the bending stress:

$$\sigma_f = \frac{3 * F * l_v}{b * h^2}$$

Equation 5-4

As a next step the strain at the edge fiber will be calculated. This strain quantity describes the change of length at the edge fiber between the bearings, relative to the distance between the bearings at both the tensile and compression side.

The calculation is carried out as follows:

$$\varepsilon_f = \frac{f}{lb} * 100$$

Equation 5-5

$$l_b = \frac{lv^2}{6 * h}$$

Equation 5-6

$$\varepsilon_f = \frac{6 * h * f}{lv^2} * 100$$

Equation 5-7

ε_f strain of the outer fiber [%]

f bending [mm]

l_b length [mm]

The samples have to be placed symmetrically on the bearings to allow a centered application of the compression fin. The longitudinal axis of the sample has to be aligned perpendicular to the bearings.

The type of failure, either shear, compressive or tensile needs to be stated in the test report. [31]

5.1.2. Schematic illustrations

The following sketches outline the functionality of the experimental set-up including the testing machine and pulling device. Two additional photographs show the testing machine.

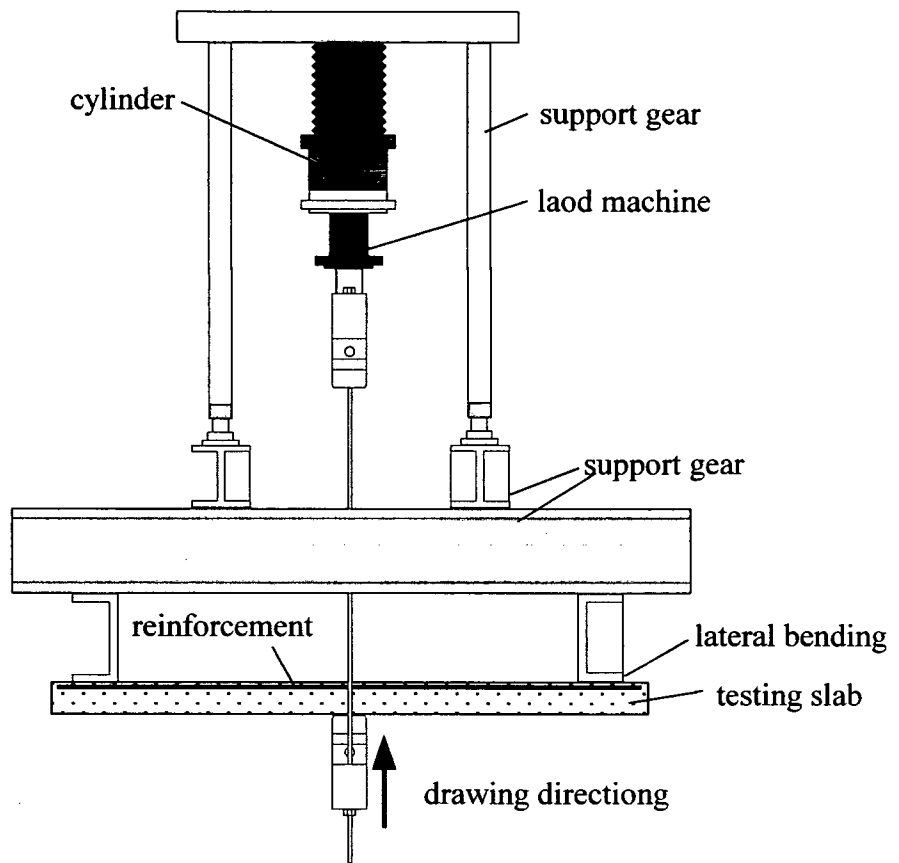


Figure 5.1.2-1 Hydraulic actuator

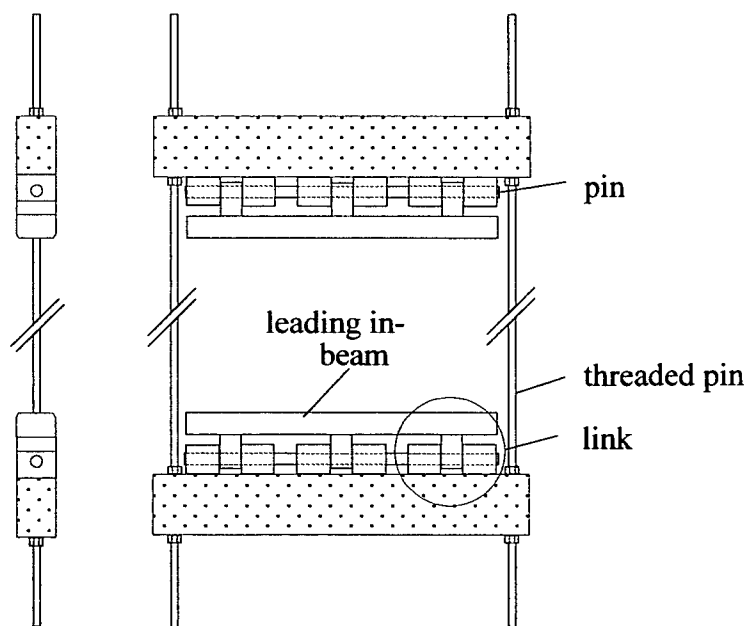
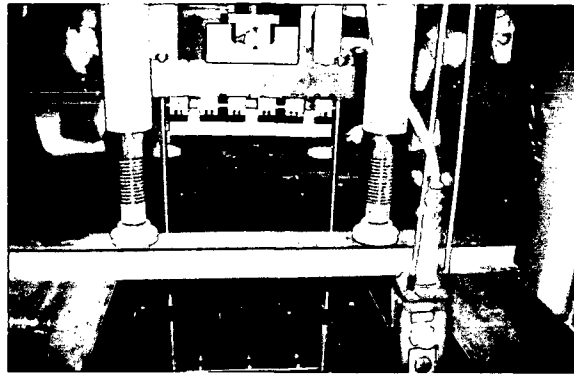
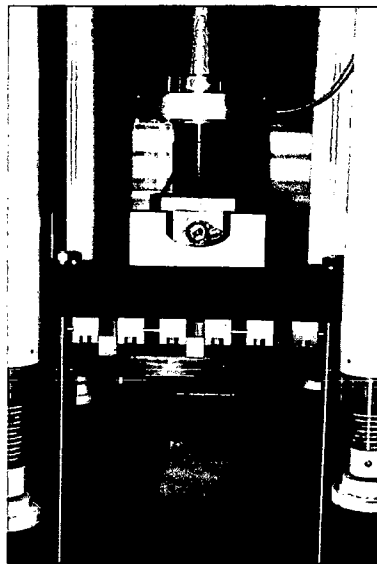


Figure 5.1.2-2 Pulling device



Picture 5.1.2-1 Test setup



Picture 5.1.2-2 Hydraulic actuator

5.1.3. Set-up of measuring unit

The measurement unit consists of two data circuits, one for the external inductive displacement transducer positioned on the slab center, and one for the force-displacement control system of the testing machine. The external sensing device was connected to the main data acquisition unit of the testing machine in order to obtain an independent simultaneous measurement.

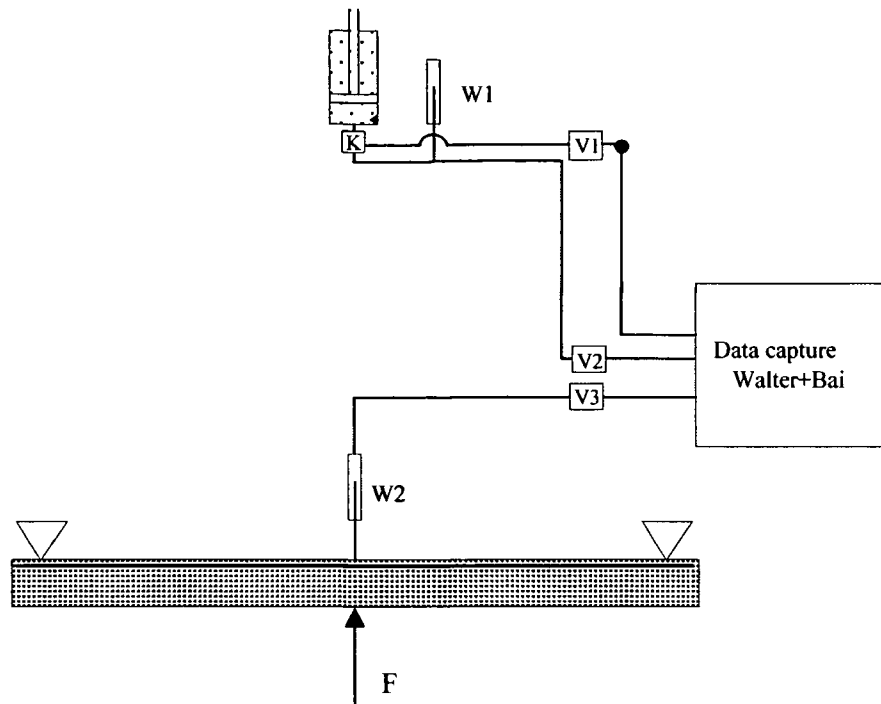


Figure 5.1.3-1 Data capture

F	bending force
W1	displacement transducer testing machine
W2	external displacement transducer
K	hydraulic forcer
V1-V3	measuring circuit of data capture

The measurement data was acquired automatically once the testing machine started to operate, after recalibration of the initial values by the computer.

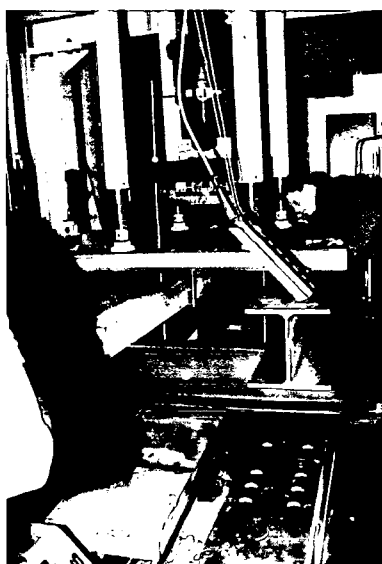
5.2. Experiments

5.2.1. Mounting of specimens

After 28 day storage in the water basins, the slabs were cleaned and the ribbed steel crooks removed after transporting the slabs to the testing laboratory. By the use of an overhead crane it was possible to exactly position the slabs into the testing machine. The clearance between the bearings was 1500 mm. The load was applied at the slab center whereby the slab was kept in position by applying little prestress. The following two pictures illustrate the rather difficult mounting of the slabs.



Picture 5.2.1-1 Assembling of specimen



Picture 5.2.1-2 Fixing of specimen

5.2.2. Tensile bending test

As already mentioned earlier, the slabs have been prepared in 3 batches each comprising 2 pieces. To summarize there are 2 slabs with a double-ply reinforcement mesh, 2 slabs with a single-layer reinforcement mesh and for reference purposes 2 slabs with conventional steel reinforcement (CQS 6, CQS 8).

The first experiment was carried out with the double-ply reinforced slabs. The initial loading speed amounted $v=1.80$ mm/min and was then increased to $v=3.00$ mm/min thereby it was possible to decrease the already vast amounts of data. The same strategy was applied when testing the single-layer reinforced slabs.

Whereas the conventional steel reinforced slabs were tested at a constant loading speed of $v=1.80$ mm/min. The upward pointing force was applied at the bottom side of the slab. The duration of the experiment ranged between 30 to 45 minutes per slab.

In the following sub chapter we will discuss the destruction of the slabs, evolution of cracks and the type of failure.

Further a description of the data analysis and results will be given and illustrated by further pictures and tables.

5.3. Results

5.3.1. Crack evolution and distribution

The evolution of cracks and their spatial growth and size has been documented for all slabs. For now the crack evolution shall be discussed based only on the double-ply carbon fiber reinforced slab.

The first visible hair crack occurred at a load of 8.34 kN almost at the center of the slab and was continually propagating in transversal direction due to the increase in load. The next crack occurred at a load of 11.77 kN at the right hand side from the slab center. All other cracks occurred alternately on both sides of the slab (left and right from the center). The experiment was stopped as the load reached 29.43 kN and crack width were measured.

The device used to measure the crack width was equipped with a magnifying focusing unit and a hair cross. The device was placed directly on the concrete surface and the crack width was determined based on a 1/10 mm scale division.

At a load of 14.72 kN seven hair cracks could be found, whereas at a load of 21.58 kN nine hair cracks were counted. A “short-time failure” was observed at a load of 32.37 kN, where at crack number 3 the initiation of failure in compression mode was noticed. Ultimate failure occurred at a stress level of 15.80 MPa (15.80 N/mm²).

The crack width of the other slabs have been measured in the same manner, with the only difference that different load levels were responsible for the occurrence and position of cracks. Longitudinal cracks have not been observed. This could be due to low

transmission of tensile stress to the flat and smooth carbon fiber lamellae or due to the high amount of transversal reinforcement.

The results given in the table below have been obtained at the measurement locations outlined in the following sketch.

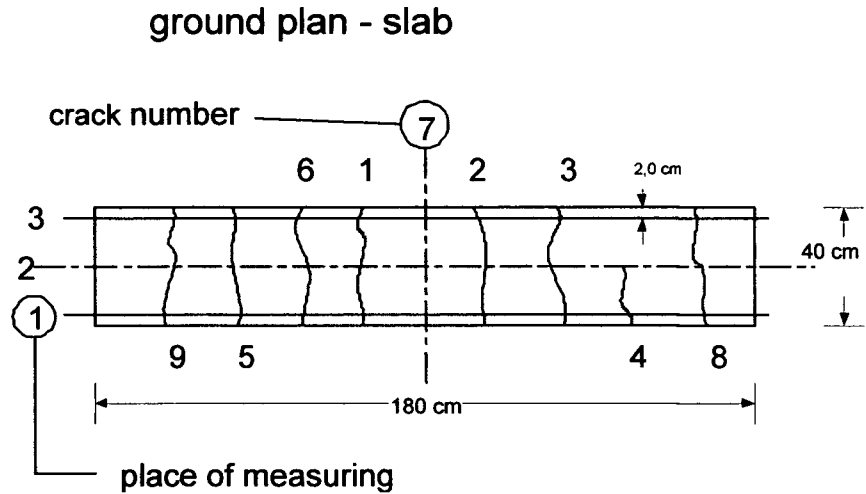


Figure 5.3.1-1 Distribution of cracks for a double-layer reinforcement (schematic)

crack-number	crack width [mm]		
	1 /	place of measuring	
1	1 / 0,30	2 / 0,20	3 / 0,20
2	1 / 0,30	2 / 0,30	3 / 0,20
3	1 / 0,40	2 / 0,30	3 / 0,60
4	1 / 0,20	2 / 0,10	3 / 0,40
5	1 / 0,10	2 / 0,20	3 / 0,30
6	1 / 0,30	2 / 0,20	3 / 0,20
7	1 / 0,40	2 / 0,40	3 / 0,10
8	1 / 0,80	2 / 0,50	3 / 0,20
9	1 / 0,30	2 / 0,60	3 / 0,40

Table 5.3.1-1 Measured crack widths for a double-layer reinforcement

The next two photographs show the distribution of cracks, however the numbering of the cracks is hardly visible.



Picture 5.3.1-1 Crack distribution of a slab



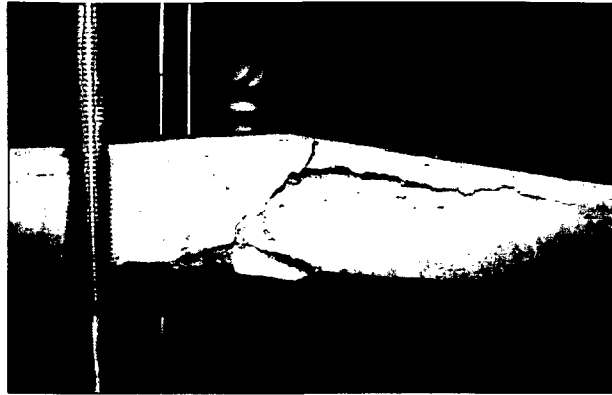
Picture 5.3.1-2 Crack distribution of a slab with numbering

5.3.2. Ultimate failure criteria

Experiments were stopped when a maximum deflection of 10 cm was reached, taking into consideration a span of 150 cm this criteria appears to be quite sufficient. As can be seen in the following analysis all slabs have reached their ultimate carrying capacity already earlier. However, the purpose of these experiments was to investigate the interaction between concrete and carbon fiber mesh at increased load levels, as well as if and how failure occurs.

The following pictures are well documenting the different failure modes of the slabs.

In the first picture a typical shear failure of a double-layer reinforced slab can be seen, but also for a single-layer reinforced slab shear failure could be observed (slabs nr. 1 and 3). Slabs nr. 2 and 4 exhibited bending tensile failure (see following pictures).



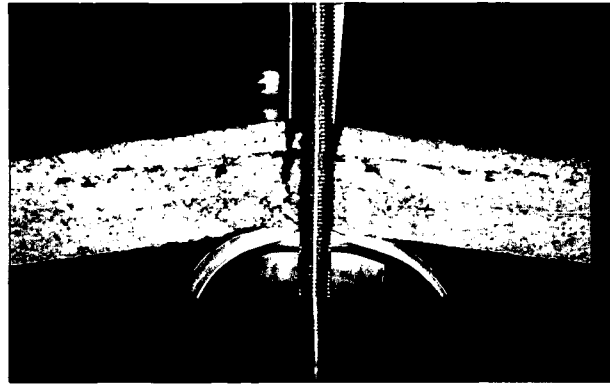
Picture 5.3.2-1 Shear failure of double-layer reinforced slab



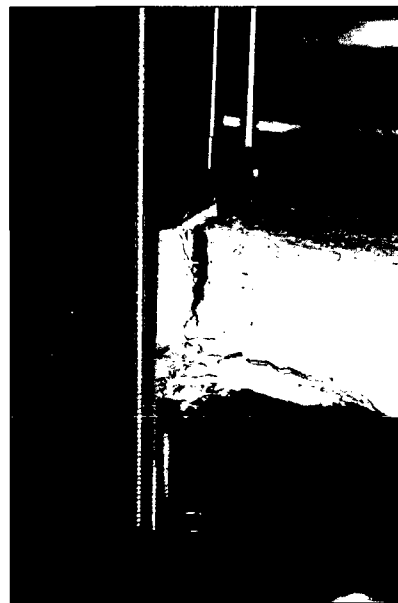
Picture 5.3.2-2 Bending tensile failure of double-layer reinforced slab



Picture 5.3.2-3 Bending tensile failure of single-layer reinforced slab



Picture 5.3.2-4 Bending tensile failure of single-layer reinforced slab (lateral)

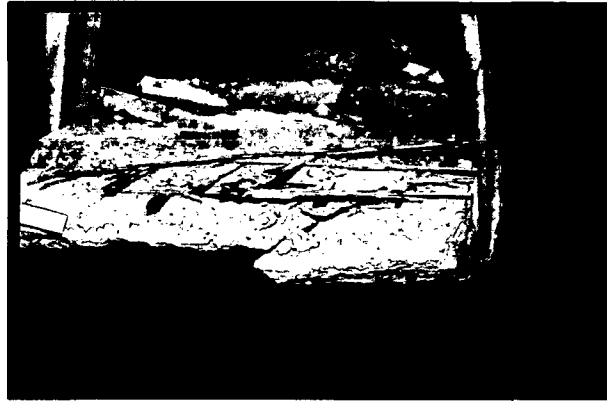


Picture 5.3.2-5 Failure of concrete cover

The pressure zone of the concrete failed after the tensile zone, whereas the whole force was sustained by the CFRP-sheets. This state ensued at a deflection of 7 – 8 cm.

5.3.3. Demolition of the slabs

In order to study the behaviour of the slabs after ultimate load they were loaded until total demolition without data acquisition. The average total deflection of the slabs was about 50 cm before rupture of the reinforcement occurred, which was accompanied by a loud noise. The reference slabs with the CQS steel mesh were more ductile.



Picture 5.3.3-1 Totally destroyed slab with CFRP reinforcement



Picture 5.3.3-2 Enlargement of picture 5.3.3-1 with visible concrete cover

The final picture shows the abraded concrete in the region of the lamellae due to the deviation of the forces and the extreme bending tensile loading which is indicated by the blank surface of the debris.



Picture 5.3.3-3 Abraded concrete close to the lamellae

5.3.4. Results

In this chapter the results are presented in form of diagrams and tables using the following division:

- Slabs 1 and 2 with double-layered CFRP-sheet reinforcement
- Slabs 3 and 4 with single-layered CFRP-sheet reinforcement
- Slabs 5 and 6 with CQS 8 and CQS 6 steel mesh reinforcement (reference slabs)

The diagrams are presented in the following form:

- The single slabs with stress – strain resp. deflection curves in one diagram
- Associated slabs in one diagram in the form of a stress – strain curve
- Table for a better comparison
- Final summary of all results

The first 3 curves show the double-layered and the next 3 the single-layered slabs with CFRP-sheet reinforcement.

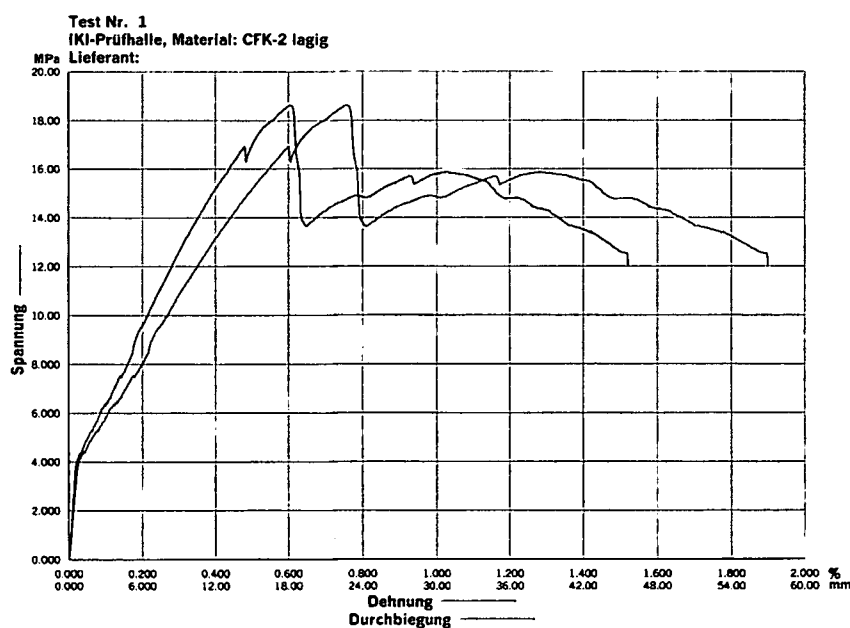


Figure 5.3.4-1 Slab 1 with double-layered CFRP-sheet reinforcement

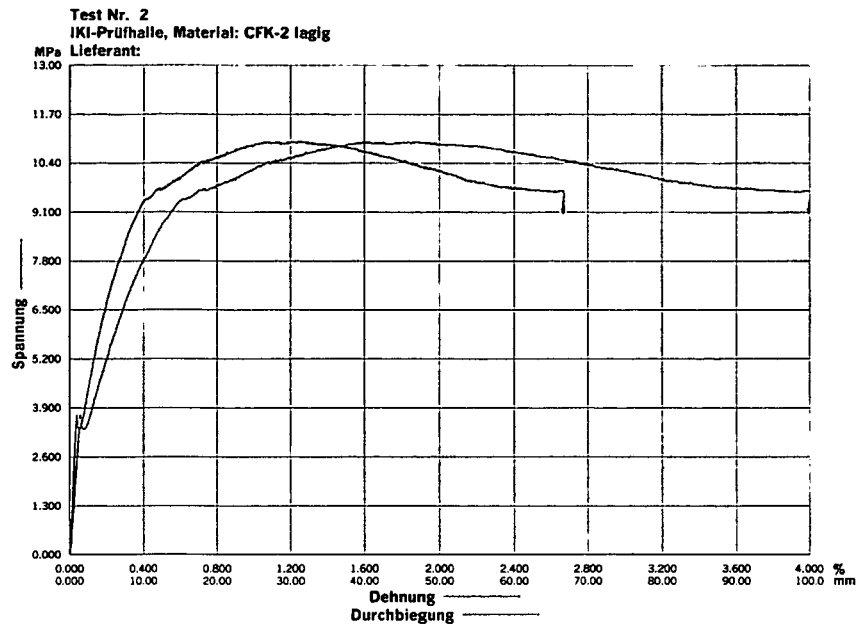


Figure 5.3.4-2 Slab 2 with double-layered CFRP-sheet reinforcement

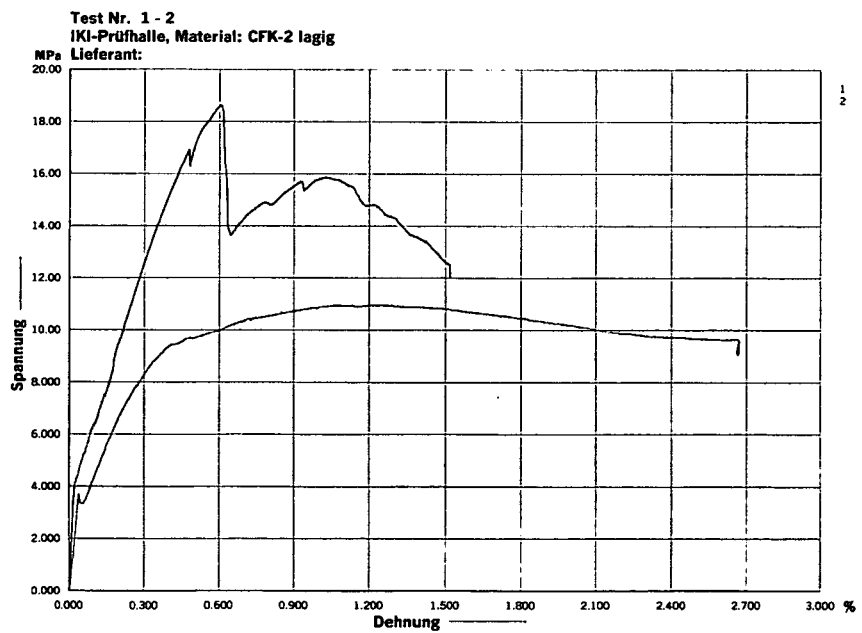


Figure 5.3.4-3 Slabs 1 and 2 with double-layered CFRP-sheet reinforcement

slab num.	max. σ [MPa]	max. F [kN]	strain %	bending [mm]
1	18,64	33,14	0,604	22,60
2	10,96	19,49	1,135	42,76
slab num.	break of testing			
1	12,00	22,11	1,520	57,00
2	9,07	17,16	2,668	99,98

Table 5.3.4-1 Ultimate stress and load with according strain resp. deflection

slab number	strain with 2 ‰		strain with 4 ‰	
	σ [Mpa]	F [kN]	σ [Mpa]	F [kN]
1	9,63	17,11	15,11	26,86
2	6,71	11,97	9,40	16,72
slab number	bending [mm]		bending [mm]	
1	7,49		15,02	
2	7,46		15,04	

Table 5.3.4-2 Stress and load at 2‰ and 4‰ strain and according deflection

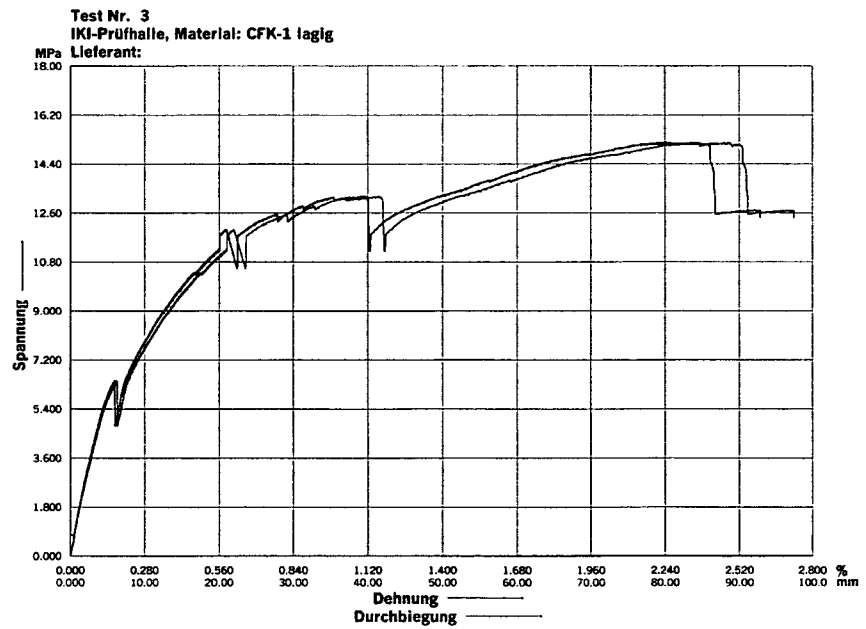


Figure 5.3.4-4 Slab 3 with single-layered CFRP-sheet reinforcement

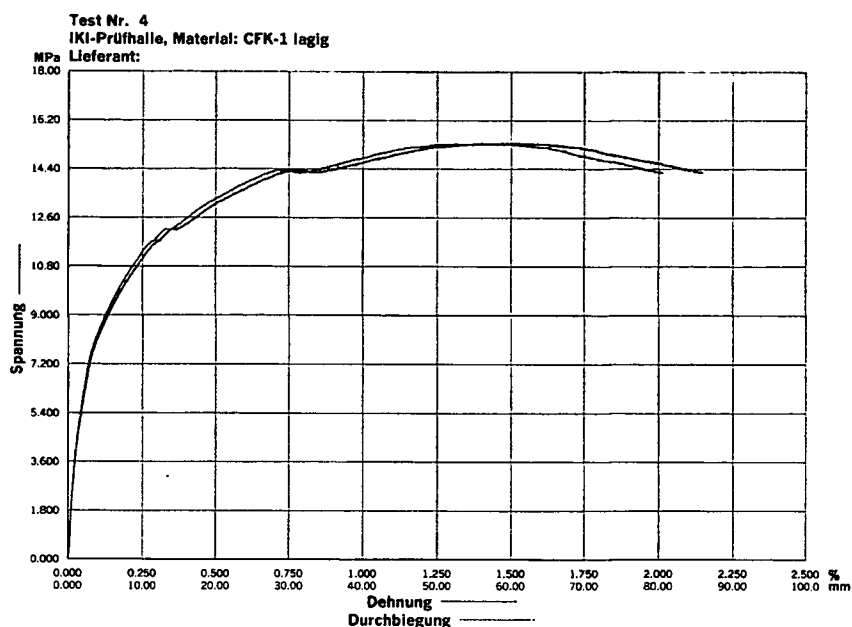


Figure 5.3.4-5 Slab 4 with single-layered CFRP-sheet reinforcement

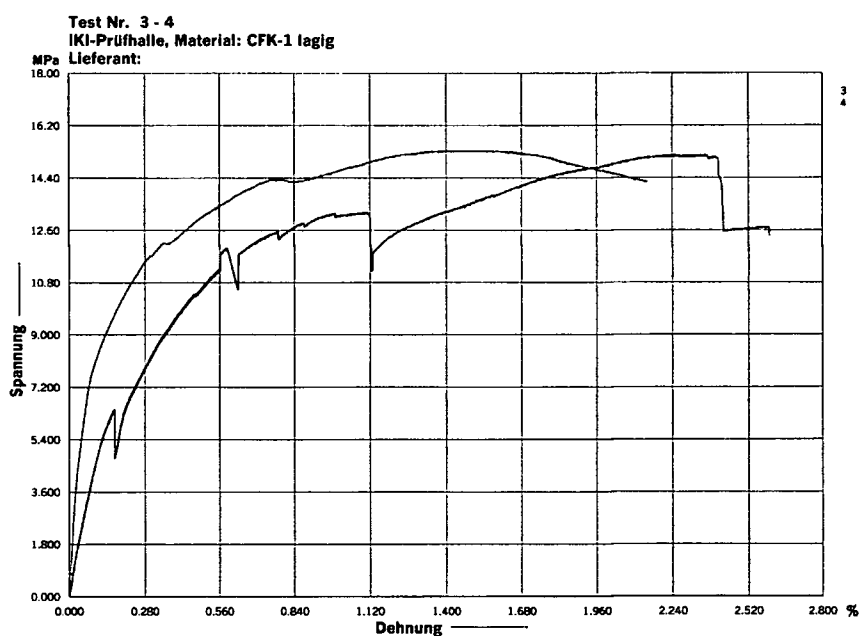


Figure 5.3.4-6 Slabs 3 and 4 with single-layered CFRP-sheet reinforcement

slab num.	max. σ [MPa]	max. F [kN]	strain %	bending [mm]
3	15,19	27,00	2,224	84,11
4	15,36	27,30	1,399	52,56
slab num.	break of testing			
3	12,47	22,50	2,598	97,44
4	14,26	25,35	2,149	80,47

Table 5.3.4-3 Ultimate stress and load with according strain resp. deflection

slab number	strain with 2 %		strain with 4 %	
	σ [Mpa]	F [kN]	σ [Mpa]	F [kN]
3	6,30	11,34	9,56	17,11
4	10,32	18,35	12,37	22,01
slab number	bending [mm]		bending [mm]	
3	7,50		14,99	
4	7,50		15,02	

Table 5.3.4-4 Stress and load at 2‰ and 4‰ strain and according deflection

Finally the reference slabs with the CQS mesh are shown.

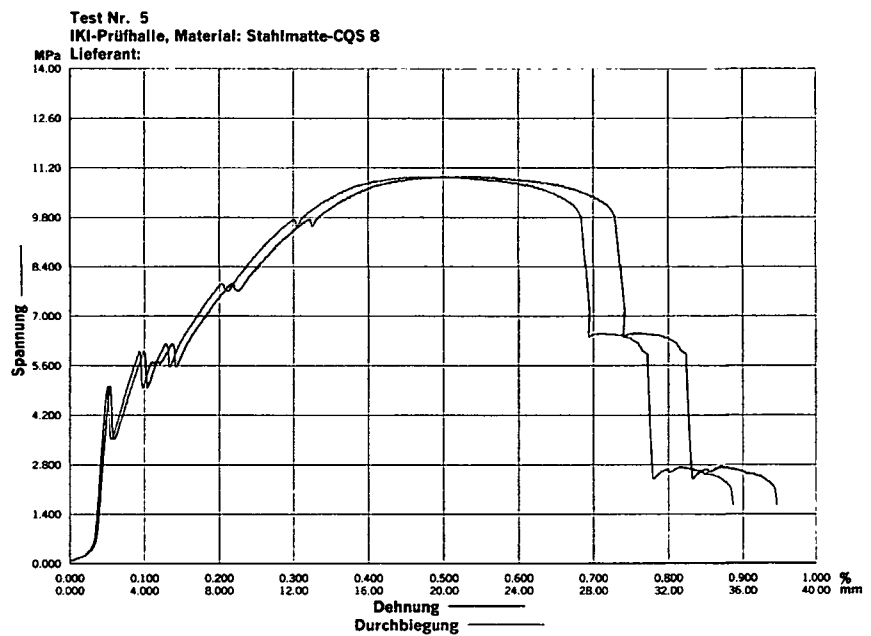


Figure 5.3.4-7 Slab 5 with CQS 8 steel mesh reinforcement

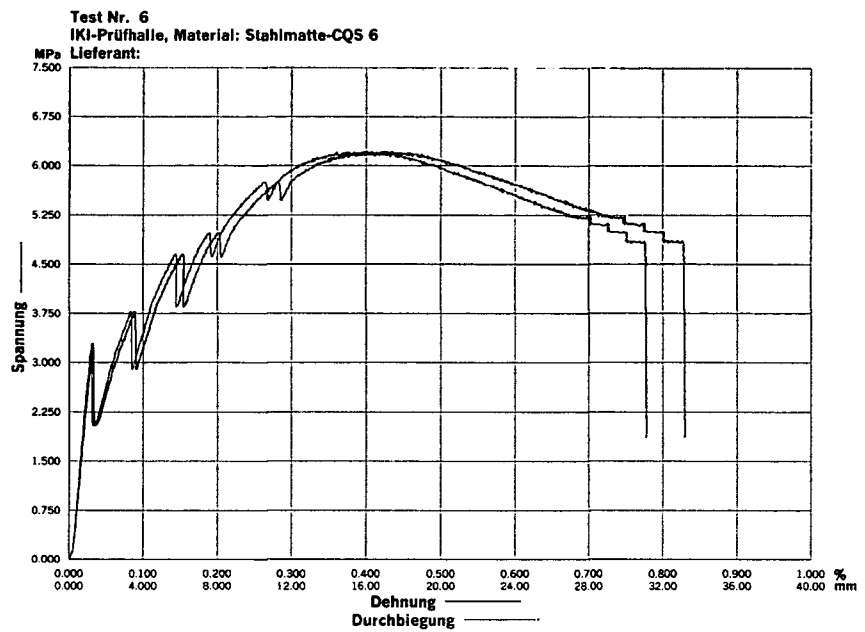


Figure 5.3.4-8 Slab 6 with CQS 6 steel mesh reinforcement

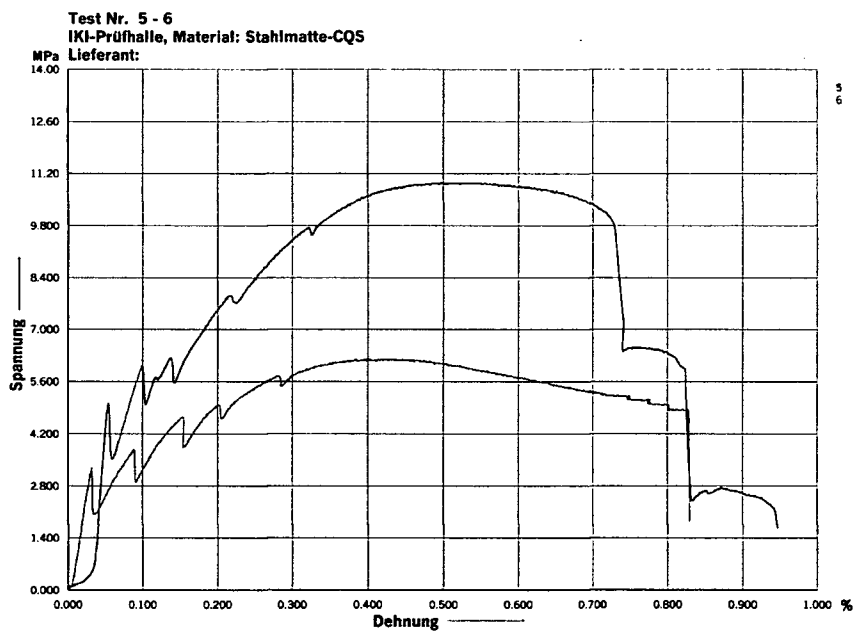


Figure 5.3.4-9 Slabs 5 and 6 with CQS steel mesh reinforcement

slab num.	max. σ [MPa]	max. F [kN]	strain %	bending [mm]
5	10,95	19,47	0,498	18,69
6	6,21	11,05	0,421	15,83
slab num.	break of testing			
5	1,65	2,94	0,946	35,48
6	1,88	8,59	0,829	31,05

Table 5.3.4-5 Ultimate stress and load with according strain resp. deflection

slab number	strain with 2 ‰		strain with 4 ‰	
	σ [Mpa]	F [kN]	σ [Mpa]	F [kN]
5	7,53	13,38	10,62	18,86
6	4,97	8,80	6,19	10,96
slab number	bending [mm]		bending [mm]	
5	7,55		14,99	
6	7,49		15,04	

Table 5.3.4-6 Stress and load at 2‰ and 4‰ strain and according deflection

For a better comparison of the results all six curves are plotted in a stress- strain – diagram, whereas the following colours are used:

- Slab 1 in black (double-layered CFRP-sheet reinforcement)
- Slab 2 in pale green (double-layered CFRP-sheet reinforcement)
- Slab 3 in dark blue (single-layered CFRP-sheet reinforcement)
- Slab 4 in pale red (single-layered CFRP-sheet reinforcement)
- Slab 5 in pale blue (CQS 8 steel mesh reinforcement)
- Slab 6 in brown (CQS 6 steel mesh reinforcement)

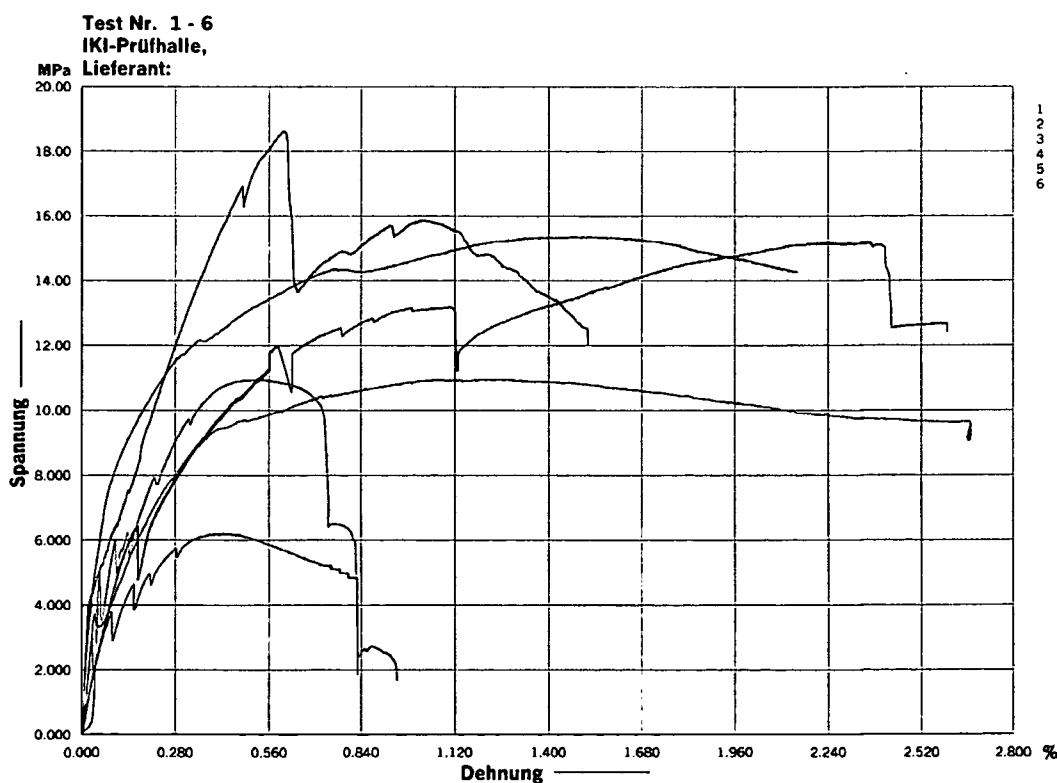


Figure 5.3.4-10 Summary of results in the stress - strain – diagram

In the final table all values are summarized.

slab_num.	max. value			break			of testing		
	σ [MPa]	F [kN]	strain %	bending [mm]	σ [MPa]	F [kN]	strain %	bending [mm]	
1	18,64	33,14	0,604	22,66	12,00	22,11	1,520	57,00	
2	10,96	19,49	1,135	42,76	9,07	17,16	2,668	99,98	
3	15,19	27,00	2,244	84,11	12,47	22,50	2,598	97,44	
4	10,95	27,30	1,399	52,56	14,26	25,35	2,149	80,47	
5	10,95	19,47	0,498	18,69	1,65	2,94	0,946	35,47	
6	6,21	11,05	0,421	15,83	1,88	8,59	0,829	31,05	

slab_num.	strain with 2 ‰			strain with 4 ‰			
	σ [MPa]	F [kN]	bending [mm]	slab number	σ [MPa]	F [kN]	bending [mm]
1	9,63	17,11	7,49	1	15,11	26,86	15,02
2	6,71	11,97	7,46	2	9,40	16,72	15,04
3	6,30	11,34	7,50	3	9,56	17,11	14,99
4	10,32	18,35	7,50	4	12,37	22,01	15,02
5	7,53	13,38	7,55	5	10,62	18,86	14,99
6	4,97	8,80	7,49	6	6,19	10,96	15,04

Table 5.3.4-7 Ultimate stress and load with according strain resp. deflection, values until stop of the tests and at the right the according values at 2‰ and 4‰ strain

5.4. Analysis of the results

In the following section the most important results are analyzed by means of fig. 5.4-1 and table 5.3.4-7.

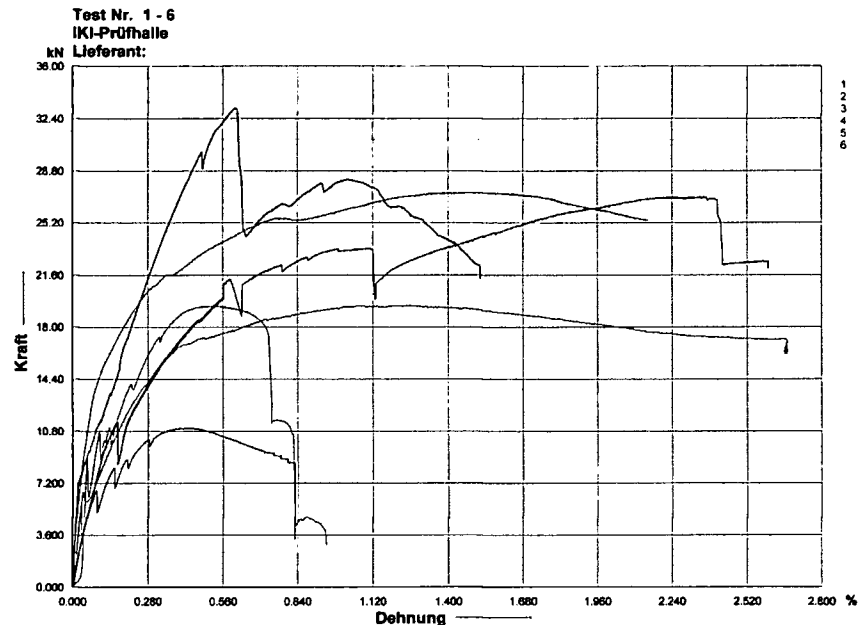


Figure 5.4-1 Summary of results with force-strain diagram

- Slab 1: The ultimate load was about 33.14 kN at a strain of 0.6% and a deflection of 22.66 mm. Then the load decreases rapidly until 24.23 kN, maybe due to a shear displacement between concrete and sheets. Another local peak can be observed at 28.18 kN. The test was stopped at a strain of 1.52% and an according deflection of 57 mm.
- Slab 2: This slab exhibited bending tensile rupture with a large crack in the middle and fine hair cracks close to it. A poor adhesion between concrete and CFRP-sheet may be assumed so that the concrete contributed only little to the load transfer. Another explanation could be the type of reinforcement arrangement, since both mats were superposed on each other and a “sliding gap” could rise between them. The main part of the load was transferred by the lamellae and due to their ductile behaviour the curve is very flat at large strains. The ultimate load was 19.49 kN at a strain of 1.13% and the according deflection of 42.76 mm.

Slab 1 and 2 show different failure modes and a different shape and peak values of the load-deflection curve: the ultimate load of slab 1 was about 70% higher.

- Slab 3 exhibited the same failure mode as slab 1 and a fine crack distribution, whereas the ultimate load was 27 kN at a strain of 2.24% and a deflection of 84.1 mm. The total failure was induced slightly afterwards.
- Slab 4: The shape of the curve and the failure mode correspond to that of slab 2, but the ultimate load is higher. This could be explained by the missing “sliding gap” between the two sheets. The ultimate load was 27.3 kN at a strain of 1.4% and a deflection of 52.56 mm.

The difference of the ultimate load of the slabs 3 and 4 is about 39%, whereas slabs with shear failure exhibit a much higher ultimate load as slabs with bending tensile failure. Crack initiation and distribution may be correlated with the load-deflection behaviour: for slabs with a fine crack distribution the load is well distributed between the concrete and reinforcement, which is reflected by jumps in the load-deflection curve.

- Slab 6 and 7: The slabs with the CQS 8 resp. CQS 6 steel mesh reinforcement showed a very fine crack distribution and nearly the same strain at ultimate load (0.5% resp. 0.42%) which corresponds to the limit strain of 0.4% according to ÖNorm and EC. The failure of the single steel bars can be observed very well in the load-deflection curve.

According to table 5.3.4-7 the deflection is very similar at strains of 0.2% resp. 0.4%. The maximum allowable deflection of $l/300$ (for a span of $l = 1500$ mm the allowable deflection is 5 mm) was exceeded in all tests: $l/200$ at 0.2% strain and $l/100$ at 0.4% strain. In the conclusive table the various deflections are listed for a better comparison.

slab number	reinforcement model	max. zul. bending	bending with 2‰	bending with 4‰	bending break test
1	CFK-double	$l/300$	$l/200$	$l/100$	$l/26$
2	CFK-double	$l/300$	$l/201$	$l/100$	$l/15$
3	CFK-single	$l/300$	$l/200$	$l/100$	$l/15$
4	CFK-single	$l/300$	$l/200$	$l/100$	$l/19$
5	CQS 8	$l/300$	$l/199$	$l/100$	$l/45$
6	CQS 6	$l/300$	$l/200$	$l/100$	$l/48$

Table 5.4-1 Maximum allowable deflections compared with the deflections of the various slabs

The exceeding of the allowable deflections may be explained by the concentrated loading in form of a 3-point bending test. Also the load increasing rate is of major importance. For the total destruction of the slabs an average deflection of 50 cm was measured which corresponds to $l/5$ is due to the high ductility of the CFRP-sheets.

Finally the calculated Young's moduli of the single slabs are presented.

test number	Charge Nr.	reinforcement model	E-moduli [GPa]	break of slab
1	slab 1	CFK double	3,022	shearing stress
2	slab 2	CFK double	2,169	bending stress
3	slab 3	CFK single	3,354	bending stress
4	slab 4	CFK single	7,525	shearing stress
5	slab 5	CQS 8	6,430	steel
6	slab 6	CQS 6	1,029	steel

Table 5.4-2 Calculated Young's moduli from the tests

6. Pull out tests

In this final chapter two types of pull-out tests are described, whereas the first one was not performed according to the standard, but for the second one the different roughness of the lamellae are taken into consideration.

6.1. Simplified pull-out test

6.1.1. Preparation

Five lamellae of the type C 200/2000 without surface treatment with the dimensions 10 mm x 1.4 mm were placed at a time with different embedment lengths and a distance of 15 cm in fresh concrete C 25/30 with maximum grain of 4 mm. After three days the formwork was dismantled and the slab was stored in a water basin for 25 days. The dimensions of the lamellae resulted from a preliminary estimation of the shear strength and hence for the embedment length there have been chosen 2, 4, 6 and 8 cm. According to the measured force at failure an average bond strength $\tau_m = 1.2 \text{ N/mm}^2$ was calculated for the CFRP-lamellae.

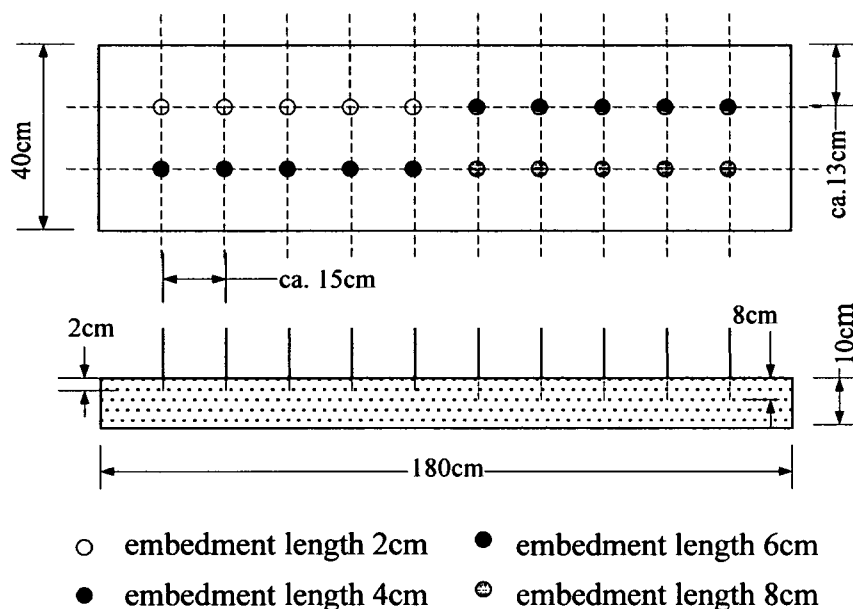
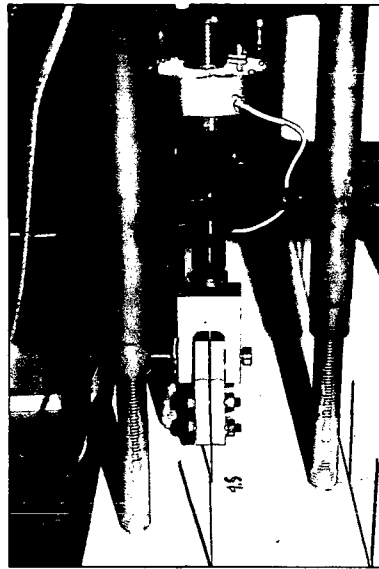


Figure 6.1.1-1 Geometry for the pull-out tests

6.1.2. Test setup

The bond strength was determined with an electro mechanic testing machine whereas the relative displacement of the lamella and the applied tensile force were measured. The load transfer to the lamella was achieved by a cramping device with a rough inner surface in order to avoid sliding of the lamella.



Picture 6.1.2-1 Testing equipment



Picture 6.1.2-2 Tested lamella at the left

6.1.3. Evaluation

According to Fig. 6.1.3-1 a nearly linear relation exists between embedment depth and bond strength which was estimated through the ultimate load divided by the surface area. The embedment depth for which the bond strength remains constant was not reached.

embedment length [cm]	Test Nr.	shearing stress			
		with way [N/mm ²]	mean value [N/mm ²]	without way [N/mm ²]	mean value [N/mm ²]
2	1	0,54		0,52	
2	2	0,05		0,05	
2	3	0,05		0,05	
2	4	1,80		1,76	
2	5	0,75	0,638	0,73	0,622
4	1	---		---	
4	2	0,94		0,93	
4	3	1,42		1,41	
4	4	1,43		1,43	
4	5	1,25	1,260	1,24	1,253
6	1	1,21		1,20	
6	2	1,05		1,05	
6	3	1,37		1,37	
6	4	1,09		1,08	
6	5	1,68	1,280	1,68	1,276
8	1	1,32		1,32	
8	2	1,64		1,59	
8	3	2,03		2,02	
8	4	1,55		1,55	
8	5	1,69	1,646	1,69	1,634

Table 6.1.3-1 Results of pull-out tests

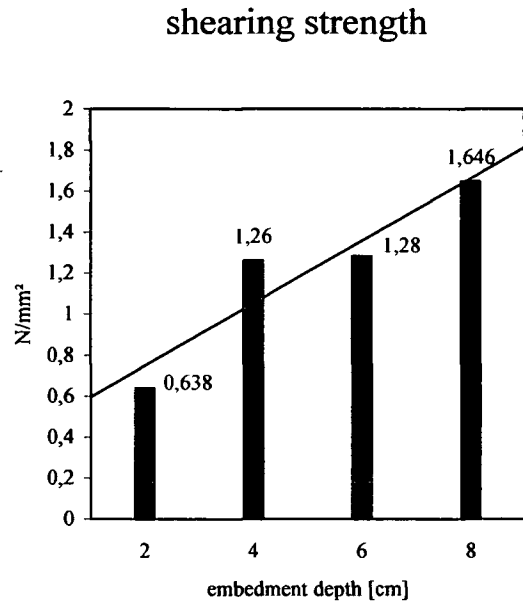


Figure 6.1.3-1 Bond stresses for different embedment depths (bars) and theoretic values (line)

6.2. Standardized pull-out test

6.2.1. Roughness of the lamellae

The surface of the lamellae was roughened with abrasive paper exhibiting different roughness:

- Type 1: not treated lamellae as delivered from the manufacturer (one side rough, the other flat)
- Type 2: both sides roughened with abrasive paper type Nr. 80
- Type 3: both sides roughened with abrasive paper type Nr. 40
- Type 4: both sides roughened with abrasive paper type Nr. 60

In the standard DIN 4760 there are defined six different surface roughness, which in reality cannot be observed separately due to the fact that the changes takes place continuously.

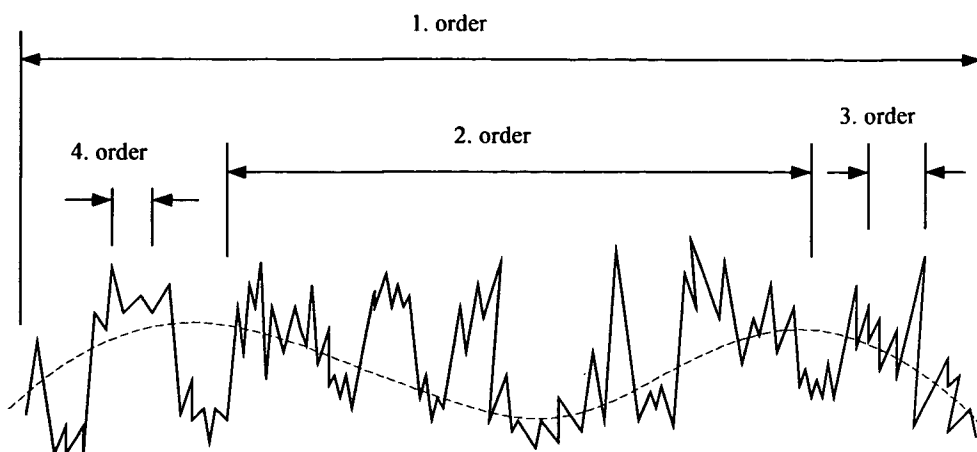


Figure 6.2.1-1 Interactions between the surface deviations

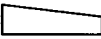
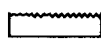
shape	example	
1. order: difference of figure 	unevenness non circularity	
2. order: wave shape 	corrugation	
3. order 	R o u g h n e s s	
4. order 		scoring scaliness
5. order no graphical representaton		crystallization chorrosion
6. order no graphical representaton		lattice structure

Table 6.2.1-1 Definition of roughness

In the following chapter the roughness parameter and their application are described. The most significant and also internationally accepted parameter is R_a , which describes the arithmetic mean of the total values referred to the absolute deviations of the tested profile and is expressed mathematically as following:

$$R_a = \frac{1}{l} * \int_0^l |y[x]| dx$$

Equation 6-1

R_t (=P_t) is the distance of the highest to the lowest point in the profile, whereas it is calculated via a reference length:

$$R_t = R_{pos} + |R_{neg}|$$

Equation 6-2

In the next figure the various parameters are illustrated schematically.

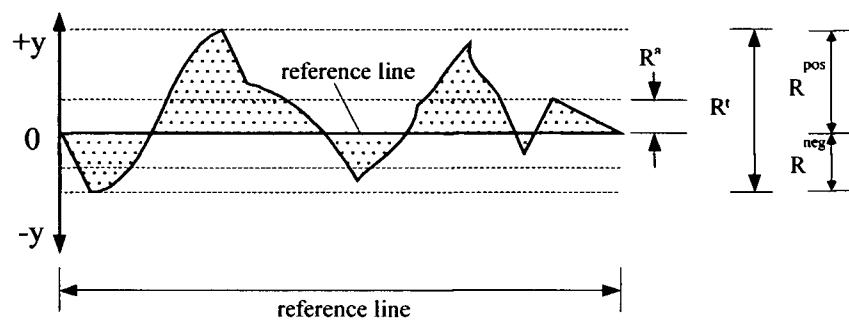


Figure 6.2.1-2 Roughness parameter

The results of the roughness measurements of the lamellae, which were treated with different abrasive papers are shown in the following table resp. diagram.

lamella	Nr.	surface	R _a [μm]	R _t [μm]
C200/2000	1	1 front	2,76	47,96
	2	1 back	0,54	5,42
C150/2000	3	1 front	5,10	57,95
	4	1 back	0,64	17,20
	5	2	1,78	18,33
	6	3	6,73	59,18
	7	4	2,45	28,43

Table 6.2.1-2 Roughness parameter of tested lamellae

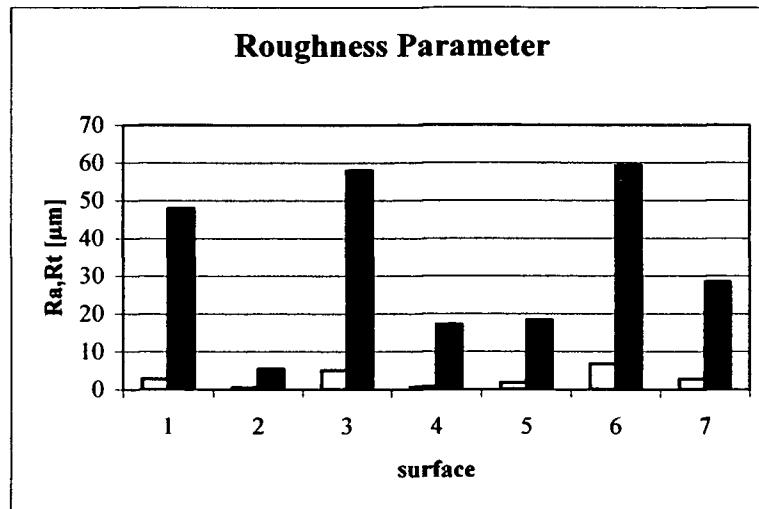


Figure 6.2.1-3 Plotted roughness parameter [29]

6.2.2. Pull-out test in general

In this chapter the pull-out test is described and failure modes are discussed. Contrary to ripped or flat steel bars the lamellae are rectangular and exhibit a relatively flat surface. The bonding of ripped steel is of crucial importance for the application of “high strength” reinforcing steels like BSt 500 and BSt 550 in RC structures. Good bonding performance enables short anchoring lengths and hence small crack distances and crack widths. The quality of the bonding is determined by the

- composition, tensile and compressive strength of structural concrete
- rib geometry and diameter of steel reinforcement
- position of steel reinforcement and concrete cover
- stress level, static / dynamic

The correlation between tensile force in the steel reinforcement resp. the bonding stress τ and the displacement Δ of the loaded steel bar relative to the surrounding concrete is determined through pull-out tests in concrete specimen with short anchoring length. Especially in the case of thick steel bars and small concrete cover longitudinal cracks can be observed, which diminish the bonding performance. Hence the anchoring length of the steel bars increases, the tensile loading of the concrete between the bending cracks decreases and the width of the bending cracks increases.

Bond models describe mathematically the load transfer from the steel bar to the surrounding concrete, whereas the basis is the separation of the bonding effect in different mechanisms:

- adhesion
- friction
- shear bond due to ribs

The amount of transferable bonding load depends on the relative displacement between the steel bar and concrete, i. e. the slip Δ .

Adhesion

Pure adhesion bases on chemical-physical binding forces between steel surface and concrete. It is effective only until the concrete is deformed without slip of the steel bar resp. the slip is very low, e. g. $\Delta < 0.001$ mm.

Friction

The friction arises from the roughness of the steel surface in the presence of a normal force, which probably originates from the cramping effect of the micro fragments of the hardened cement paste. Another contribution to the friction yields the “lack of fit”-effect. Due to the variation of the diameter of the steel bars (waviness) an additional friction is activated at large slips (see next figure).

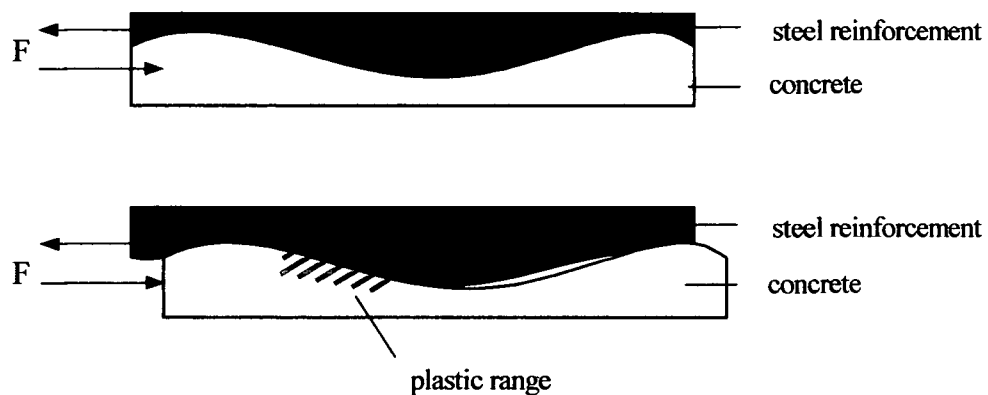


Figure 6.2.2-1 Bonding effect due to “lack of fit”

Shear bond

Shear bonding originates from the shear resistance of the concrete between the steel ribs. The concentrated load transfer on the rib flanks leads to plastic deformations of an increasing concrete volume until fracture occurs. The fracture surface may develop parallel or inclined to the steel bar. The first leads to a drastic decrease of bonding stress (zipper effect and missing friction), the

latter causes an increasing cramping force due to the wedging effect of the sheared concrete cone. In this way a further load increase is possible until the tensile ring stresses cause bursting cracks around the steel bar. The decisive parameter for the rib geometry was introduced by REHM as the “referred rib area”.

Bonding failure due to longitudinal cracking

It is distinguished from the pure bonding failure, where the steel bar is pulled out of the concrete with nearly constant load without formation of longitudinal cracks.

Rib geometry and concrete cover determine the failure mode. For cyclic and alternating loading differences could be observed between ribbed and flat steel bars. Ribbed steels exhibited damage or even bonding failure already at small slips, whereas flat steel bars were able to transfer almost the same load at the beginning of slip and at considerably displacements. [32]

Regarding the type of loading RC beam may be divided into three regions:

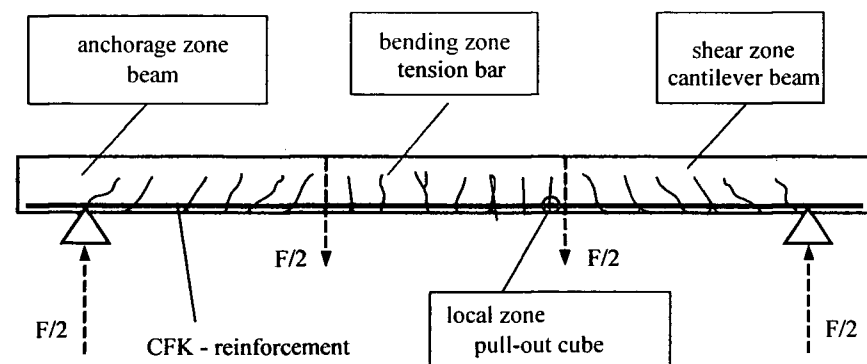


Figure 6.2.2-2 Loading regions of a reinforced concrete beam

6.2.3. Testing variants

In this section the different shapes of specimen are compared and evaluated according to the following aspects:

- **Applicability:** suitability of the testing method to simulate special loading regions in the structure and possible effects on the results
- **Setup:** characteristic structural features of the specimen
- **Testing:** testing equipment and possible measurements

Aim of bond tests is to determine the relation between the slip of the reinforcing steel bar relative to the concrete and the according bond stress $\tau = f(\Delta)$ and fracture behaviour of the bonding. Criteria are good simulation of a certain loaded region of a structure, simple setup, testing method and evaluation.

Strain specimen

Regarding the bonding effect only the slip measurement on the ends can be simply evaluated, whereas the distribution of the steel strain, displacements and bond stresses along the specimen are difficult to measure resp. to calculate from deformations and crack widths obtained at the concrete surface.



Figure 6.2.3-1 Simple strain specimen

The test is simple because it can be performed in a standard testing machine without special supplies. The following measurements can easily be performed: strain distribution at the concrete surface, slip of steel bar at the ends of the specimen, crack distances and widths and length and width of eventually longitudinal cracks. The steel bar may also be placed eccentrically in order to simulate the conditions in bending regions.

Console shaped pull-out specimen

The steel bar is placed in the salient part of the specimen with small concrete cover. In case of a specimen with real console the eccentricity of the testing load has to be compensated by horizontal loads in a complicated manner. This problem is avoided if a slotted console specimen is used.

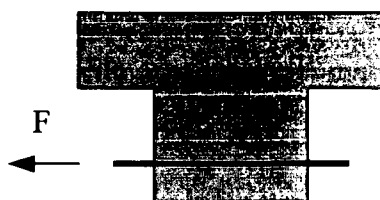


Figure 6.2.3-2 Console shaped pull-out specimen

Compared to the standard strain specimen the possibility of application of the console shaped pull-out specimen is extended considerably because the concrete is loaded in tension, no vault

effect resp. horizontal reaction load appears inside the bond length, no impediment of transverse strain originates so that longitudinal cracks can be formed without falsifying influences. Therefore the results may be transferred well on the bonding behaviour in the structural element.

Pull-out specimen with tensile loading of concrete

Tensile loading of concrete usually is achieved by loading of several cast-in-place steel bars in opposite direction, whereas on one end there is pulled only the tested bar. The slip may be measured at the loaded or at the not loaded end.



Figure 6.2.3-3 Pull-out specimen with tensile loading

This kind of loading corresponds better to the real conditions than the standard strain specimen. Therefore the test results may be representative for the bond behaviour in the structure. Due to the unavoidable formation of separating cracks the bond can be investigated only for small slips.

Beam or beam sections

The beam section in fig. 6.2.3-4 exhibits the principal structural features like not bonded ends for variable anchoring lengths, stirrups for transverse loading and complicated beam joints.

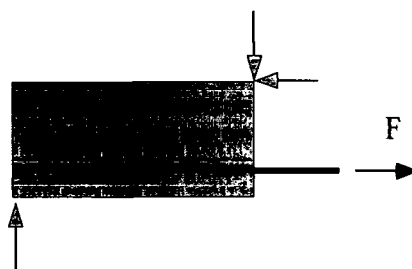


Figure 6.2.3-4 Beam or beam section

Beam sections require a sophisticated bearing to resist the concrete compressive forces and the joint has to be adjusted non-positively. This testing method simulates very well the conditions in the regions of bearings or shear loading.

Pull-out specimen

The set-up of a pull-out specimen is very simple and hence it is commonly used. A few disadvantages may be reduced by special set-up features and an increased number of influences on the bonding behaviour, e. g. small anchoring lengths for determining the basic bonding law and the ultimate bonding stress can be acquired.

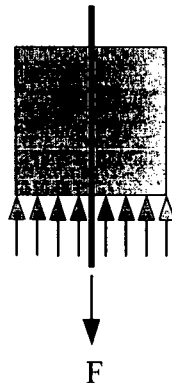


Figure 6.2.3-5 Pull-out specimen

Testing with pull-out specimens is suitable for comparative purposes. In this way defined influences on the bonding behaviour can be studied, e. g. rib form, surface condition (corrosion, coatings, contamination), bar diameter, concrete type and position of the reinforcing bar. Direct information about the bonding behaviour inside the structural element cannot be gained. Due to the simple testing method it is practical to perform an increased number of tests so that only one parameter must be changed and the statistical information is adequate. [32]

For this reasons and by comparing the possibilities this testing method was chosen to perform the pull-out tests.

6.2.4. Bursting effect resulting from bonding

As already mentioned the tensile ring stresses around the steel bar may lead to the formation of bursting cracks. If the allowable steel stress is applied for the minimum concrete cover longitudinal cracks may originate. Another cause for longitudinal cracks can be the bursting effect of corrosion products on the steel surface, but this is irrelevant for CFRP-lamellae.

Due to the fact that in praxis longitudinal cracks usually are existing, one may expect adequate calculations only if basic laws are utilized in which the formation of longitudinal cracks is

considered. Hereby it has to be distinguished whether the longitudinal crack width is limited by a transverse reinforcement or not.

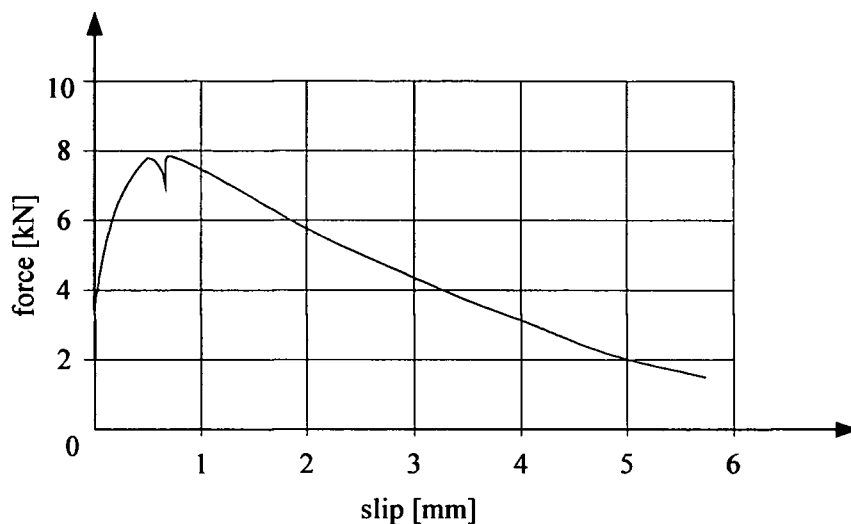


Figure 6.2.4-1 Example for a basic bond law

6.2.5. Experimental set-up of the pull-out tests

The chosen testing method corresponds to that shown in fig. 6.2.3-5, whereas further distinctions according to the next figure have to be considered.

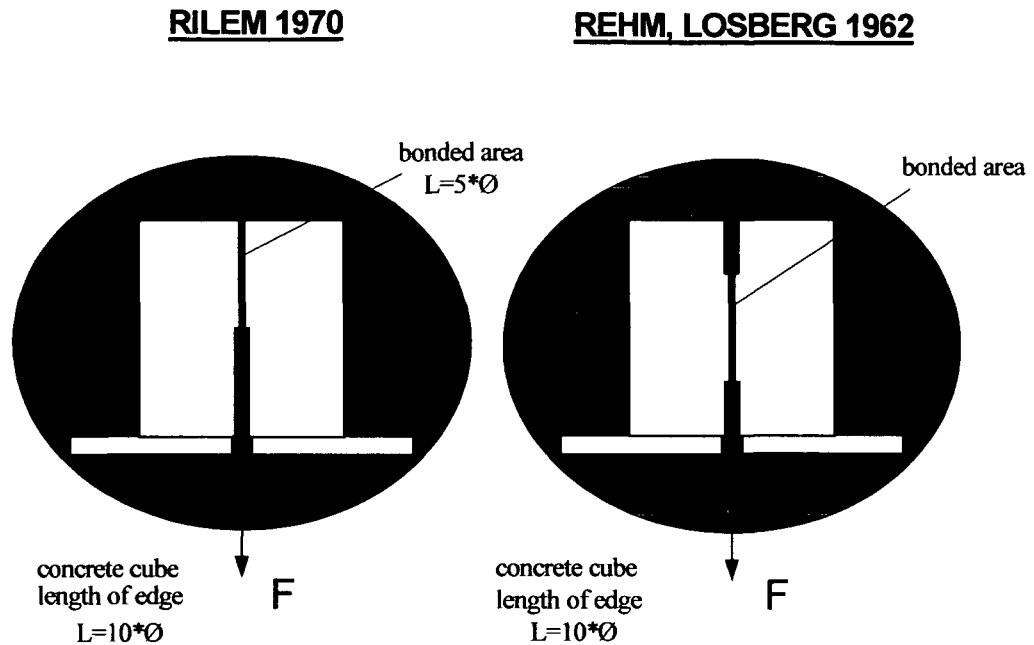


Figure 6.2.5-1 Example for two different pull-out tests

A common way to determine the elastic bond between matrix and fiber consists of defining the maximum bond stress τ_{\max} and the bond modulus κ by means of analytical models (shear lag theory) using the results of the pull-out tests. Under the assumption of fixed boundary conditions these models are described by complex algebraic equations (see chapter 6.3.). [33]

By means of the tests the bonding failure mechanisms can be determined and constitutive bonding laws may be defined and tested e. g. with a finite element program. It is also possible to introduce a mathematical formulation which might be appropriate for the praxis.

6.2.6. Manufacturing

Four series of concrete cubes with three single different lamellae were casted in a usual commercial formwork.

serie	lamella with [mm]	lamella thickness [mm]	surface [mm]	embedded length [mm]	cube dimension [mm]	concr. ---	test number ---
1	5	1,40	smooth - Type 1	50	100	SCC	1-3
2	5	1,40	rough - Type 4	50	100	SCC	4-6
3	10	1,40	smooth - Type 1	50	100	SCC	7-9
4	10	1,40	rough - Type 4	50	100	SCC	10-12

Table 6.2.6-1 Tested materials

In the following figures the formwork and the geometry of the cubes are illustrated. The lower 50 mm of the CFRP-lamellae are covered and their position is fixed by a steel profile.

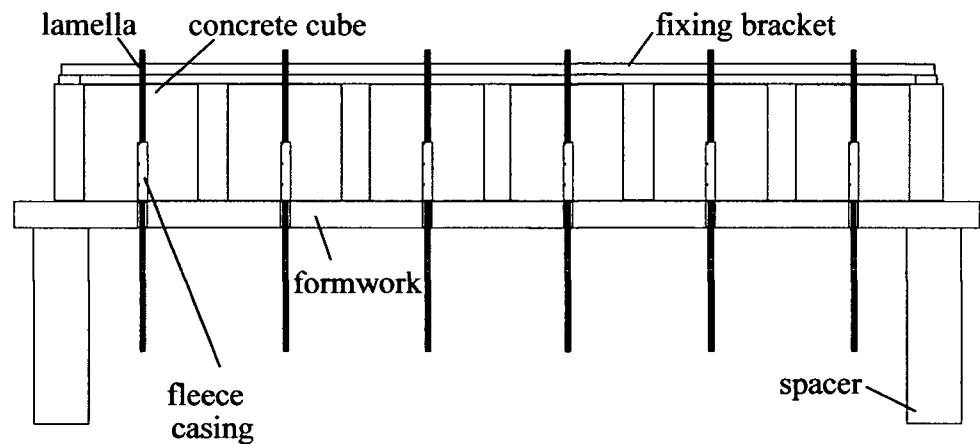


Figure 6.2.6-1 Formwork of specimen

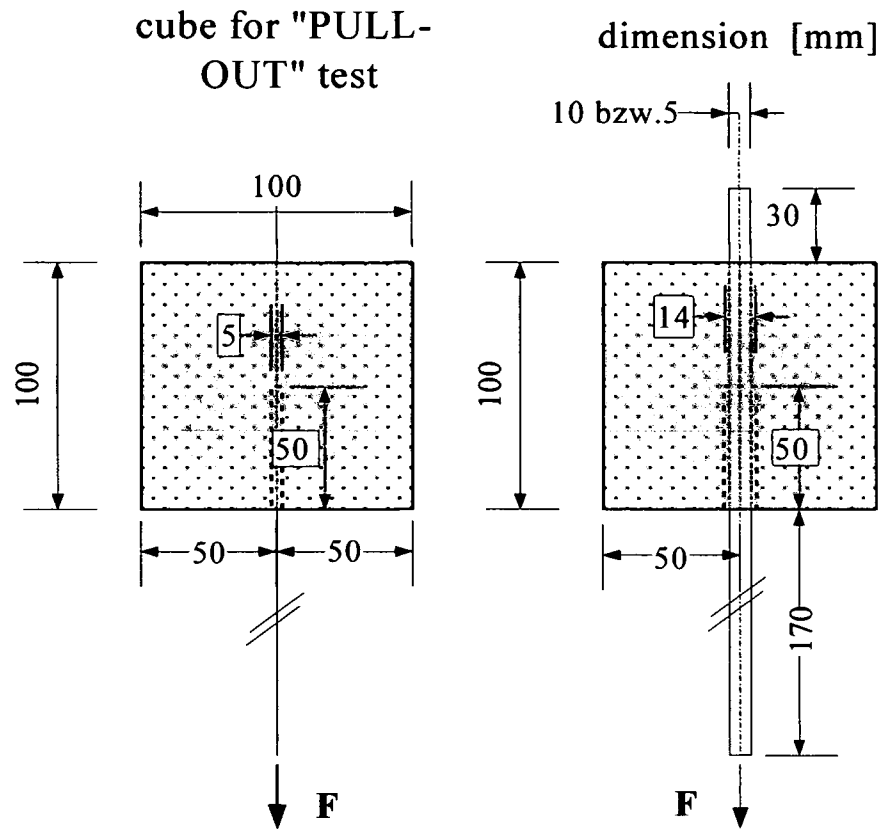
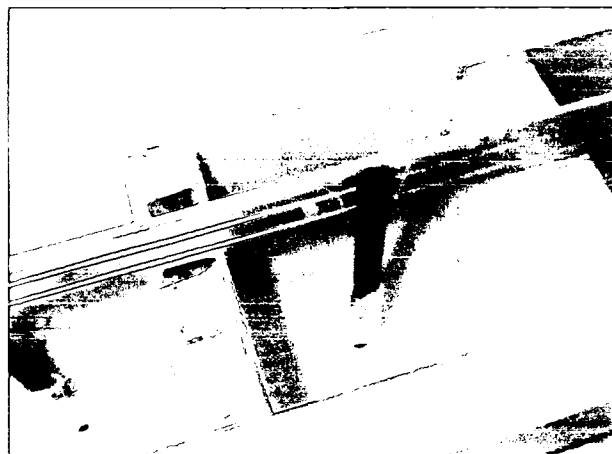


Figure 6.2.6-2 Cube geometry and anchoring length of CFRP-lamellae



Picture 6.2.6-1 Detail of formwork with lamellae

6.2.7. Data acquisition system

The slip of the CFRP-lamella was measured at the free end and at the loaded end by means of displacement transducers with an accuracy of 1/100 mm. After conditioning and A/D-converting the signals were stored in a personal computer (see next fig.).

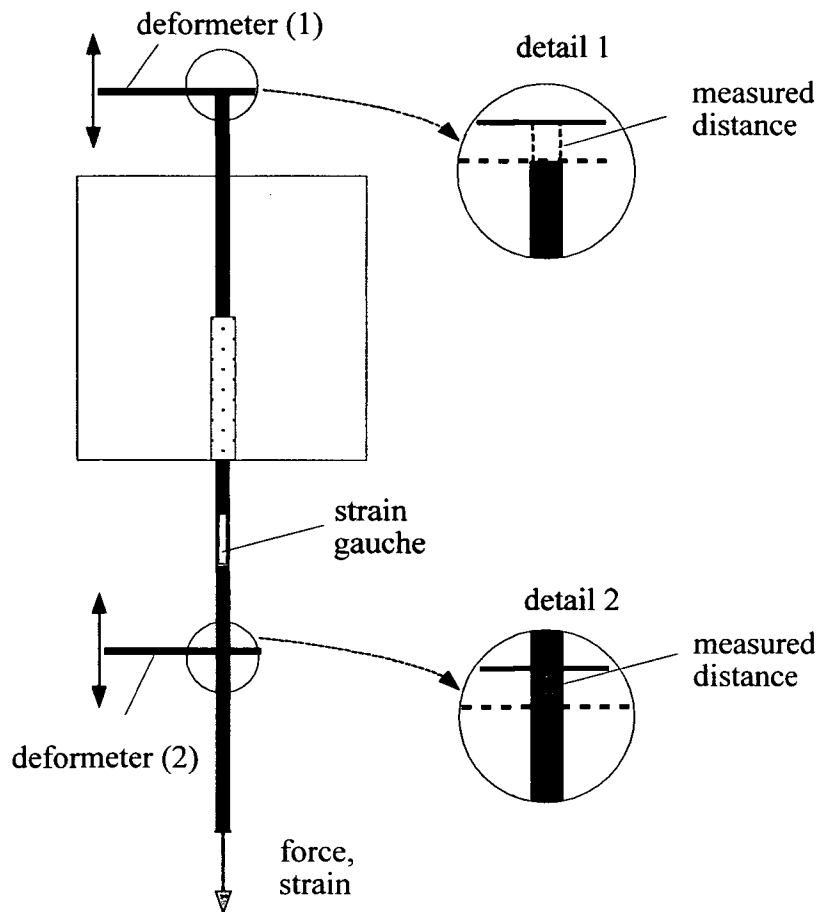
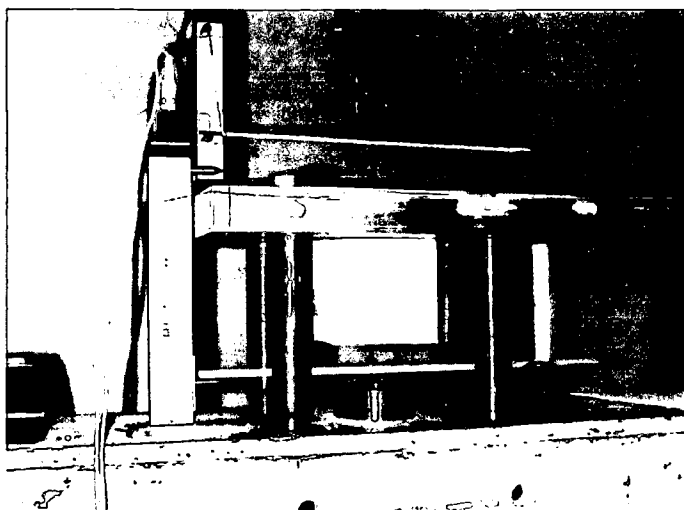


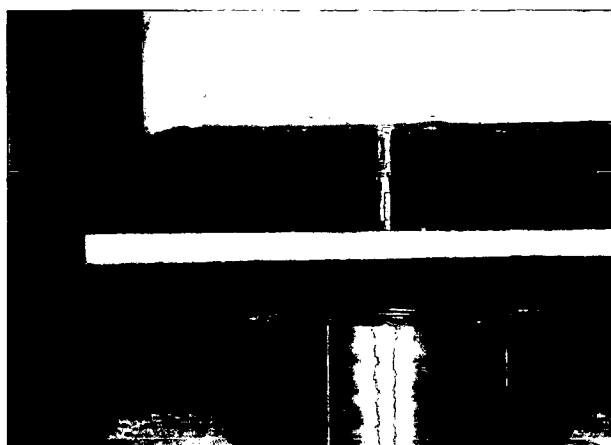
Figure 6.2.7-1 Test and measurement setup

The displacement transducer at the free end measured the slip between lamella and concrete, at the loaded end also the strain of the lamella was recorded, which had to be corrected in the further evaluation.



Picture 6.2.7-1 Pulling device with test specimen

By means of a hydraulic actuator the lamella is loaded in tension and the load is measured by a load cell. The loading speed was 0.1 mm/min.



Picture 6.2.7-2 Damaged lamella after testing

6.2.8. Test results

Four different lamella surfaces were tested with each series consisting of three tests. In the next figures there are shown the results of lamellae with a flat and a rough surface, whereas the width was 5.0 mm and the thickness 1.4 mm (cross section of 7 mm²). The blue line represents the slip at the free end, the red one stands for the slip inclusive the linear strain of the lamella measured at a height of 150 mm beyond the concrete surface. To obtain the corrected value the linear strain is subtracted from the

measured slip (orange line). The linear part of the orange line represents the bond modulus κ . It can also be clearly seen that the blue and the orange line are almost identical.

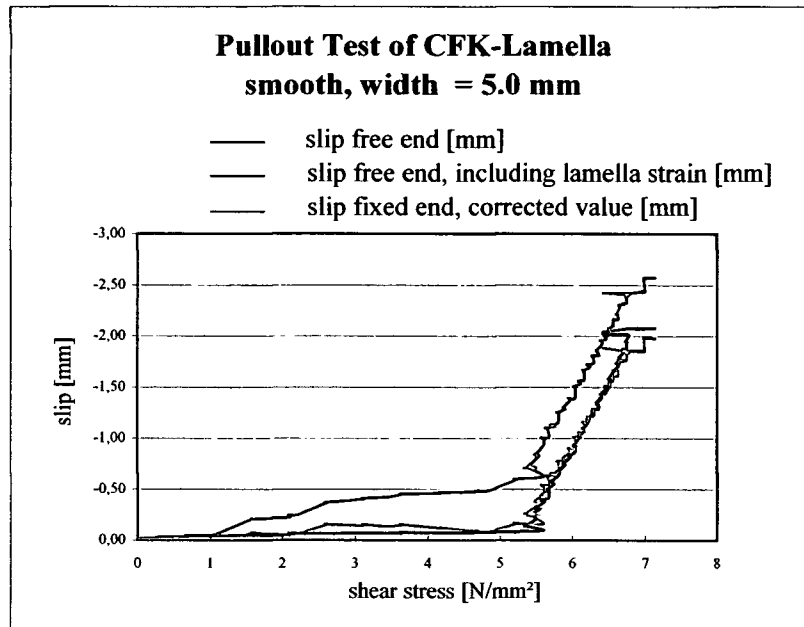


Figure 6.2.8-1 Stress-slip relation of a lamella with flat surface and a width of 5 mm

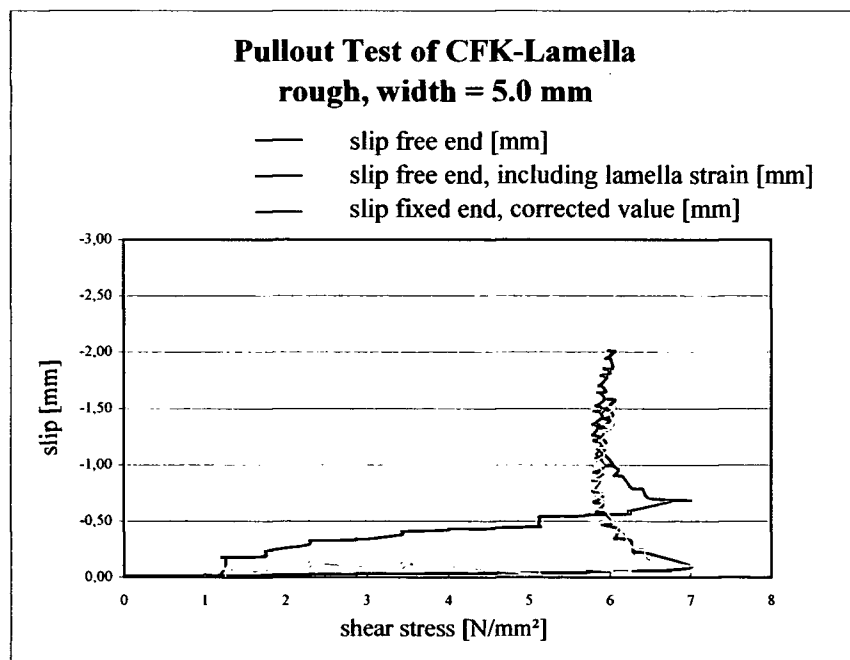


Figure 6.2.8-2 Stress-slip relation of a lamella with rough surface and a width of 5 mm

6.2.9. Analysis of the results

The two different surfaces cause a different slip behaviour. The flat lamella failed at a stress of about 5.7 N/mm² and an according slip of 0.1 mm. The subsequent quasi-linear part indicates that only few debris of hardened cement paste were detached in the sliding gap and hence the cramping effect is almost missing (see chapter 6.2.2.). Therefore the stress increment until total failure at 6.8 N/mm² is moderate and the according slip of 1.8 mm is rather high. The rough lamella exhibited a linear behaviour until the maximum stress of nearly 7 N/mm² at a slip of 0.1 mm and a subsequent decrease until a constant level of 5.9 N/mm². The bond of the rough lamella is more stiff compared to the flat one. In the next figure the lamellae with a width of 5 mm and 10 mm are compared.

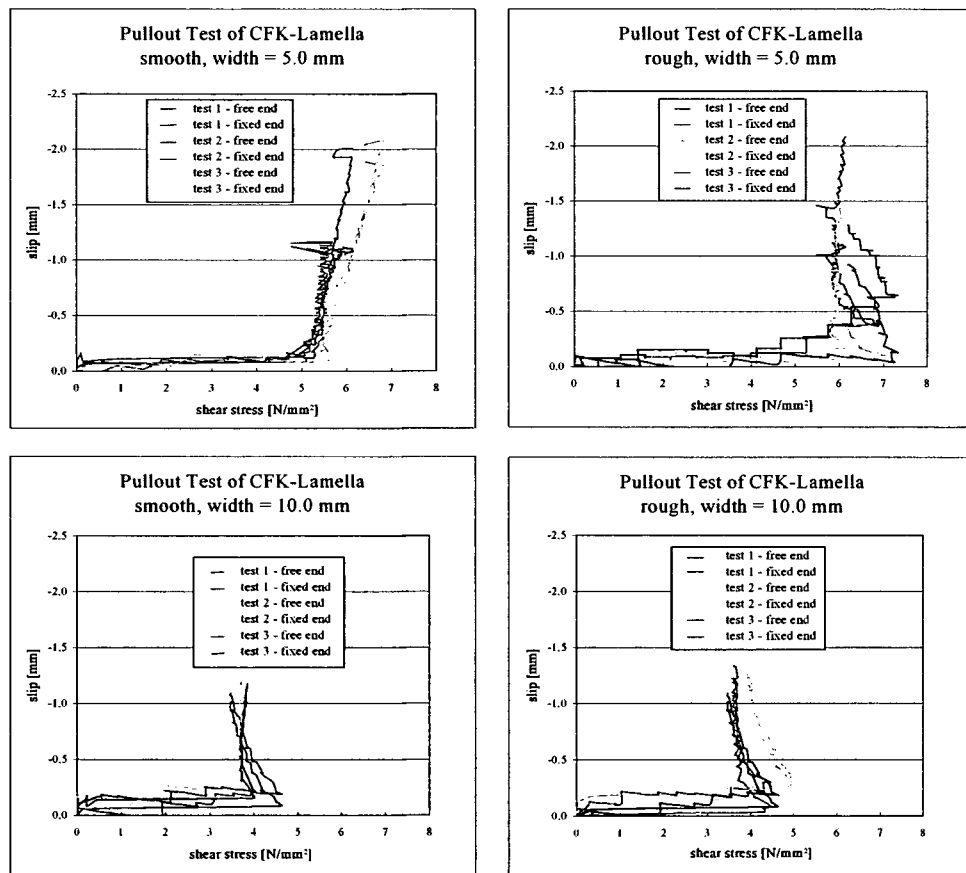


Figure 6.2.9-1 Pullout test results of 5 mm and 10 mm wide lamellae

Finally the ultimate values of the single tests are summarized in the following table.

surface	width [mm]	bond modulus [N/mm ³]	slip [mm]	sheared stress [N/mm ²]	load [N]
smooth	5,00	39,08	0,132	5,08	3251,20
rough	5,00	57,52	0,129	6,92	4428,80
smooth	10,00	21,18	0,197	4,17	4756,10
rough	10,00	20,54	0,223	4,62	5226,80

Table 6.2.9-1 Summary of main results

6.3. Simplified evaluation

The basis consists of the simple pullout test with the already mentioned disadvantages and of the shear lag theory of elasticity, which was introduced by COX.

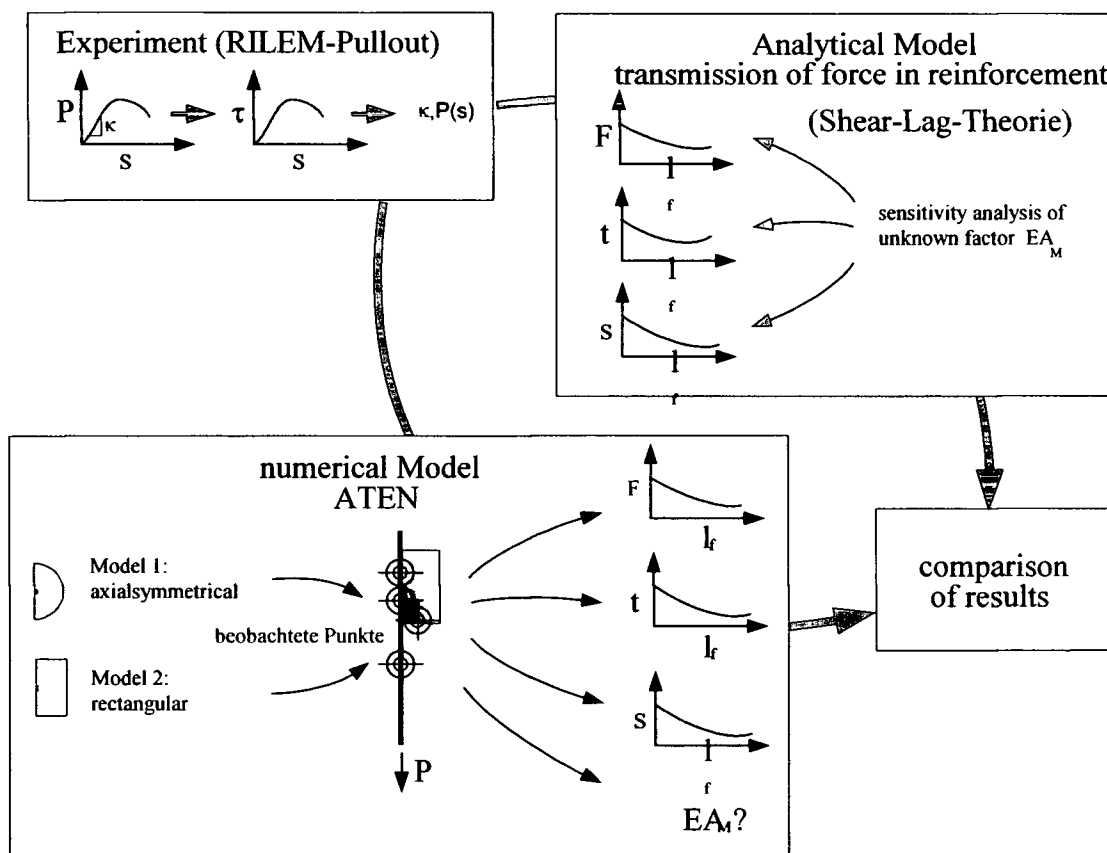


Figure 6.3-1 Steps to compare model and test [29]

The following assumptions are valid:

- Fiber and matrix are cylindrical
- Constant distribution of forces and displacements over the cross section of the fiber, i. e. the partial cross sections remain plane
- Only displacements in longitudinal direction occur
- Shear deformations arise only in the contact zone due to the difference $s(x)$ – slip, displacement between fiber and matrix
- The linear relation between local bond stress $\tau(x)$ and $s(x)$ for the perfect bond is characterized by the bond modulus κ in N/mm^3

$$\tau(x) = \kappa * s(x) \tag{Equation 6-3}$$

- Linear elastic material behaviour, i. e.

$$F(x)_{F,M} = \epsilon(x)_{F,M} * (EA)_{F,M} \tag{Equation 6-4}$$

With the fiber circumference U the equilibrium condition at the fiber element yields

$$\frac{dF(x)}{ds} = U * \tau(x) = t(x) \tag{Equation 6-5}$$

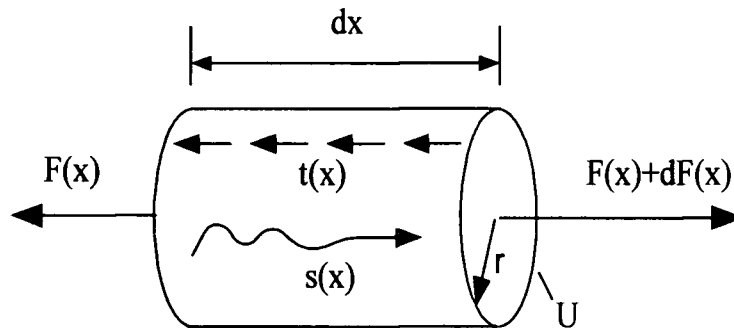


Figure 6.3-2 Forces and stresses at the fiber element

The local slip $s(x)$ is defined as the difference between local displacement of the fiber $u_F(x)$ and the matrix $u_M(x)$ and is attained by

$$s(x) = u_F(x) - u_M(x)$$

Equation 6-6

$$\frac{du(x)}{dx} = \varepsilon(x)$$

Equation 6-7

$$\frac{ds(x)}{dx} = \varepsilon F(x) - \varepsilon M(x)$$

Equation 6-8

$$\frac{d\tau(x)}{dx} = \kappa \frac{ds(x)}{dx} = \kappa(\varepsilon F(x) - \varepsilon M(x))$$

Equation 6-9

After elimination of the strain of fiber and matrix one gets the difference equation which is valid under the assumptions made in the shear lag theory:

$$\begin{aligned} \frac{d^2 FF(x)}{dx^2} &= U * \frac{d\tau(x)}{dx} = U * \kappa \frac{s(x)}{dx} = U * \kappa * (\varepsilon F(x) - \varepsilon M(x)) = \\ &= U * \kappa * \left[\frac{FF(x)}{EAF} - \frac{FM(x)}{EAM} \right] \end{aligned}$$

Equation 6-10

The equilibrium of the internal forces of fiber and matrix at x yields

$$F_F(x) = -F_M(x)$$

Equation 6-11

With these force equilibrium conditions the force $F_M(x)$ can be eliminated. Using the factor λ

$$\lambda = \sqrt{U * \kappa \left[\frac{1}{EAF} + \frac{1}{EAM} \right]}$$

Equation 6-12

The bearing condition is

$$F''_F(x) - \lambda^2 * F_F(x) = 0$$

Equation 6-13

This pullout type is suitable for the variant according to RILEM and may be applied due to the force distribution $F_F(x=0) = 0$ and $F_F(x=l/2) = P$ holds.

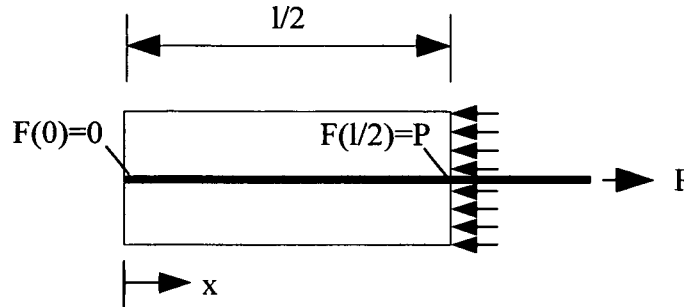


Figure 6.3-3 Pullout cube system

Distribution of load $F_F(x)$ in the fiber

$$F_F(x) = \frac{P * \sinh(\lambda x)}{\sinh(\frac{1}{2} \lambda l)}$$

Equation 6-14

Derivation of $F_F(x)$ yields the shear flow

$$\tau(x) = \frac{P * \lambda \cosh(\lambda x)}{\sinh(\frac{1}{2} \lambda l)}$$

Equation 6-15

and the slip $s(x)$

$$s(x) = \frac{P * \lambda \cosh(\lambda x)}{\kappa * U \sinh(\frac{1}{2} \lambda l)}$$

Equation 6-16

Hereby the formulas for the perfect bond are completed. [33]

7. Summary

Carbon fibers and carbon fiber laminate show a large scope of application in modern structural engineering. Due to their corrosion resistance, fiber reinforced polymer materials gain increasingly more attention as a reinforcing option for concrete. Today, high costs make those new materials little attractive for general applications, but there are some special cases where it makes sense to apply lamellas instead of steel. The lamella type used for the main part of this work shows tensile strength of 2.700 – 3.000 N/mm² and a Young's modulus of 165.000 N/mm². The density of the material is 1.8 g/cm³.

The investigated application of the carbon lamella is a type of reinforcement grid, which is woven of carbon lamella bars and combined with self-compacting concrete. The bonding behaviour with concrete and the bending behaviour of slabs, reinforced with this kind of grid are tested. The crack widths and the crack distances are measured and turn out to be in the range of common steel reinforced slabs. The mesh sizes are varied to quantify the required reinforcement ration for concrete slabs.

Though the crack formations give information about the bond between lamella and concrete, the difference between the bond behaviour of a smooth and a rough lamella has to be investigated. Pullout tests with a RILEM cube [10cm x 10cm x 10 cm] quantify the bonding between the two surfaces. Four lamella surface types are analyzed by means of an embedded length of 50 mm and two cross sections of the lamella.

Four types are tested. Type 1 is a not treated lamella, type 2-4 are roughened with abrasive paper Nr. 40 to 80. For example, the pullout tests show that the roughened lamella with a width of 10 mm fails at load values of approximately 5.200 N, the smooth lamella fails at a load value of 4.800 N.

This result shows a gain in bond of about 10% due to the roughening. In the case of the smaller lamellas the gain due to roughness turned out to be more than 35%. Two tested lamellas with 5.0 mm and 10.0 mm width show an increase in bond of about 30% in the case of the roughened surface type 4.

A comparison of the Pullout tests results and a simplified analysis of force distribution, shear stress and slip in the embedded part of the lamella turn out that the best accordance of results can be found for the case that the concrete area around the lamella has a radius of at least 10.0 mm.

The contents of this diploma thesis are applied in investigations to find an ideal reinforcement content and to test practical applications for these reinforcement systems. One example is the reinforcement of shell structures.

Literature

- [1] Lafarge Perlmooser: Zement und Beton, 31. verbesserte und erweiterte Auflage, Wien, Zement + Beton Handels- und Werbe-GmbH, J.C.König & Ebhardt AG, 1997 / 98
- [2] Böhm, Geiger, Valentin: Stahlbetonbau, 3-te verbesserte und erweiterte Auflage, Wien, Manzsche Verlags- und Universitätsbuchhandlung, 1984
- [3] ÖNORM B 4200, Teil 10, Beton – Herstellung und Überwachung, Österreichisches Normungsinstitut, Wien, Johann Zellmayer's Söhne Ges.m.b.H., 1983
- [4] Huber G.: Baustoffkunde III, 1. Auflage, Wien, Manzsche Verlags- und Universitätsbuchhandlung, Österreichischer Bundesverlag GmbH., 1981
- [5] Michl H.: Anorganische Chemie, 2. Teil, Institut für Chemie, Universität für Bodenkultur, Wien, ÖH - Wirtschaftsbetriebe GmbH., 1988
- [6] Bergmeister K.: Konstruktion I, 4. Auflage, Institut für Konstruktiven Ingenieurbau, Universität für Bodenkultur, Wien, 1997
- [7] Ramberger, Hartl: Stahlbau und konstruktiver Holzbau, 1. Auflage, 1. Teil, Wien, Manzsche Verlags - und Universitätsbuchhandlung, Österreichischer Bundesverlag GmbH., 1985
- [8] Bouche, Leitner, Sass: Dubbel, Taschenbuch für den Maschinenbau, 13-te Auflage, 1.Band, Springer - Verlag, Berlin / Heidelberg, 1974
- [9] Bergmeister K.: Ingenieurtragwerke - konstruktiver Stahlbau, 4. Auflage, 1. Band, Institut für Konstruktiven Ingenieurbau, Universität für Bodenkultur, Wien, 1997 / 98
- [10] Universität Aachen: [http:// www.rwth-aachen.de /imb/publik/umdrucke/mb1,MI Baustoffe](http://www.rwth-aachen.de/imb/publik/umdrucke/mb1,MI_Baustoffe)

-
- [11] Bergmeister K.: Stahlbetonbau, 1. Auflage, Institut für Konstruktiven Ingenieurbau, Universität für Bodenkultur, Wien, 1991
- [12] Bindseil P.: Massivbau – Bemessungen im Stahlbetonbau, 2. Auflage, Vieweg und Sohn, Verlagsgesellschaft mbH., Braunschweig / Wiesbaden, 2000
- [13] Bergmeister K.: Ingenieurtragwerke - Spannbeton, 4. Auflage, 1. Band, Institut für Konstruktiven Ingenieurbau, Universität für Bodenkultur, Wien, 1997 / 98
- [14] Derschmidt M.: Diplomarbeit über vergleichende Betrachtung der Biegezugfestigkeit und Würfeldruckfestigkeit von CF-verstärktem Beton, Institut für Konstruktiven Ingenieurbau, Universität für Bodenkultur, Wien, 1999
- [15] Abel M., Thormählen U.: Kreative Ingenieurleistungen - Neubau und Ertüchtigung von Brücken mit externer Vorspannung, Institut für Statik, Technische Universität Darmstadt, Institut für konstruktiven Ingenieurbau, Universität für Bodenkultur, Wien, Darmstadt, Wien, 1998
- [16] Halser H.: Ertüchtigung von Biegebalken durch Kohlenstofffasern - Versuche und nicht lineare FE-Analysen, Diplomarbeit, Baufakultät – Architektur und Bauingenieurwesen, Leopold - Franzens Universität, Innsbruck, 2000
- [17] Meier U.: Technische Forschungs - und Beratungsstelle der Schweizerischen Zementindustrie, Tagungsband, Verstärken von Tragwerken mit CFK-Lamellen- Kapitel 1, Schulungszentrum TFB, Wildeg, Schweiz, 1997
- [18] Scherer J., Hochleitner F.: MBrace® - Systeme für Bauteilverstärkungen, Broschüre von MBT Austria Bauchemie, Lanzendorf, 1999
- [19] ÖNORM B 4700, Stahlbetontragwerke, Eurocode nahe Berechnung, Bemessung und konstruktive Durchbildung, Österreichisches Normungsinstitut, Wien, 1995
-

-
- [20] Bergmeister K.: Verstärken mit CFK - Lamellen In: Neue Normen und Technologien für Beton - und Spannbetonbauten, Ltg. Wicke M., Österreichischer Betonverein, 22. Auflage, Innsbruck, 1999
- [21] Deutsches Institut für Bautechnik: Allgemeine bauaufsichtliche Zulassung, Verstärkung von Stahlbeton - und Spannbetonbauteilen durch schubfest aufgeklebte Kohlenfasernlamellen "Sika CarboDur", 1999
- [22] Deuring M.: Verstärken von Stahlbeton mit gespannten Faserverbundwerkstoffen, EMPA (Eidgenössische Materialprüfungs - und Forschungsanstalt) Forschungsbericht Nr.224, Zürich, Schweiz, 1993
- [23] Scherer J.: Kreative Ingenieurleistungen - Faserverbundwerkstoffe in der Bauverstärkung, Technische Universität Darmstadt, Institut für Konstruktiven Ingenieurbau, Universität für Bodenkultur, Wien, Darmstadt, Wien, 1998
- [24] Deutsches Institut für Bautechnik: Richtlinien für das Verstärken von Betonbauteilen durch ankleben von Stahllaschen, Deutschland, Schweiz, 1993
- [25] Meier U.: Composite Materials in Bridges, In: Bridge Engineering Conference 2000, Past Achievements, Current Practices, Future Technologies, Sinai, Egypt, 26-30 March, 2000
- [26] Burkhardt H., Keller A., Schwegler G.: Stahlbetonverbund-Brücke mit CFK-Spannkabeln, Schweizer Ingenieur und Architekt, Heft 17, April, 1999
- [27] Guidotti N., Keller T., Como C., Haldemann C.: Konzentriert umgelenkte Karbonkabel - erstmaliger Einsatz, Schweizer Ingenieur und Architekt, Heft 17, April, 1999
- [28] MBT Austria GesmbH.: Master Builder Technologies, GLENIUMTM - die Pionierleistung für Beton, Broschüre von MBT Austria GesmbH., Österreich, Zentrale und Verwaltung - Roseggerstraße 10, A - 8670 Krieglach
-

-
- [29] Guggenberger A.: Dissertation über Carbon Fiber Reinforcement in Structural Engineering Analysis and Applications, Institut für Konstruktiven Ingenieurbau, Universität für Bodenkultur, Wien, März, 2000
- [30] 100 Jahre Beton- und Stahlbetonbauten, der Betonbau in Geschichte, Gegenwart und Zukunft – Tradition und Innovation, Heft 4, 96. Jahrgang, Ernst & Sohn, Verlag für Architektur und technische Wissenschaften GmbH, Böhrlingstraße 10, D – 13086, Berlin, April, 2001
- [31] Meßphysik: Laborgeräte Ges.m.b.H., Anwendungsliteratur, Normierung zum 3 Punkt Biegeversuch, Fürstenfeld, Österreich
- [32] Zilch K., Kupfer H.: Schlußbericht zum Forschungsvorhaben Verbund-Grundgesetze unter dem Einfluß der Sprengwirkung und der Betondeckung (Ku 239 50-1/2), Bericht Nr.1500, Institut für Tragwerkslehre, Lehrstuhl für Massivbau, Technische Universität München, München, März, 1995
- [33] Brameshuber W., Banholzer B., Brümmer G.: Ansatz für eine vereinfachte Auswertung von Faser Pull-Out-Versuchen, ibac, Institut für Bauforschung, RWTH Aachen, Deutschland

Bibliographie

- Abel M., Thormählen U.:** Kreative Ingenieurleistungen - Neubau und Ertüchtigung von Brücken mit externer Vorspannung, Institut für Statik, Technische Universität Darmstadt, Institut für konstruktiven Ingenieurbau, Universität für Bodenkultur, Wien, Darmstadt, Wien, 1998
- Bergmeister K.:** Ingenieurtragwerke - konstruktiver Stahlbau, 4. Auflage, 1. Band, Institut für Konstruktiven Ingenieurbau, Universität für Bodenkultur, Wien, 1997 / 98
- Bergmeister K.:** Konstruktion I, 4. Auflage, Institut für Konstruktiven Ingenieurbau, Universität für Bodenkultur, Wien, 1997
- Bergmeister K.:** Stahlbetonbau, 1. Auflage, Institut für Konstruktiven Ingenieurbau, Universität für Bodenkultur, Wien, 1991
- Bergmeister K.:** Ingenieurtragwerke - Spannbeton, 4. Auflage, 1. Band, Institut für Konstruktiven Ingenieurbau, Universität für Bodenkultur, Wien, 1997 / 98
- Bergmeister K.:** Verstärken mit CFK - Lamellen In: Neue Normen und Technologien für Beton - und Spannbetonbauten, Ltg. Wicke M., Österreichischer Betonverein, 22. Auflage, Innsbruck, 1999
- Bindseil P.:** Massivbau – Bemessungen im Stahlbetonbau, 2. Auflage, Vieweg und Sohn, Verlagsgesellschaft mbH., Braunschweig / Wiesbaden, 2000
- Bouche, Leitner, Sass:** Dubbel, Taschenbuch für den Maschinenbau, 13-te Auflage, 1. Band, Springer - Verlag, Berlin / Heidelberg, 1974
- Böhm, Geiger, Valentin:** Stahlbetonbau, 3-te verbesserte und erweiterte Auflage, Wien, Manzsche Verlags- und Universitätsbuchhandlung, 1984

-
- Brameshuber W., Banholzer B., Brümmer G.:** Ansatz für eine vereinfachte Auswertung von Faser Pull-Out-Versuchen, ibac, Institut für Bauforschung, RWTH Aachen, Deutschland
- Burkhardt H., Keller A., Schwegler G.:** Stahlbetonverbund-Brücke mit CFK-Spannkabeln, Schweizer Ingenieur und Architekt, Heft 17, April, 1999
- Derschmidt M.:** Diplomarbeit über vergleichende Betrachtung der Biegezugfestigkeit und Würfeldruckfestigkeit von CF-verstärktem Beton, Institut für Konstruktiven Ingenieurbau, Universität für Bodenkultur, Wien, 1999
- Deuring M.:** Verstärken von Stahlbeton mit gespannten Faserverbundwerkstoffen, EMPA (Eidgenössische Materialprüfungs - und Forschungsanstalt) Forschungsbericht Nr.224, Zürich, Schweiz, 1993
- Deutsches Institut für Bautechnik:** Richtlinien für das Verstärken von Betonbauteilen durch ankleben von Stahllaschen, Deutschland, Schweiz, 1993
- Deutsches Institut für Bautechnik:** Allgemeine bauaufsichtliche Zulassung, Verstärkung von Stahlbeton - und Spannbetonbauteilen durch schubfest aufgeklebte Kohlenfasernlamellen "Sika CarboDur", 1999
- Guggenberger A.:** Dissertation über Carbon Fiber Reinforcement in Structural Engineering Analysis and Applications, Institut für Konstruktiven Ingenieurbau, Universität für Bodenkultur, Wien, März, 2000
- Guidotti N., Keller T., Como C., Haldemann C.:** Konzentriert umgelenkte Karbonkabel – erstmaliger Einsatz, Schweizer Ingenieur und Architekt, Heft 17, April, 1999
- Halser H.:** Ertüchtigung von Biegebalken durch Kohlenstofffasern - Versuche und nicht lineare FE-Analysen, Diplomarbeit, Baufakultät – Architektur und Bauingenieurwesen, Leopold - Franzens Universität, Innsbruck, 2000
-

-
- Huber G.:** Baustoffkunde III, 1. Auflage, Wien, Manzsche Verlags - und Universitätsbuchhandlung, Österreichischer Bundesverlag GmbH., 1981
- Lafarge Perlmooser:** Zement und Beton, 31. verbesserte und erweiterte Auflage, Wien, Zement + Beton Handels- und Werbe-GmbH, J.C.König & Ebhardt AG, 1997 / 98
- MBT Austria GesmbH.:** Master Builder Technologies, GLENIUM™ – die Pionierleistung für Beton, Broschüre von MBT Austria GesmbH., Österreich, Zentrale und Verwaltung – Roseggerstraße 10, A – 8670 Krieglach
- Meier U.:** Technische Forschungs - und Beratungsstelle der Schweizerischen Zementindustrie, Tagungsband, Verstärken von Tragwerken mit CFK-Lamellen- Kapitel 1, Schulungszentrum TFB, Wildeg, Schweiz, 1997
- Meier U.:** Composite Materials in Bridges, In: Bridge Engineering Conference 2000, Past Achievements, Current Practices, Future Technologies, Sinai, Egypt, 26-30 March, 2000
- Meßphysik:** Laborgeräte Ges.m.b.H., Anwendungsliteratur, Normierung zum 3 Punkt Biegeversuch, Fürstenfeld, Österreich
- Michl H.:** Anorganische Chemie, 2. Teil, Institut für Chemie, Universität für Bodenkultur, Wien, ÖH - Wirtschaftsbetriebe GmbH., 1988
- ÖNORM B 4700,** Stahlbetontragwerke, Eurocode nahe Berechnung, Bemessung und konstruktive Durchbildung, Österreichisches Normungsinstitut, Wien, 1995
- ÖNORM B 4200,** Teil 10, Beton – Herstellung und Überwachung, Österreichisches Normungsinstitut, Wien, Johann Zellmayer`s Söhne Ges.m.b.H., 1983
- Ramberger, Hartl:** Stahlbau und konstruktiver Holzbau, 1. Auflage, 1. Teil, Wien, Manzsche Verlags - und Universitätsbuchhandlung, Österreichischer Bundesverlag GmbH., 1985
-

Scherer J., Hochleitner F.: MBrace® - Systeme für Bauteilverstärkungen, Broschüre von MBT Austria Bauchemie, Lanzendorf, 1999

Scherer J.: Kreative Ingenieurleistungen – Faserverbundwerkstoffe in der Bauverstärkung, Technische Universität Darmstadt, Institut für Konstruktiven Ingenieurbau, Universität für Bodenkultur, Wien, Darmstadt, Wien, 1998

Universität Aachen: <http://www.rwth-aachen.de/imb/publik/umdrucke/mb1>, MI Baustoffe

Zilch K., Kupfer H.: Schlußbericht zum Forschungsvorhaben Verbund-Grundgesetze unter dem Einfluß der Sprengwirkung und der Betondeckung (Ku 239 50-1/2), Bericht Nr.1500, Institut für Tragwerkslehre, Lehrstuhl für Massivbau, Technische Universität München, München, März, 1995

100 Jahre Beton- und Stahlbetonbauten, der Betonbau in Geschichte, Gegenwart und Zukunft – Tradition und Innovation, Heft 4, 96. Jahrgang, Ernst & Sohn, Verlag für Architektur und technische Wissenschaften GmbH, Bühringstraße 10, D – 13086, Berlin, April, 2001

Picture register

Chapter 2

Picture 2.1.3-1	Microphoto of a ground surface concrete..2-4
Picture 2.1.3-2	Cement stone, w/c = 0.5, after 7 days, 5000 times enlarged.....2-5
Picture 2.1.4-1	Structural constitution of concrete.....2-6
Picture 2.1.4-2	Content of meal grains: at the left too little, at the right ok.....2-8
Picture 2.4.3-3	Internal view of the Hünenburg bridge, external prestressing elements VBF-CMM D for timed shifting [30].....2-26
Picture 2.4.3-2	Internal view of Rümmecke bridge (exclusively external prestressing elements).....2-26

Chapter 4

Picture 4.1.1-1	Base material for production of CFRP-sheets.....4-2
Picture 4.3.1-1	Finished formwork with sheet reinforcement.....4-12
Picture 4.3.1-2	Sealing of joints.....4-12
Picture 4.3.2-1	Casting of the concrete cover.....4-14
Picture 4.3.2-2	Positioning of the reinforcement sheet...4-15
Picture 4.3.4-1	Transport of slabs to the water basin.....4-16
Picture 4.3.4-2	Storage of slabs under water.....4-17
Picture 4.3.4-3	Covering of basins.....4-17

Chapter 5

Picture 5.1.2-1	Test setup.....5-6
Picture 5.1.2-2	Hydraulic actuator.....5-6
Picture 5.2.1-1	Assembling of specimen.....5-8
Picture 5.2.1-2	Fixing of specimen.....5-8

Picture 5.3.1-1	Crack distribution of a slab.....5-11
Picture 5.3.1-2	Crack distribution of a slab with numbering.....5-11
Picture 5.3.2-1	Shear failure of double-layer reinforced slab.....5-12
Picture 5.3.2-2	Bending tensile failure of double-layer reinforced slab.....5-12
Picture 5.3.2-3	Bending tensile failure of single-layer reinforced slab.....5-12
Picture 5.3.2-4	Bending tensile failure of single-layer reinforced slab (lateral).....5-13
Picture 5.3.2-5	Failure of concrete cover.....5-13
Picture 5.3.3-1	Totally destroyed slab with CFRP reinforcement.....5-14
Picture 5.3.3-2	Enlargement of picture 5.3.3-1 with visible concrete cover.....5-14
Picture 5.3.3-3	Abraded concrete close to the lamellae...5-14

Chapter 6

Picture 6.1.2-1	Testing equipment.....6-2
Picture 6.1.2-2	Tested lamella at the left.....6-2
Picture 6.2.6-1	Detail of formwork with lamellae.....6-16
Picture 6.2.7-1	Pulling device with test specimen.....6-18
Picture 6.2.7-2	Damaged lamella after testing.....6-18

Appendix

Picture A – 1	Rovings on spools , which are pulled together in the first production step.....A-10
Picture A – 2	Consolidation and spread prozess.....A-10
Picture A – 3	Impregnation with liquid matrix – glass fiber.....A-10

Picture A – 4	Profiling and hardening prozess in casting forms with lateral rolled-on borders which are removed finally.....A-11
Picture A – 5	Heated nip roll, which gives the fitting thickness to the matrix by means of high pressure.....A-11
Picture A – 6	Post curing with hot air – result of the nip roll, shown in picture A – 5.....A-12
Picture A – 7	Pull-off process by means of a rubber cylinder and cutting in fitting width.....A-12
Picture A – 8	Separator and rewinder of the glassfiberlaminat.....A-12
Picture A – 9	conveyer band with heated nipp rolls....A-13
Picture A – 10	Square cut of carbon fiber laminate to be applied for example for sports goods.....A-13

Table register

Chapter 2

Table 2.1.3-1	The main cement colour codes.....2-3
Table 2.1.4-1	Limits for the content of smaller and larger grains.....2-7
Table 2.1.6-1	Concrete strength vs. w/c-ratio.....2-9
Table 2.1.6-2	Concrete consistencies [6].....2-10
Table 2.1.7-1	Common types of additives.....2-11
Table 2.1.8-1	Concrete strength classes and specifications according to EC2 (in N/mm ²) [10, 12]...2-12
Table 2.1.8-2	Concrete strength classes and specifications according to DIN 1045 (in N/mm ²) [10]..2-12
Table 2.1.8-3	Concrete strength classes and specifications according to ÖN 4700 (in N/mm ²) [19]...2-12
Table 2.1.8-4	Concrete strength classes and specifications according to ÖN 4200 part 10 (in N/mm ²) [2,3].....2-13
Table 2.2-1	Steel classes according to ÖN 4200 part 7 (units in N/mm ²) [6].....2-17
Table 2.2-2	Steel classes according to DIN ISO 898 (units in N/mm ²) [6].....2-17

Table 2.2-3	Steel classes according to ÖN 4700 (units in N/mm ²) [19].....2-17
--------------------	--

Chapter 3

Table 3.2.2-1	Strength values of CFRP-lamellae with 70% fiber content [17].....3-5
Table 3.2.2-2	Technical elasticity parameters of CFRP-lamellae with 70% fiber content [17].....3-5
Table 3.2.2-3	Thermal properties of CFRP-lamellae with 60% fiber content [17].....3-5
Table 3.2.2-4	Electric resistance of CFRP-lamellae with 60% fiber content [17].....3-5
Table 3.2.3-1	Properties of duroplastics and thermoplastics.....3-6
Table 3.4.2-1	Relative equivalent Young's modulus....3-11
Table 3.4.6-1	Overview of carbon and glass fiber composite materials.....3-13
Table 3.4.6-2	For comparison: structural steel.....3-14

Chapter 4

Table 4.1.1-1	Dimensions of CFRP-sheets and reference slabs.....4-3
Table 4.1.2-1	Composition of concrete.....4-4
Table 4.1.3-1	Values of dry grading curve.....4-5
Table 4.1.4-1	Concrete composition in weight and volume percent.....4-7
Table 4.1.4-2	Corrected concrete composition in weight and volume percent.....4-7
Table 4.2-1	Composition of SCC [29].....4-9
Table 4.2-2	result of analyses about zero concrete [29]4-11
Table 4.3.2-1	Results of the slump test.....4-14
Table 4.3.3-1	Mechanical properties of base concrete...4-16

Chapter 5

Table 5.3.1-1	Measured crack widths for a double-layer reinforcement.....5-10
Table 5.3.4-1	Ultimate stress and load with according strain resp. deflection.....5-16
Table 5.3.4-2	Stress and load at 2‰ and 4‰ strain and according deflection.....5-17
Table 5.3.4-3	Ultimate stress and load with according strain resp. deflection.....5-18
Table 5.3.4-4	Stress and load at 2‰ and 4‰ strain and according deflection.....5-19
Table 5.3.4-5	Ultimate stress and load with according strain resp. deflection.....5-20
Table 5.3.4-6	Stress and load at 2‰ and 4‰ strain and according deflection.....5-21
Table 5.3.4-7	Ultimate stress and load with according strain resp. deflection, values until stop of the tests and at the right the according values at 2‰ and 4‰ strain.....5-22
Table 5.4-1	Maximum allowable deflections compared with the deflections of the various slabs..5-24
Table 5.4-2	Calculated Young's moduli from the tests.....5-25

Chapter 6

Table 6.1.3-1	Results of pull-out tests.....6-3
Table 6.2.1-1	Definition of roughness.....6-5
Table 6.2.1-2	Roughness parameter of tested lamellae...6-6
Table 6.2.6-1	Tested materials.....6-15
Table 6.2.9-1	Summary of main results.....6-21

Figure register

Chapter 1

Figure 1.2-1 Qualitative comparison of different types of fibers.....1-2

Chapter 2

Figure 2.1.3-1 The most important test and quality seals of cement.....2-2

Figure 2.1.4-1 Various grain mixtures (schematic) [4]....2-7

Figure 2.2-1 Ferrum-carbon-diagramm.....2-14

Figure 2.2-2 Stress-strain-diagram [7].....2-15

Figure 2.4.3-1 Strothetal bridge (timed shifting, composite construction).....2-26

Chapter 3

Figure 3.2.1-1 Chemism of manufacturing and microstructure of carbon fibers.....3-2

Figure 3.2.1-2 Young's modulus of prestressed hybrid laminate.....3-3

Figure 3.2.2-1 Single procedures of a pultrusion equipment.....3-4

Figure 3.2.2-2 Comparison of Young's moduli of CFRP-lamellae and steel.....3-6

Figure 3.4.1-1 Shift in a bending crack due to large shear stress [22].....3-9

Figure 3.4.1-2 Tensile strength of the CFRP-lamella for design [18].....3-10

Figure 3.4.2-1 Operating line of prestressed steel and CFRP cable.....3-11

Figure 3.4.6-1 Operating line of composite materials....3-14

Figure 3.5-1 Fire protection measures [18].....3-15

Chapter 4

Figure 4.1.1-1	Sheets of series 1 and 2.....	4-3
Figure 4.1.3-1	Single grading curve for maximum grain size 4.....	4-5
Figure 4.1.3-2	Grain size distribution for maximum grain size 4.....	4-6
Figure 4.2-1	Grain size distribution for SCC with maximum grain 4.....	4-10
Figure 4.2-2	Grain size distribution for SCC with maximum grain 16.....	4-10

Chapter 5

Figure 5.1.1-1	Test setup.....	5-2
Figure 5.1.2-1	Hydraulic actuator.....	5-5
Figure 5.1.2-2	Pulling device.....	5-5
Figure 5.1.3-1	Data capture.....	5-7
Figure 5.3.1-1	Distribution of cracks for a double-layer reinforcement (schematic).....	5-10
Figure 5.3.4-1	Slab 1 with double-layered CFRP-sheet reinforcement.....	5-15
Figure 5.3.4-2	Slab 2 with double-layered CFRP-sheet reinforcement.....	5-16
Figure 5.3.4-3	Slabs 1 and 2 with double-layered CFRP-sheet reinforcement.....	5-16
Figure 5.3.4-4	Slab 3 with single-layered CFRP-sheet reinforcement.....	5-17
Figure 5.3.4-5	Slab 4 with single-layered CFRP-sheet reinforcement.....	5-18
Figure 5.3.4-6	Slabs 3 and 4 with single-layered CFRP-sheet reinforcement.....	5-18
Figure 5.3.4-7	Slab 5 with CQS 8 steel mesh reinforcement.....	5-19
Figure 5.3.4-8	Slab 6 with CQS 6 steel mesh reinforcement.....	5-20
Figure 5.3.4-9	Slabs 5 and 6 with CQS steel mesh reinforcement.....	5-20

Figure 5.3.4-10	Summary of results in the stress - strain – diagram.....5-21
Figure 5.4-1	Summary of results with force-strain diagram.....5-23
 Chapter 6	
Figure 6.1.1-1	Geometry for the pull-out tests.....6-1
Figure 6.1.3-1	Bond stresses for different embedment depths (bars) and theoretic values (line)...6-4
Figure 6.2.1-1	Interactions between the surface deviations.....6-5
Figure 6.2.1-2	Roughness parameter.....6-6
Figure 6.2.1-3	Plotted roughness parameter [29].....6-7
Figure 6.2.2-1	Bonding effect due to “lack of fit”.....6-8
Figure 6.2.2-2	Loading regions of a reinforced concrete beam.....6-9
Figure 6.2.3-1	Simple strain specimen.....6-10
Figure 6.2.3-2	Console shaped pull-out specimen.....6-10
Figure 6.2.3-3	Pull-out specimen with tensile loading...6-11
Figure 6.2.3-4	Beam or beam section.....6-11
Figure 6.2.3-5	Pull-out specimen.....6-12
Figure 6.2.4-1	Example for a basic bond law.....6-13
Figure 6.2.5-1	Example for two different pull-out tests..6-14
Figure 6.2.6-1	Formwork of specimen.....6-15
Figure 6.2.6-2	Cube geometry and anchoring length of CFRP-lamellae.....6-16
Figure 6.2.7-1	Test and measurement setup.....6-17
Figure 6.2.8-1	Stress-slip relation of a lamella with flat surface and a width of 5 mm.....6-19
Figure 6.2.8-2	Stress-slip relation of a lamella with rough surface and a width of 5 mm.....6-19
Figure 6.2.9-1	Pullout test results of 5 mm and 10 mm wide lamellae.....6-20
Figure 6.3-1	Steps to compare model and test [29].....6-21
Figure 6.3-2	Forces and stresses at the fiber element..6-22

Figure 6.3-3	Pullout cube system.....	6-24
---------------------	--------------------------	------

Appendix

Figure A-1	Schematical description of the function of a glenium molecule.....	A-14
Figure A-2	two phase effect of molecule.....	A-15
Figure A-3	protocol from test results - slab [31].....	A-20
Figure A-4	Slab 1 – double CFK-reinforcement.....	A-21
Figure A-5	Slab 2 – double CFK-reinforcement.....	A-21
Figure A-6	Slab 3 – single CFK-reinforcement.....	A-22
Figure A-7	Slab 4 – single CFK-reinforcement.....	A-22
Figure A-8	Slab 5 – CQS 8 steel reinforcement.....	A-23
Figure A-9	Slab 6 – CQS 6 steel reinforcement.....	A-23
Figure A-10	Strain-stress-function for various loads [10].....	A-25

Release for publication

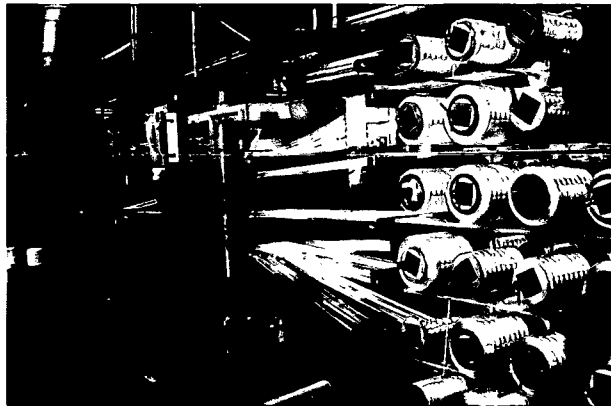
- Isosport Verbundbauteile GmbH.A-27
- Degussa Construction Chemicals Austria GmbH.A-28

Produktion of Carbon Fiber Plastics

The following pictures and comments show the production process of carbon fiber plastics, which is similar to the production of glass fiber plastics. Due to the fact that during our visit in the ISOSPORT fabric no carbon fiber plastic was produced, the pictures show rolls with glass fibers.



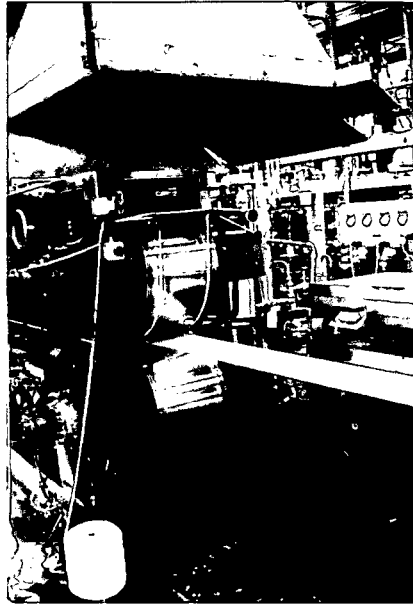
Picture A – 1 Rovings on spools , which are pulled together in the first production step.



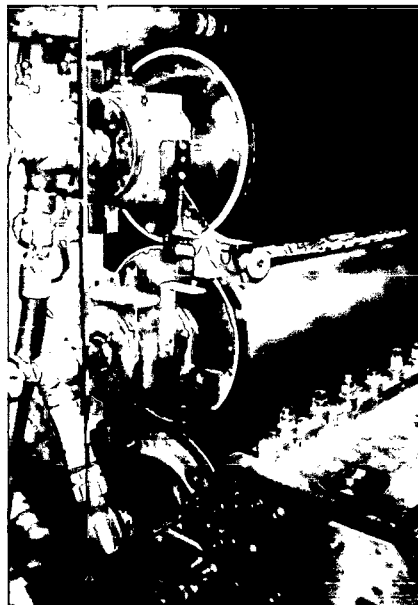
Picture A – 2 Consolidation and spread prozess



Picture A – 3 Impregnation with liquid matrix – glass fiber



Picture A – 4 Profiling and hardening process in casting forms with lateral rolled-on borders which are removed finally



Picture A – 5 Heated nip roll, which gives the fitting thickness to the matrix by means of high pressure



Picture A – 6 Post curing with hot air – result of the nip roll, shown in picture A-5



Picture A – 7 Pull-off process by means of a rubber cylinder and cutting in fitting width

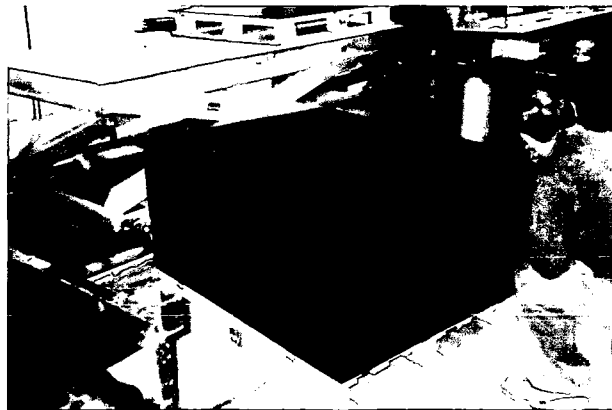


Picture A – 8 Separator and rewinder of the glassfiberlaminate

Another alternative to form carbon fiber lamellas



Picture A – 9 conveyer band with heated nipp rolls



Picture A – 10 Square cut of carbon fiber laminate to be applied for example for sports goods

Mechanism of SCC

Additional to chapter 4.2. the mode of functioning of SCC “Self compacting concrete” is described.

The system of SCC is based on the behaviour of a GLENIUM molecule. Glenium is a new type of a high effective plasticiser, based on a modified polycarboxylether and applied in many different product types. Balanced with the application it is possible to consider various conditions like for example transport concrete in summer or winter, prefabrication of concrete units and to force the hydratation process.

The glenium molecule is complex and flexible, built of different groups with various chain length.



Figure A – 1 Schematical description of the function of a Glenium molecule

- Hydratation

The chemical reaction called hydration starts after mixing the cement with water. The surface of the cement particles is softened and sheets of drift are build. With progressive hydration the sheets turn to hardened cement paste.

- Dispergierungseffekt (A)

The Glenium molecule accumulates on the surface of the cement particles. Due to this process result electrostatic forces which disperse the particles and the green concrete can be used very good.

- Sterical effect (B)

The molecule carries longsome side chains (B), which build a sterical barrier and avoid contact with the hydration products (C) (setting of cement).

Two-phase effect

High temperatures demand longtime “opentime” of green concrete. Today, the loss of workability can be well balanced by the new mechanism (delayed effectiveness).

A glenium molecule interacts time shared with the others, activated and controlled by the high alkalinity of the cement paste. This makes is possible to extend the workability without the effect of delay in setting. [28]

This type of concrete keeps it’s consistence during the whole process of application, with the effect of correct levelling. The relation of water/cement could be reduced extremely without a loss of processibility.

After striking, the surface of the concrete shows no imperfections, which makes it perfect to be used as a fairfaced concrete.

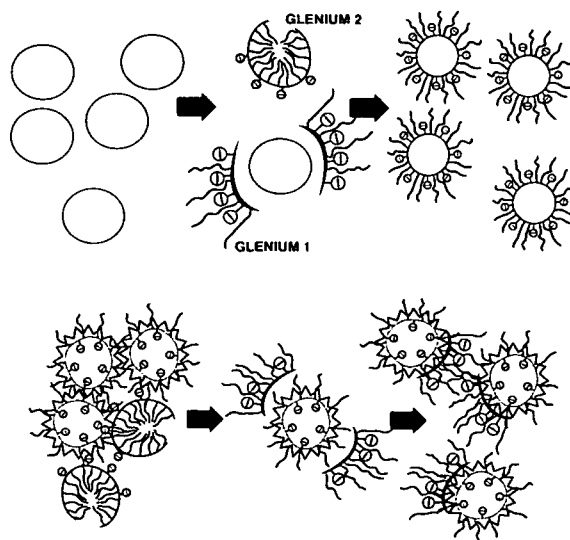


Figure A – 2 two phase effect of molecule

LOG-IN Data for the evaluation program

100;Test Standard;;IKI-
 Prüfhalle;;F;F;30;;;F;100;
 101;Prüfer/in;;WENZL
 Wolfgang;;F;F;30;;;F;101;
 102;Material;;CFK-2 lagig;;F;F;30;;;F;102;
 104;Lieferant;;;F;F;30;;;F;104;
 106;Testdatum;Datum;1998-09-07;;F;F;-
 2;;F;106;
 200;Chargennummer;ChNo;Plattel;;T;F;;;F;200;
 201;Temperatur;T;20;°C;F;T;;;F;201;
 202;Querschnitt;;0.000;;F;F;;;F;202;
 203;Dicke;a;100;mm;F;T;;;F;203;
 204;Breite;b;400.0;mm;F;T;;;F;204;
 205;Durchmesser;d;0;mm;F;T;;;F;205;
 206;Aussen Ø;D;0;mm;F;T;;;F;206;
 207;Wandstärke;wd;0;mm;F;T;;;F;207;
 208;Gesamtlänge;Lt;0;mm;F;T;;;F;208;
 209;Spez. Gewicht;rho;0;g/cm³;F;T;;;F;209;
 210;Masse;m;0;g;F;T;;;F;210;
 211;Bekannte Fläche;S0;0;mm²;F;T;;;F;211;
 212;Schiebelehre;;n.i.;F;F;;;F;212;
 213;Waage;;n.i.;F;F;;;F;213;
 216;Erwarteter E-Modul;eE;;GPa;F;F;;;F;216;
 218;Richtung;Richtung;gerade;;F;F;;;F;218;
 223;Stützweite;Ls;1500;mm;F;T;;;F;223;
 224;Freie Biegelänge;Ll;750;mm;F;T;;;F;224;
 300;Prüfmaschine;;;F;F;;;F;300;
 301;Geschwindigkeit
 1;v1;0|0.6|mm/min;;T;F;;;F;301;
 302;Geschwindigkeit
 2;v2;0.6|3.0|mm/min;;T;F;;;F;302;
 303;Geschwindigkeit
 3;v3;|0|mm/min;;F;F;;;F;303;
 304;Geschwindigkeit
 4;v4;|0|mm/min;;F;F;;;F;304;
 305;Geschwindigkeit
 5;v5;|0|mm/min;;F;F;;;F;305;
 306;Vorspannung;"0;0.1;MPa;T;F;;;F;306;
 307;Bruchkriterium 1;;99;%;F;F;;;F;307;
 308;Bruchkriterium 2;;500;%/min;F;F;;;F;308;
 309;Bruchkriterium 3;;250;MPa/s;F;F;;;F;309;
 310;Automatischer Rücklauf;;;F;F;;;F;310;
 311;Beanspruchungsrichtung
 auf;;;T;F;;;F;311;
 312;Krümmungssensor;;ME46;;T;F;;;F;312;
 313;Extensometer quer;;ME46;;F;F;;;F;313;
 314;Testmethode;;1.000;;F;F;;;F;314;

325;Blockprogramm;;DEFAULT;;F;F;;;F;325;
 330;ME46 Längs-Setup;ME46-L;;;F;F;;;F;330;
 350;Deflektometer-
 Messlänge;Lb;1500;mm;F;F;;;F;350;
 352;Load DAQ criterium;;;MPa;T;F;;;F;352;
 353;Stroke DAQ criterium;;;mm;F;F;;;F;353;
 354;Strain DAQ
 criterium;;0.001;%;T;F;;;F;354;
 355;Time DAQ criterium;;;sec;F;F;;;F;355;
 400;Diagramm X-
 Achse;;4.000;%;F;F;3;0;2;F;400;
 401;Diagramm Y-
 Achse;;2.000;MPa;F;F;3;0;20;F;401;
 402;Daten speichern;;1.000;;F;F;;;F;402;
 403;Offset;;0;;F;F;;;F;403;
 404;Diagramm X-Typ;;0.000;;F;F;;;F;404;
 405;Diagramm Y-Typ;;0.000;;F;F;;;F;405;
 406;Diagramm Y-Achse
 2;;2;MPa;F;F;1;0;1000;F;406;
 500;Vorwahlbiegung 1;;1;%;T;F;;;F;500;
 501;Vorwahlbiegung 2;;2;%;T;F;;;F;501;
 502;Vorwahlbiegung 3;;3;%;T;F;;;F;502;
 503;Vorwahlbiegung 4;;4;%;T;F;;;F;503;
 504;Vorwahlspannung 1;;100;MPa;T;F;;;F;504;
 505;Vorwahlspannung 2;;200;MPa;T;F;;;F;505;
 506;Vorwahlspannung 3;;300;MPa;T;F;;;F;506;
 507;Vorwahlspannung 4;;400;MPa;T;F;;;F;507;
 508;x%-Dehnspannung;;2.5;%;T;F;;;F;508;
 509;E-Modulsberechnung;;1.000;;T;F;;;F;509;
 510;E-Modulsuntergrenze;;4;MPa;T;F;;;F;510;
 511;E-Modulobergrenze;;6;MPa;T;F;;;F;511;
 600;Querschnittsfläche;A0;40000;mm²;F;T;;;F;
 600;
 601;Maximalkraft;Fmax;33138;N;T;T;;;F;601;
 602;Bruchdehnung;"fB;1.520;%;T;T;;;F;602;
 603;Biegefestigkeit;"fM;18.64;MPa;T;T;;;F;60
 3;
 604;Referenzlänge;Lr;3750;mm;F;T;;;F;604;
 605;Extensometer Referenzlänge;Ler;-
 999.0;mm;F;T;;;F;605;
 606;Volumsbez.
 Brucharbeit;Wv(B);0.207;mJ/mm³;F;T;;;F;606;
 607;Volumsbez. Arbeit bis
 Fmax;W(Fmax);0.072;mJ/mm³;F;T;;;F;607;
 608;Testdauer;t;-9.838;s;T;T;;;F;608;
 609;Spannung/Kraft bei
 1%;"f(1%);15.80;MPa;F;T;;;F;609;
 610;Spannung/Kraft bei
 2%;"f(2%);n.a.;MPa;F;T;;;F;610;
 611;Spannung/Kraft bei
 3%;"f(3%);n.a.;MPa;F;T;;;F;611;

612;Spannung/Kraft bei
 4%;"f(4%);n.a.;MPa;F;T;;;;;F;612;
 613;Biegung/Weg bei
 100MPa;"f(100MPa);n.a.;%;F;T;;;;;F;613;
 614;Biegung/Weg bei
 200MPa;"f(200MPa);n.a.;%;F;T;;;;;F;614;
 615;Biegung/Weg bei
 300MPa;"f(300MPa);n.a.;%;F;T;;;;;F;615;
 616;Biegung/Weg bei
 400MPa;"f(400MPa);n.a.;%;F;T;;;;;F;616;
 620;E-Modul;Ef;3.022;GPa;T;T;;;;;F;620;
 621;5%-
 Dehnspannung;"fS5;n.a.;MPa;F;T;;;;;F;621;
 622;1%-
 Dehnspannung;"fS1;13.25;MPa;F;T;;;;;F;622;
 623;0.2%-
 Dehnspannung;"fS0.2;13.72;MPa;F;T;;;;;F;623;
 624;x%-
 Dehnspannung;"fS2.5;n.a.;MPa;F;T;;;;;F;624;
 625;Streckspannung;"fY;16.93;MPa;F;T;;;;;F;625
 ;
 627;Dehnung bei
 Biegefestigkeit;"fM;0.604;%;T;T;;;;;F;627;
 630;Verfestigungsexponent;n;n.a.;F;T;;;;;F;630;
 631;Volumsbez. Arbeit bis
 "fY;W("fY);0.050;mJ/mm³;F;T;;;;;F;631;
 637;Bruchspannung;"fB;12.00;MPa;T;T;;;;;F;637;
 642;Streckdehnung;"fY;0.480;%;F;T;;;;;F;642;
 643;Nom.Dhg. bei Biegefestigkeit;"tfM;5.60E-6;%;F;T;;;;;F;643;
 644;Nom.Dhg. bei Bruch;"tfB;5.60E-6;%;F;T;;;;;F;644;
 645;Widerstandsmoment;W;666667;mm³;F;T;;;;;F;645;
 646;Spannungsfaktor;SF;1778;mm²;F;T;;;;;F;646;
 647;Prozentisches
 Kriechen;Kn;0.000;%;F;T;;;;;F;647;
 678;Spezifisches
 Gewicht;rho;n.a.;kg/m³;F;T;;;;;F;678;
 682;Weg bei Biegefestigkeit;smax;2.10E-4;mm;F;T;;;;;F;682;
 686;Weg bei Bruch;f;2.10E-4;mm;F;T;;;;;F;686;
 704;Scheinbare Scherfestigkeit;-
 ;0.400;MPa;F;T;;;;;F;704;
 708;Innen Ø;id0;0.000;mm;F;T;;;;;F;708;
 999;Kommentar;Kommentar;CFK 2-
 lagig;;T;F;;;;;F;999;
 @DATA
 8280 21.0000 -999.0000 100.0000
 9280 42.0000 -999.0000 99.980000

10280	21.0000	-999.0000	99.970000
11280	42.0000	-999.0000	99.950000
12280	21.0000	-999.0000	99.950000
13280	42.0000	-999.0000	99.950000
14280	0.0000	-999.0000	99.940000
15280	168.0000	-999.0000	99.920000
16280	210.0000	-999.0000	99.910000
17280	273.0000	-999.0000	99.900000
18280	378.0000	-999.0000	99.890000
19280	210.0000	-999.0000	99.900000
20280	378.0000	-999.0000	99.880000
21280	525.0000	-999.0000	99.870000
22280	609.0000	-999.0000	99.860000
23280	588.0000	-999.0000	99.860000
24280	609.0000	-999.0000	99.860000
25280	651.0000	-999.0000	99.850000
26280	840.0000	-999.0000	99.830000
27280	693.0000	-999.0000	99.850000
28280	798.0000	-999.0000	99.840000
29280	945.0000	-999.0000	99.820000
30280			1071.0000 -
999.0000			99.810000
31280	1092.0000	-999.0000	99.810000

[31]

This data show the required input parameter and a small part of data from the beginning of a bending test. The first column gives the time in [ms], the second column shows the applied force in [N], the further columns the strain in [mm]. The whole data material comprises about 1230 A4 pages.

TEST PROTOCOL

MESSPHYSIK Laborgeräteges.m.b.H.

Prüfbericht

Biegeversuch

Test Standard.....IKI-Prüfhalle
 Prüfer/in.....WENZL Wolfgang

Material.....
 Testdatum.....

Prüfmaschine.....
 Krümmungssensor.....ME46
 Geschwindigkeit 1.....0 % -> 1.8 mm/min

Artikel / Projekt.....PLATTEN
 Parametersatz.....PLATTEN

Legende

ChNo.....Chargennummer
 Ef.....E-Modul
 Fmax.....Maximalkraft
 *fM.....Biegefestigkeit
 *fM.....Dehnung bei Biegefestigkeit
 *fB.....Bruchdehnung
 *fB.....Bruchspannung
 Kommentar.....Kommentar

Test Nr.	ChNo	Ef GPa	Fmax kN	*fM MPa	*fM %	*fB %	*fB MPa	LI mm	Kommentar
1	Platte1	3.022	33.14	18.64	0.604	1.520	12.00	750.0	CFK 2-lagig
2	Platte2	2.169	19.49	10.96	1.135	2.668	9.072	750.0	CFK 2-lagig
3	Platte3	3.354	27.00	15.19	2.244	2.598	12.47	750.0	CFK 1-lagig
4	Platte4	7.525	27.30	15.36	1.399	2.149	14.26	750.0	CFK 1-lagig
5	Platte5	6.430	19.47	10.95	0.498	0.946	1.654	750.0	Stahl CQS 6
6	Platte6	1.029	11.05	6.213	0.421	0.829	1.878	750.0	Stahl CQS 8
Mittelwert:		3.922	22.91	12.89	1.050	1.785	8.556	750.0	
Minimum:		1.029	11.05	6.213	0.421	0.829	1.654	750.0	
Maximum:		7.525	33.14	18.64	2.244	2.668	14.26	750.0	
Var. Koeff. %:		64.36	34.09	34.10	66.71	45.24	64.49	0.000	
Werte:		6	6	6	6	6	6	6	

Figure A-3 protocol from test results - slab [31]

FORCE – STRAIN - CURVE

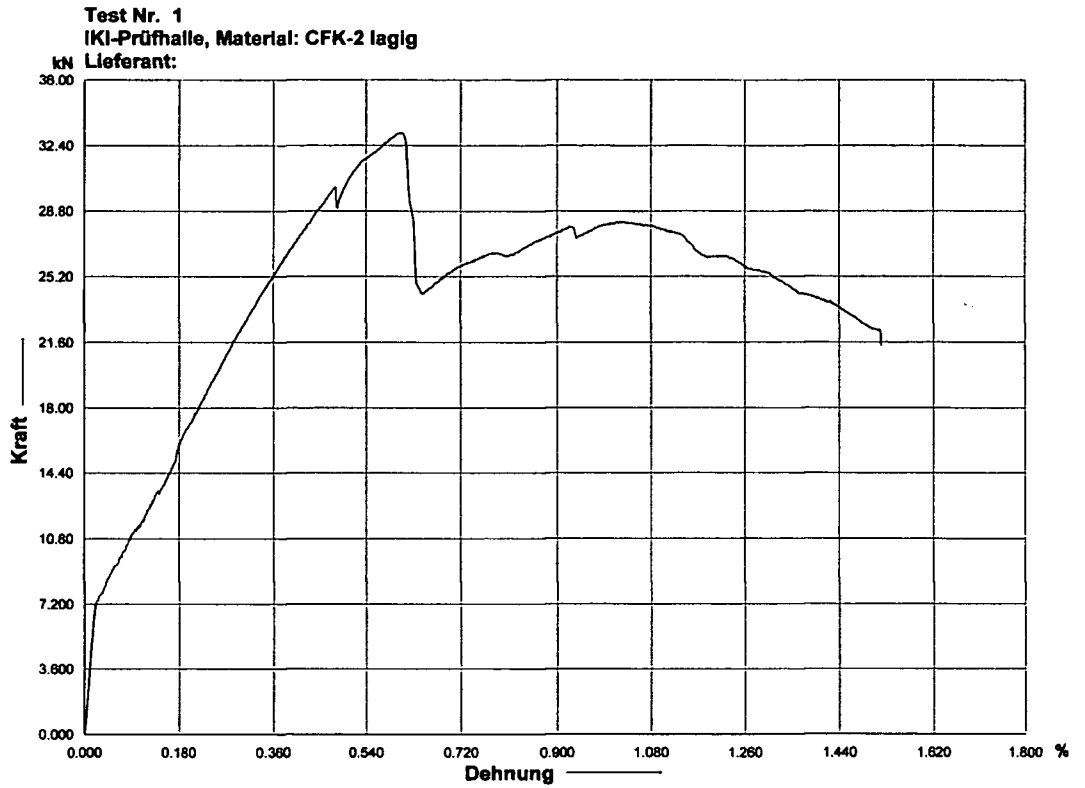


Figure A-4 Slab 1 – double CFK-reinforcement

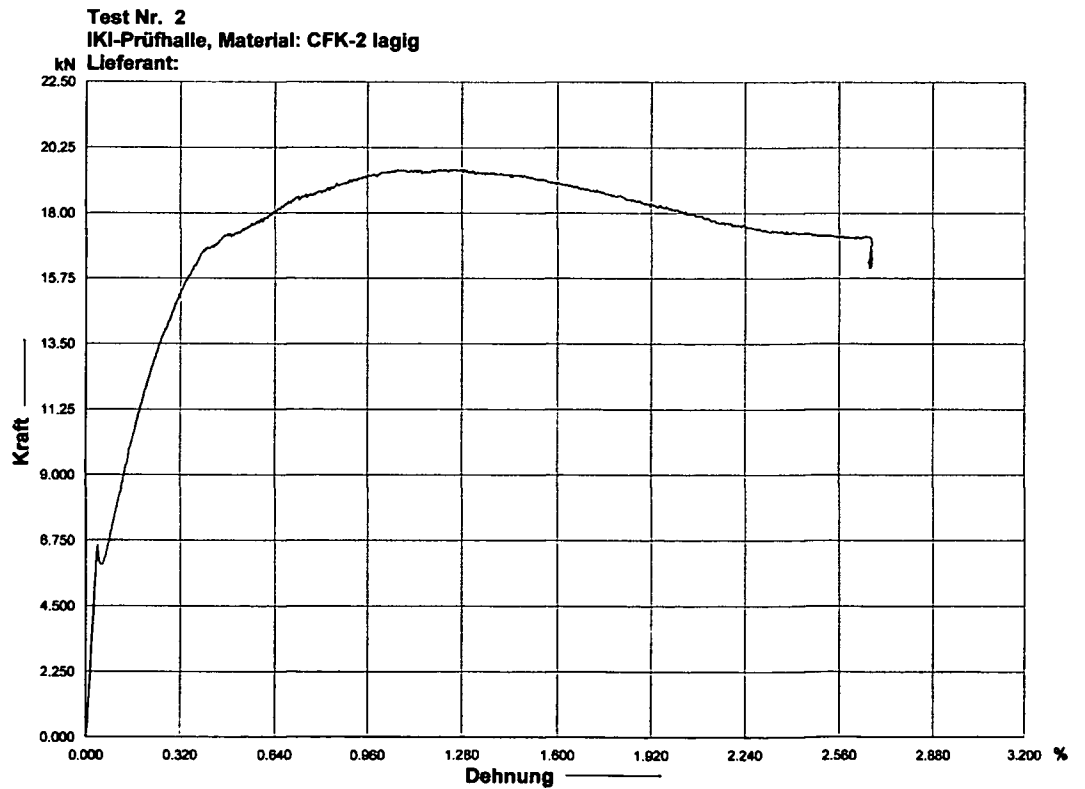


Figure A-5 Slab 2 – double CFK-reinforcement

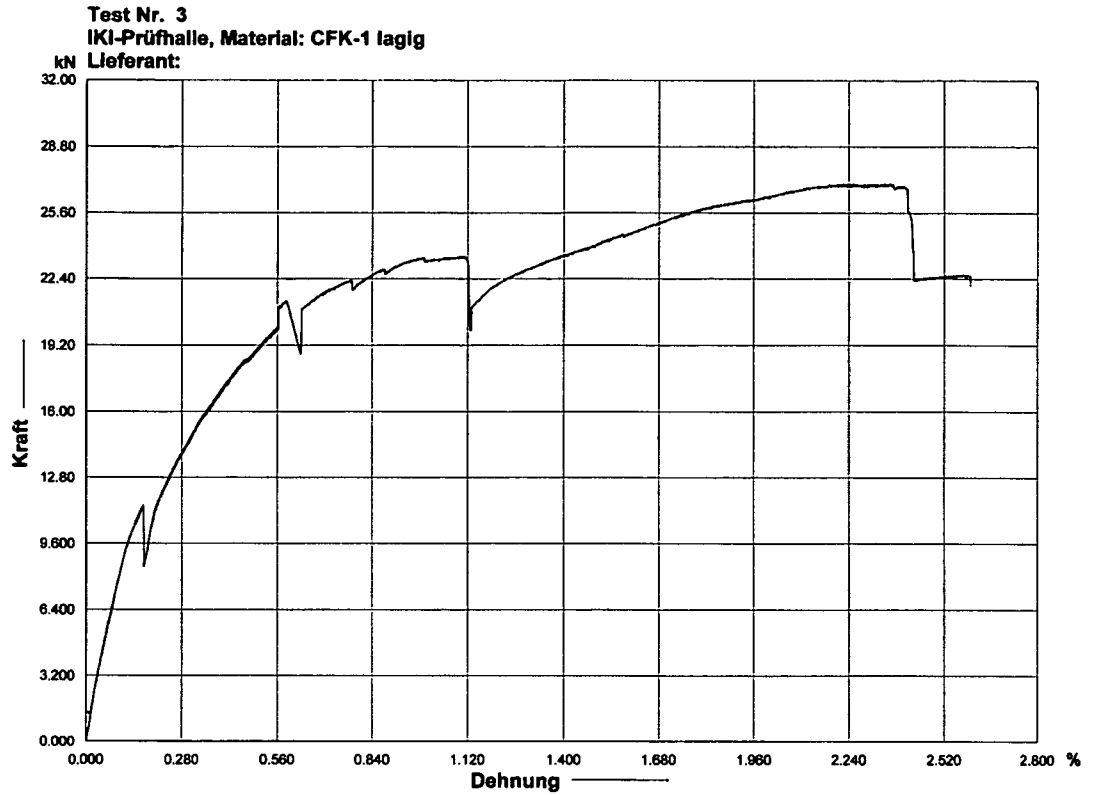


Figure A-6 Slab 3 – single CFK-reinforcement

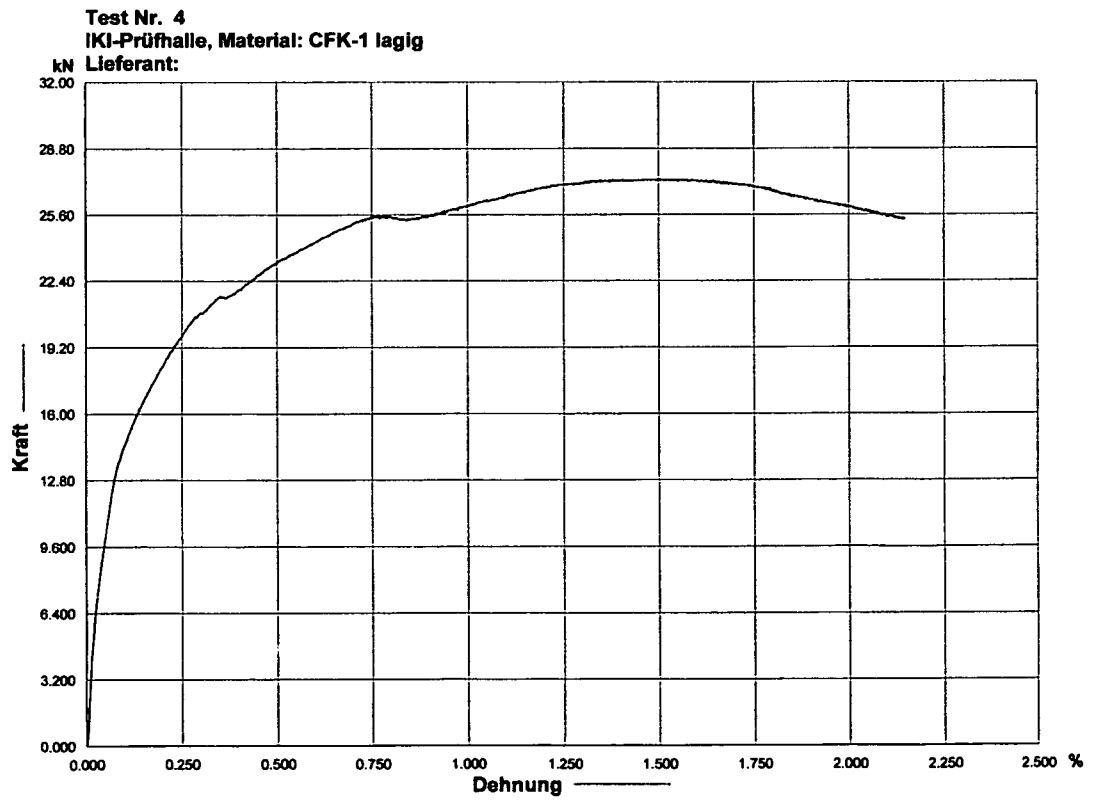


Figure A-7 Slab 4 – single CFK-reinforcement

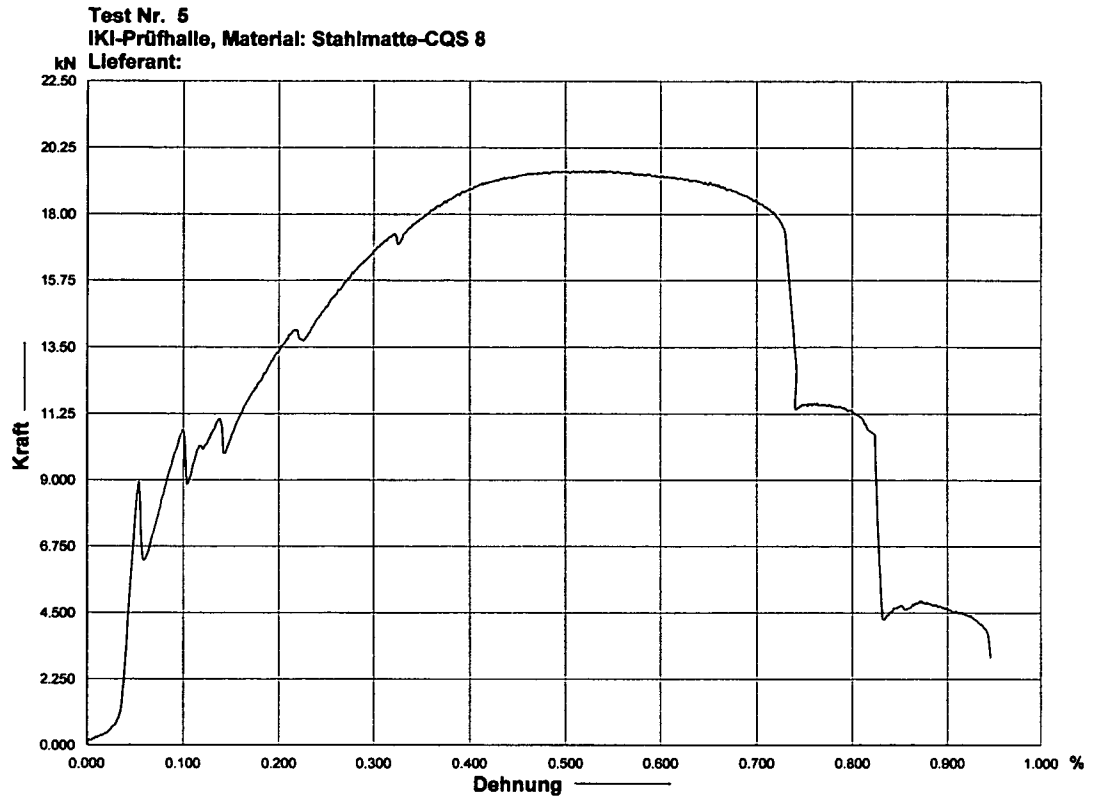


Figure A-8 Slab 5 – CQS 8 steel reinforcement

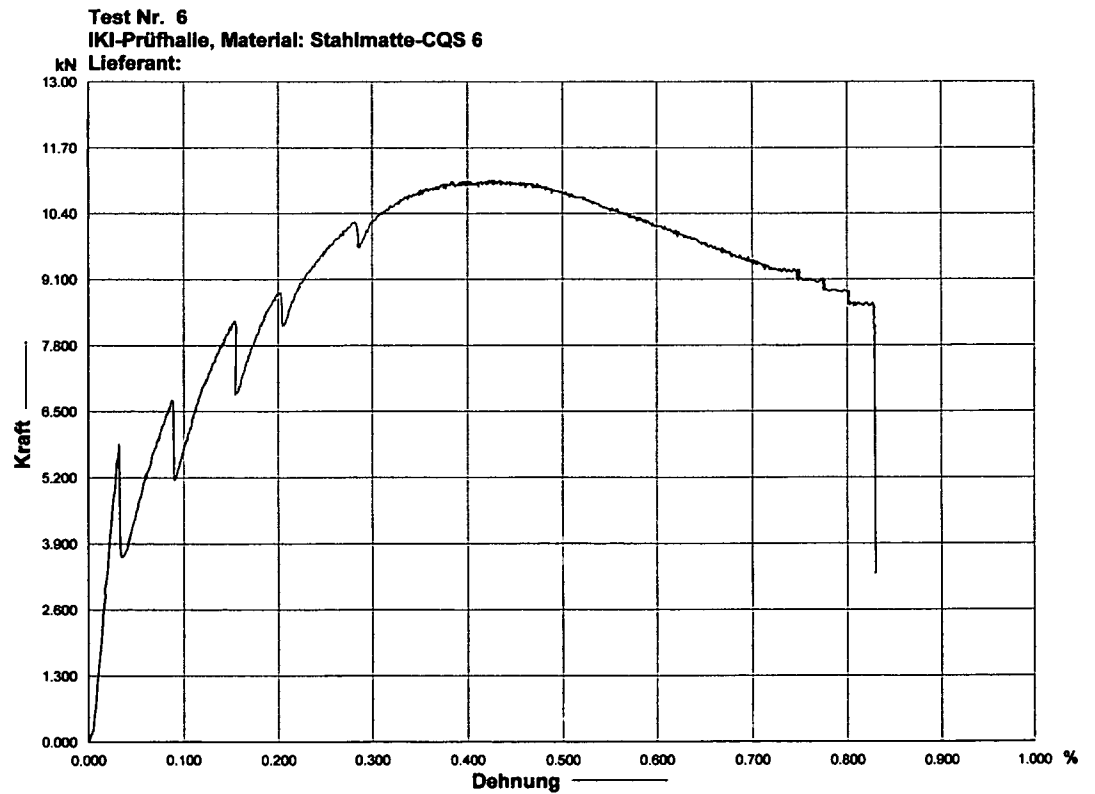


Figure A-9 Slab 6 – CQS 6 steel reinforcement

INFLUENCE FACTS OF LOADING RATE TO THE CONCRETE

The deformation behaviour under load is important to evaluate the properties of building materials. The distribution of stress in the cross section can not be measured but the resulting strains. To get conclusions on stress the correlation between stress and strain must be well known. The most common interrelationship between stress and strain is Hook's law, in detail

$$E = \frac{\sigma}{\varepsilon}$$

Equation A-1

with

E	Young's modulus [N/mm ²]
σ	Stress in the cross section [N/mm ²]
ε	Strain [%].

The basis is the assumption of a constant Young's Modulus. The relation between strain and stress can be shown in a function. The essential influence facts on this function and on the deformation behaviour of concrete are the loading rate, the loading duration and the concrete strength.

The following diagrams show the strain-stress-functions, which have been explored with various constant strain rates. It can be seen, that a low deformation rate leads to a smaller peak value, to a slowly decrease of bearing load and to an increase of deformation (creep of concrete).

The influence of the load regulation on the strain-stress-function with constant strainrate $d\varepsilon/dt$, load-rate controlled ($d\sigma/dt=\text{const.}$) and strain-rate controlled ($d\varepsilon/dt=\text{const.}$) can be seen in Picture A-10 on the right hand side of the diagram.

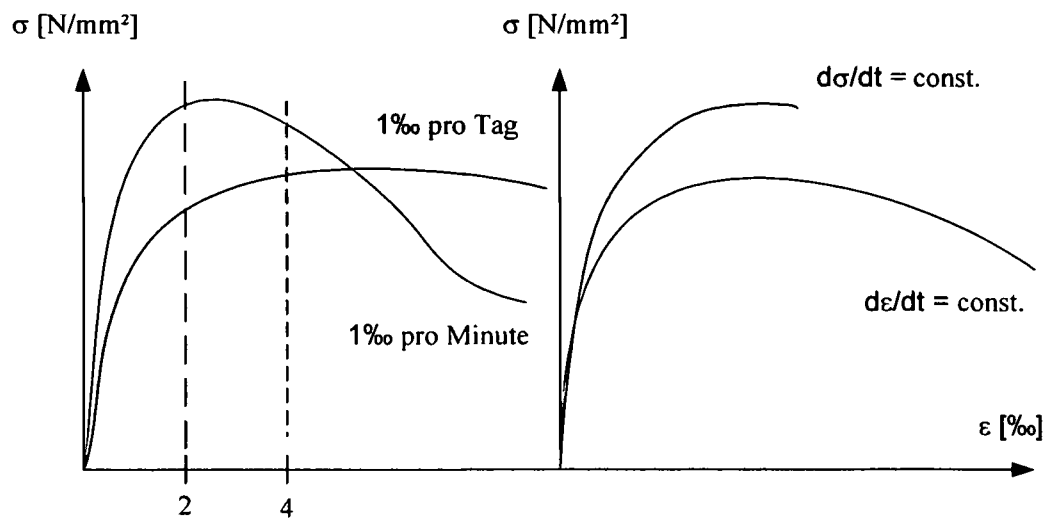


Figure A-10 Strain-stress-function for various loads [10]

Considering the case of constant loading rate ($d\sigma/dt = \text{const.}$) the development of microcracks causes the acceleration in the deformation behaviour above average. Reaching the peak value of load, the deformation rate should be infinite in theory with the result of failure without indication. Strain-stress-functions of that case are of little importance. Due to that fact the functions with constant deformation rates ($d\varepsilon/dt = \text{const.}$) are preferred. The test can be continued till the resistance in load approximates zero.

The functions and peak values for the compressive strength describe the short-time strength. To use the values for design of structural components under constant load, they have to be attenuated. Both, EC2 and DIN 1045 take that fact into account with the decrease factor of $\alpha = 0.85$, the fatigue strength. Both standards support two strain-stress-functions, the parable-rectangle-diagram and the bilinear sprain-stress-function [10].

Release for publication the illustrations from the company`s

- Isosport Verbundbauteile GmbH. and
- Degussa Construction Chemicals Austria GmbH.

Firmensitz / headquarter Eisenstadt

Industriestrasse 2-8
A-7000 Eisenstadt

Telefon +43 2682 / 703-0
Fax +43 2682 / 703-4222

e-mail office@isosport.com
Internet <http://www.isosport.com>

Werk / plant Hall

Josef-Dinkhauser-Strasse 4
A-6060 Hall in Tirol

Telefon +43 5223 / 5859-0
Fax +43 5223 / 5859-8111

e-mail office.hall@isosport.com
Internet <http://www.isosport.com>



Hrn. Wenzl Wolfgang

Wiesflecker Strasse 6
A-7423 Pinkafeld

Eisenstadt, 28.03.2006

Betreff: Diplomarbeit

Sehr geehrter Herr Wenzl!

Die Firma ISOSPORT hat keine Einwände gegenüber der Veröffentlichung der Fotos (Bild A-1, A-2, A-3, A-4, A-5, A-6, A-7 und A-8) aus Ihrem Schreiben vom 13.03.2006 im Rahmen Ihrer Diplomarbeit.

Wir wünschen viel Glück und verbleiben

mit freundlichen Grüßen
ISOSPORT Verbundbauteile GmbH
Geschäftsleitung

Ing. G. Mikats

degussa.
creating essentials

Degussa Construction
Chemicals Austria GmbH
Roseggerstraße 101
A-8670 Krieglach

T +43 3855 2371 0
F +43 3855 2371 23

Herr
Wolfgang Wenzl

Wiesflecker Strasse 6
A – 7423 Pinkafeld

Donnerstag, 16. März 2006

Dieter Schmidt
Leiter Customer Service
Assistent Geschäftsleitung

Freigabe Bilder zur Diplomarbeit

T +43 3855 2371 39
F +43 3855 2371 23

Dieter.Schmidt.ds@
degussa.com

Sehr geehrter Herr Wenzl!

Vielen Dank für Ihr Interesse an unseren Bildern. Selbstverständlich dürfen Sie diese für Ihre Diplomarbeit verwenden. Ich darf Ihnen als weitere Hilfe unsere Homepage

www.degussa-cc.at

empfehlen. Gleichzeitig würde es uns freuen eine Kopie Ihrer Diplomarbeit zu erhalten.

Für Rückfragen stehe ich Ihnen jederzeit gerne zur Verfügung.

Mit den besten Wünschen für Ihre weitere berufliche Laufbahn verbleiben wir

Mit freundlichen Grüßen
Degussa Construction
Chemicals Austria GmbH



Dieter Schmidt
Assistent Geschäftsleitung
Leiter Customer Service

UID-Nr. ATU 30158101
ARA-Lizenznummer: B41
Firmenbuch-Nr. FN 46111 k
Firmenbuchgericht: LG Leoben

Bankverbindung: BA-CA Leoben
Kto. 0069-6716000 BLZ 12000
IBAN-Nummer:
AT17110000696716000